In presenting the dissertation as a partial fulfillment of the requirements for an advanced degree from the Georgia Institute of Technology, I agree that the Library of the Institute shall make it available for inspection and circulation in accordance with its regulations governing materials of this type. I agree that permission to copy from, or to publish from, this dissertation may be granted by the professor under whose direction it was written, or, in his absence, by the Dean of the Graduate Division when such copying or publication is solely for scholarly purposes and does not involve potential financial gain. It is understood that any copying from, or publication of, this dissertation which involves potential financial gain will not be allowed without written permission.

7/25/68

NEUTRON ACTIVATION CROSS SECTIONS OF MEDIUM-Z NUCLEI AT 14.4 Mev

A Dissertation

Presented to

The Faculty of the Graduate Division

by

Winston Wen-deh Lu

In Partial Fulfillment

of the Requirements for the Degree

Doctor of Philosophy in the School of Chemistry

Georgia Institute of Technology

August 1970

NEUTRON ACTIVATION CROSS SECTIONS

OF MEDIUM-Z NUCLEI AT 14.4 Mev

Approved:

Chairman

Date approved by Chairman: October 8, 1970

ACKNOWLEDGMENTS

The author wishes to express his appreciation to Professor R. W. Fink for his guidance throughout the work reported in this dissertation. He also expresses appreciation to Drs. P. Vanugopala Rao and N. Ranakumar for their assistance in the experiments and to Mrs. A. K. Hankla for her experimental (n,2n) cross section data on heavy elements.

The author thanks Chung Shan Institute of Science and Technology, Taiwan, Republic of China, for fellowship support throughout the work.

TABLE OF CONTENTS

LIST OF TABLES

LIST OF FIGURES

LIST OF FIGURES (Continued)

SUMMARY

In the present research cross sections were measured by using the mixed powder method with Ge(Li) gamma detection first developed by Rao and Fink. This method generally gives results of much improved accuracy. Many of the cross sections were measured for the first time in the present work. For several of the lightest stable isotopes of even-Z elements, i.e. Ni^{58}, Ru^{96}, Cd^{106}, and Sn^{112} rather large [(n,np) + (n,pn) + (n,d)] cross sections were observed. Since the product of the (n,np) +... reaction is usually mixed with the daughter of the corresponding (n,2n) product, a method based on radioactive decay laws with or without radiochemical separation of the product was developed to resolve these two components. The main advantage of the method is that the cross section ratio of the (n,np) +... reaction to the corresponding (n,2n) reaction can be determined directly from the counting rates and half-lives involved without knowing the detection efficiencies and detailed decay schemes of the nuclides involved.

From the measured (n,2n) cross sections an empirical formula as a function of only Z and A of the target nucleus is obtained. This formula reproduces the (n,2n) cross sections from the present work to within about ±20% with a few exceptions. The predictions of Pearlstein and Gardner with some modifications generally give good agreement with experiment, i.e. within about ±20%, for (n,2n) cross sections. For (n,p) cross sections the predictions from Levkovskii's empirical formula give much better agreement than those of Gardner and Rosenblum. However, there are

several cases in which the values from Levkovskii's formula are too small by factors up to 2.5 compared with experimental values. For (n,α) cross sections, the statistical model calculations of Facchini et al. using energy independent level density parameter $\underline{a}$ are generally an order of magnitude too small compared with experiment.

Rather large [(n,np) + (n,pn) + (n,d)] cross sections of Ni^{58}, Ru^{96}, Cd^{106}, and Sn^{112} were observed. The cross sections were seen to be linearly related to both Z and A of the target nuclei. Empirical equations were obtained to predict the [(n,np) + (n,pn) + (n,d)] cross sections for target nuclei of the lightest stable isotopes of even-Z elements.

From the statistical model with the constant nuclear temperature approximation for level densities and other approximations, equations were derived in the present work to calculate (n,2n), (n,np), (n,pn), (n,p), (n,α), and (n,d) cross sections. The predictions from these equations generally give better agreement with experiment compared with other predictions for all (n,2n), (n,p), and (n,α) cross sections measured in the present work. In all the calculations an average nuclear temperature of 1.5 Mev taken to be constant for all types of 14 Mev neutron reactions and for all nuclei as suggested by Cuzzocrea et al. was used. No normalization procedure is involved in the present calculations. However, when neutron emissions following a first particle emission are involved, effective thresholds obtained by adding to ground state thresholds 0.5 Mev and 1 Mev, respectively, for the second and third neutron emissions appeared necessary to get good agreement with experiment. The agreements with experiment are generally within about ±15%, ±20%, and ±30%, respectively, for (n,2n), (n,p), and (n,α) cross sections measured in the present work.

For the [(n,np) + (n,pn) + (n,d)] cross sections the calculated value agrees with the measured cross section for Ni^{58} which is known from the angular and energy distribution measurements of Glover and Weigold to go mainly through compound nucleus formation. For the cases of Ru^{96}, Cd^{106}, and Sn^{112} the calculated values are far too small compared with measured cross sections suggesting that they likely go by some kind of direct interactions.

No odd-even effects in Z and no shell effects at Z = 28, 50, and at N = 50, 82 were observed in (n,2n) cross sections. Moreover, no shell effects for proton shell closures at Z = 28 and 50 in (n,p) cross sections were seen. For (n,α) reactions the cross sections of Mo^{92} and Ba^{138}, which have neutron shell closures at N = 50 and 82, respectively, appeared to be greatly enhanced. However, the enhancement may also be due to direct interactions.

CHAPTER I

INTRODUCTION

As neutron activation cross section data at 14-15 Mev for (n,2n), (n,p), and (n,α) reactions accumulated over the years since 1953, systematic studies revealed some general trends for the measured cross sections; and empirical or semi-empirical calculational methods were developed to predict cross sections at one neutron energy as well as excitation functions. The compound-nucleus statistical model with various approximations is widely used. Since the existing experimental cross section data were obtained by various workers using different experimental methods and somewhat different neutron energies between 14 and 15 Mev and have relatively large errors and often exhibit gross disagreements, each method had some success, although there are wide variations in the predictions from the various methods. There is also considerable controversy about shell structure effects on cross sections.

The purpose of the present research is to test various predictions for (n,2n), $\left[(n,np) + (n,pn) + (n,d)\right]$, (n,p), and (n,$\alpha$) cross sections at 14.4 Mev by comparing the predicted values with values measured under uniform experimental conditions with much improved accuracy and to search for possible shell structure effects on neutron activation cross sections. The medium Z region is selected because: (1) in this region there are a number of isotopes of each element whose (n,2n) products are radioactive, offering good possibilities for accurate measurement by means of gamma detection; (2) there are a number of (n,p) reactions for which

controversial predictions exist; (3) a search for shell effects can be made since this region includes the proton shell closure at Z = 50 and the neutron closures at N = 50 and 82. The single nucleus Ni^{58} is especially interesting because of its proton shell closure at Z = 28 and its large [(n,np) + (n,pn) + (n,d)] and (n,p) and small (n,2n) cross sections.

In nuclear engineering precise neutron cross sections are usually needed and the present work will provide some more neutron cross sections for that purpose. Also, from the measured cross sections some empirical or semi-empirical relationships may be set up which will enable one to predict cross sections for those isotopes that are inaccessible to experimental determination. In the statistical model calculation of cross sections different results are usually obtained from different approximations on nuclear level density and from different choices of values of parameters involved such as the level density parameter. Therefore, accurately measured cross sections are needed to test the applicability of the statistical model to various types of reactions induced by 14.4 Mev neutrons.

In the present research cross sections were measured using the mixed powder method with Ge(Li) gamma detection first developed by Rao and Fink.[1] This method generally gives results of much improved accuracy. Many of the cross sections were measured for the first time in the present work. Details in experiments and prime discussions are given in the following sections.

CHAPTER II

EXPERIMENTAL METHODS

2.1. Basic Equations for the Calculation of Cross Sections

In the present investigation there are many cases in which the measured activities arise from two sources, as is usually the case when the daughter activity of the reaction product is measured. To derive the equations for the calculation of cross sections, the following reaction-decay sequence is considered:

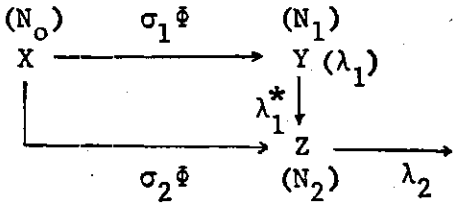

where X is the target nucleus; Y and Z are reaction products which are both assumed to be radioactive with decay constants λ_1 and λ_2, respectively; λ_1^* is the partial decay constant of Y leading to Z; σ_1 and σ_2 are the cross sections of the corresponding reactions; and Φ is the neutron flux.

During the irradiation, the production rates of Y and Z are, respectively,

$$\frac{dN_1}{dt} = N_o\sigma_1\Phi - \lambda_1 N_1 \qquad (2\text{-}1)$$

and

$$\frac{dN_2}{dt} = N_o\sigma_2\Phi + \lambda_1^* N_1 - \lambda_2 N_2 \qquad (2\text{-}2)$$

where N_o, N_1, and N_2 are, respectively, the number of nuclides of X, Y, and Z present at time t. Since the products $\sigma_1\Phi$ and $\sigma_2\Phi$ are very small for all cases in the present investigation, i.e. of the order of 10^{-14} sec^{-1}, the decrease in the number of the target nuclei N_o during the irradiation is neglected. In terms of activities defined by

$$A_i = \lambda_i N_i \qquad (i = 1,2) \qquad (2\text{-}3)$$

equations (2-1) and (2-2), respectively, can be converted to

$$\frac{dA_1}{dt} = \lambda_1 N_o \sigma_1 \Phi - \lambda_1 A_1 \qquad (2\text{-}4)$$

and

$$\frac{dA_2}{dt} = \lambda_2 N_o \sigma_2 \Phi + \lambda_2 A_1^* - \lambda_2 A_2 \qquad (2\text{-}5)$$

where

$$A_1^* = \lambda_1^* N_1 \qquad (2\text{-}6)$$

For short irradiations the neutron flux can be kept constant, but when the irradiation time is long it decreases approximately exponentially with half-lives ranging from 30 minutes to several hours, i.e.

$$\Phi = \Phi_o e^{-\Delta t} \qquad (2\text{-}7)$$

where Δ is the average decay constant of the neutron flux. Since Δ varies from one irradiation to another, it must be determined for every irradiation.

Substituting equation (2-7) into equations (2-4) and (2-5) for Φ and solving for A_1 and A_2 the results are

$$A_1 = N_o\sigma_1\Phi_o \frac{\lambda_1}{\lambda_1 - \Delta}(e^{-\Delta t} - e^{-\lambda_1 t}) \tag{2-8}$$

and

$$A_2 = N_o\Phi_o(\sigma_2 + \frac{\lambda_1^*}{\lambda_1 - \Delta}\sigma_1)\frac{\lambda_2}{\lambda_2 - \Delta}(e^{-\Delta t} - e^{-\lambda_2 t}) - N_o\sigma_1\Phi_o\frac{\lambda_1^*}{\lambda_1 - \Delta}\frac{\lambda_2}{\lambda_1 - \lambda_2}(e^{-\lambda_2 t} - e^{-\lambda_1 t}) \tag{2-9}$$

where the boundary conditions are

$$A_1 = A_2 = 0 \qquad \text{at} \qquad t = 0 .$$

At the end of the irradiation

$$t = T \qquad A_1 = A_1^o \qquad \text{and} \qquad A_2 = A_2^o$$

Then equations (2-8) and (2-9), respectively, become

$$A_1^o = N_o\sigma_1\Phi_o g_1 \tag{2-10}$$

and

$$A_2^o = N_o\Phi_o g_2\left[\sigma_2 + \frac{\lambda_1^*}{\lambda_1 - \lambda_2}(1 - \frac{\lambda_2 g_1}{\lambda_1 g_2})\sigma_1\right] \tag{2-11}$$

where

$$g_i = \frac{\lambda_i}{\lambda_i - \Delta} (e^{-\Delta T} - e^{-\lambda_i T}) \qquad i = 1,2; \tag{2-12}$$

At time t after the end of the irradiation, the time derivatives of A_1 and A_2 are, respectively, given by

$$\frac{dA_1}{dt} = - \lambda_1 A_1 \tag{2-13}$$

and

$$\frac{dA_2}{dt} = \lambda_2 A_1^* - \lambda_2 A_2 \tag{2-14}$$

Letting

$$k = \lambda_1^*/\lambda_1 = A_1^*/A_1 \tag{2-15}$$

Equations (2-13) and (2-14) are, respectively, integrated to give

$$A_1 = A_1^o \, e^{-\lambda_1 t} \tag{2-16}$$

and

$$A_2 = A_2^o \, e^{-\lambda_2 t} + \frac{k\lambda_2}{\lambda_1 - \lambda_2} A_1^o (e^{-\lambda_2 t} - e^{-\lambda_1 t}) \tag{2-17}$$

where the time t is measured from the end of the irradiation.

For simplicity a composite activity A^o_{cps} at zero time is defined by

$$A^o_{cps} = A_2^o + \frac{k\lambda_2}{\lambda_1 - \lambda_2} A_1^o \tag{2-18}$$

and equation (2-17) is then rewritten as

$$A_2 = A^o_{cps}\, e^{-\lambda_2 t} - \frac{k\lambda_2}{\lambda_1 - \lambda_2} A^o_1\, e^{-\lambda_1 t} \qquad (2\text{-}19)$$

The counting rates C_1 and C_2 corresponding, respectively, to A_1 and A_2 can be written as

$$C_1 = A^o_1 p_1\, e^{-\lambda_1 t} \qquad (2\text{-}20)$$

and

$$C_2 = A^o_{cps} p_2\, e^{-\lambda_2 t} - \frac{k\lambda_2}{\lambda_1 - \lambda_2} A^o_1 p_2 e^{-\lambda_1 t} \qquad (2\text{-}21)$$

where

$$p_i = C_i/A_i = \epsilon_i f_{di} f_{si} \qquad (i = 1,2) \qquad (2\text{-}22)$$

in which ϵ, f_d, and f_s are, respectively, detection efficiency, number of gammas per decay, and self-absorption correction factor. The determination of ϵ, f_d, and f_s is given in Section 2.4.

It is seen that if $\lambda_1 > \lambda_2$, the second term in equation (2-21) tends to zero when t is sufficiently large; while the first term will tend to zero if $\lambda_1 < \lambda_2$. Therefore, either A^o_{cps} or A^o_1 can be determined by measuring the counting rate C_2 after one of the two activities has died off. It is also possible that both A^o_{cps} and A^o_1 are determined simultaneously if several values of C_2 can be measured at various times before the short-lived activity dies off. For cases where $\lambda_1 > \lambda_2$, equation (2-21) may be multiplied by $e^{\lambda_2 t}$ on both sides to give

$$C_2 e^{\lambda_2 t} = A^o_{cps} p_2 - \frac{k\lambda_2}{\lambda_1 - \lambda_2} A^o_1 p_2 e^{-(\lambda_1 - \lambda_2) t} \tag{2-23}$$

which is a linear equation of the form

$$y = B - Mx \tag{2-24}$$

with

$$y = C_2 e^{\lambda_2 t} \tag{2-25}$$

$$B = A^o_{cps} p_2 \tag{2-26}$$

$$M = \frac{k\lambda_2}{\lambda_1 - \lambda_2} A^o_1 p_2 \tag{2-27}$$

and

$$x = e^{-(\lambda_1 - \lambda_2) t} \tag{2-28}$$

Therefore if several values of C_2 can be measured at various times before x becomes small, both A^o_{cps} and A^o_1 can be determined either by least squares fitting to equation (2-23) or by solving two simultaneous equations similar to equation (2-23).

If a composite cross section is defined by

$$\sigma_{cps} = \sigma_2 + \frac{\lambda_1^*}{\lambda_1 - \lambda_2} \sigma_1 \tag{2-29}$$

then from equations (2-10), (2-11), and (2-18) it can be shown that

$$A^o_{cps} = N_o \sigma_{cps} \Phi_o g_2 \tag{2-30}$$

which is similar to equation (2-10). In general the activity and the cross section are related by

$$A^o = N_o \sigma \Phi_o g \tag{2-31}$$

In the present investigation no absolute measurement of the neutron flux was made. Instead, a standard reaction with known cross section was used to eliminate Φ_o. The equation for the calculation of the cross sections thus becomes

$$\sigma = (A_x^o/A_s^o)(N_{os}/N_{ox})(g_s/g_x) \qquad (2\text{-}32)$$

where the subscripts s and x, respectively, denote the standard reaction and the reaction under investigation. The values of the g's are calculated from equation (2-12). The N_o's are calculated from the equation

$$N_o = \frac{W}{M} a\, N_{avo} \qquad (2\text{-}33)$$

where W is the weight of the element in the sample, M, its atomic weight, a, the isotopic abundance of a given isotope, and N_{avo}, Avogadro's number.

For most of the cases, in which the measured activity arises from the product of a single reaction, the cross sections are calculated from equation (2-32) and the related equations. For cases, in which the product nucleus has an isomeric state which decays partially or completely by an isomeric transition to the ground state with a half-life shorter than that of the ground state, the cross section corresponding to the isomeric state and the composite cross section corresponding to both states are determined separately. The isomeric cross section is determined by measuring the gamma decay of the isomeric state; and the composite cross section, by measuring the gamma activity of the ground state after the isomeric state has decayed completely. The ground state cross section is then obtained from

$$\sigma_g = \sigma_{cps} - \frac{\lambda_m^*}{\lambda_m - \lambda_g} \sigma_m \qquad (2\text{-}34)$$

where the subscripts m and g, respectively, denote the isomeric and the ground states. In the present work the half-life of the isomeric state is usually very short compared with that of the ground state so that the composite cross section amounts to practically the total cross section of the reaction if the isomeric state decays completely by isomeric transition to the ground state. Some special cases are discussed individually in Section 3.1.

2.2. Neutron Sources

Neutrons were produced by the $H^3(d,n)He^4$ reaction in the Georgia Tech 200-kV accelerator. A thick titanium-tritium target (1-inch diameter) of composition Ti/T $\approx$ 1 having about 7 mg/cm^2 Ti on 0.010-inch copper backing was used for the production of neutrons. The target was cooled by flowing water behind it, and is situated at 45° to the deuteron beam. At 90° and 100-cm above the target, a Si(Au) detector was used to count $\approx$ 3.7 Mev alpha particles from the $T(d,n)He^4$ reaction. The total neutron output can then be determined from the counting rate of the associated alpha particles.[2] The total neutron yields thus measured were in the range of 1-3 x 10^{10}n/sec, which decreased with the irradiation time. In the present work, the associated alpha particles are not used to determine the absolute neutron flux received by the sample target, because the sample target is placed very close to the neutron source target so that the solid angle subtended by the sample target cannot be calculated accurately. Figure 1 shows the geometry of the target system schematically.

To monitor the decrease of the neutron flux, the associated alpha

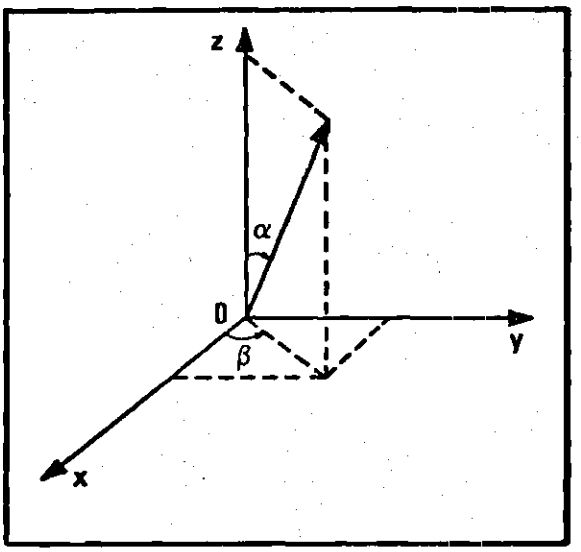

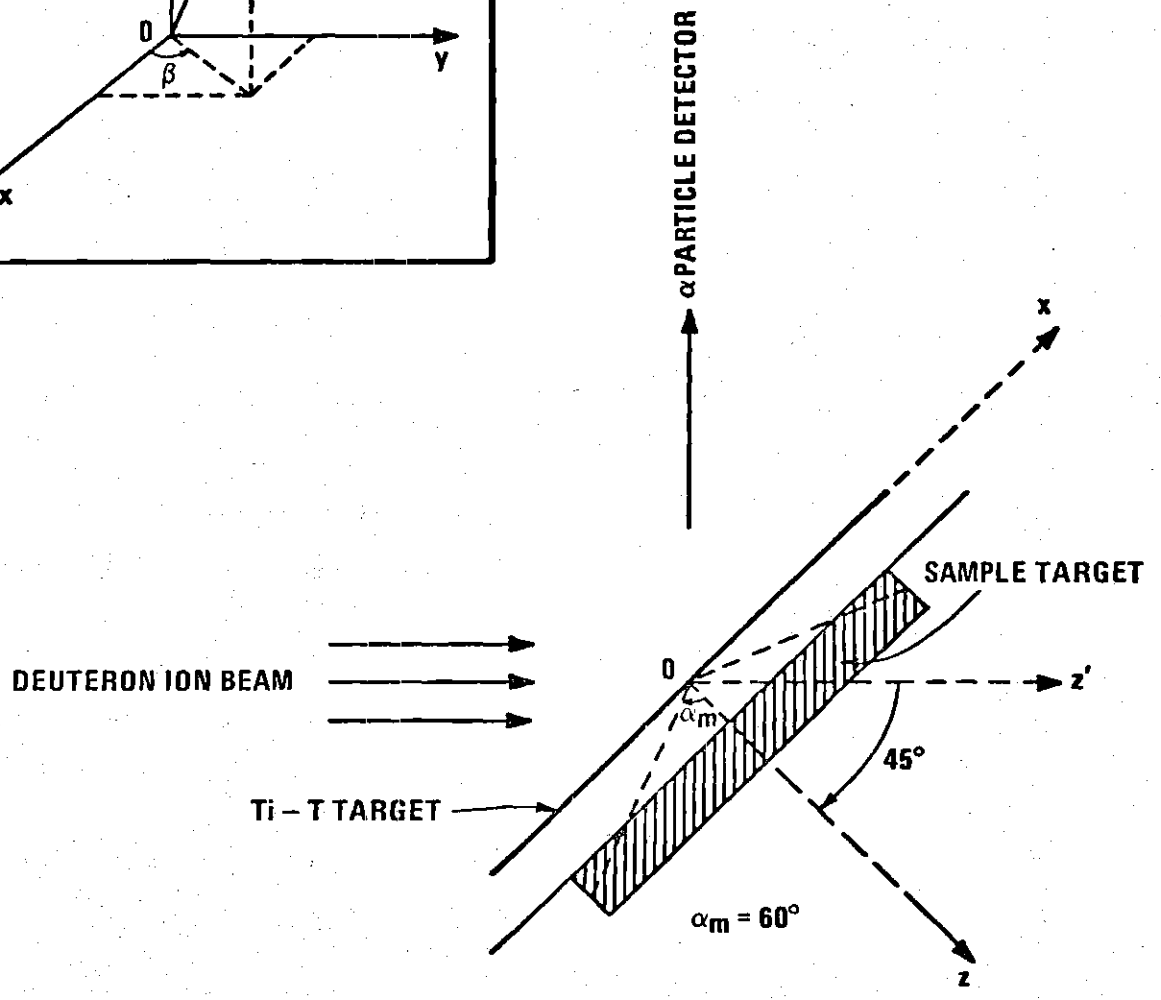

Figure 1 Geometry of the Target System

particles were counted at successive time intervals during the irradiation. The average decay constant Δ of the neutron flux in equation (2-7) was determined by fitting the counting rates into an exponential function.

The average energy of the neutrons received by the sample target was estimated by averaging over the solid angle subtended by the sample target, i.e.

$$\bar{E}_n = \frac{\int_o^{\alpha_m} \sin\alpha\, d\alpha \int_o^{2\pi} [n_1(\alpha,\beta)E_1(\alpha,\beta) + n_2(\alpha,\beta)E_2(\alpha,\beta)]d\beta}{\int_o^{\alpha_m} \sin\alpha\, d\alpha \int_o^{2\pi} [n_1(\alpha,\beta) + n_2(\alpha,\beta)]\, d\beta} \qquad (2\text{-}35)$$

where α, β are spherical polar angles as shown in Figure 1; $n_1(\alpha,\beta)$ and $n_2(\alpha,\beta)$ are the number of neutrons per unit solid angle emitted in the direction (α,β) for 100keV and 200keV deuterons, respectively; $E_1(\alpha,\beta)$ and $E_2(\alpha,\beta)$ are the corresponding neutron energies at (α,β) and α_m is the maximum half angle subtended by the sample target as shown in Figure 1. For a thick Ti-T target, the neutron yield is not isotropic. However, its variation with emission angle is small for deuteron energies smaller than 200 keV.[3] Therefore $n_1(\alpha,\beta)$ and $n_2(\alpha,\beta)$ are approximately constant. The deuteron ion beam is thought to consist mainly of D_2^+ and D^+. The ratio D_2^+/D^+ may vary considerably from run to run (i.e. from 3 to 1), depending on ion source operating conditions. However, the variation of D_2^+/D^+ does not affect the neutron energy spread significantly because the maximum deuteron energy (200keV) is small compared with the Q-value of 17.6 Mev for the $H^3(d,n)He^4$ reaction (the average energy of the neutrons received by the sample target changes only slightly, i.e. from 14.42 to 14.39 Mev as the ratio D_2^+/D^+ varies from 1 to 3). The

neutron yield of 200-keV deuterons is about 3 times larger than that of 100-keV deuterons.[3] With $D_2^+/D^+ = 2$ it can be shown that

$$n_1(\alpha,\beta) = 0.57n_o \quad \text{and} \quad n_2(\alpha,\beta) = 0.43n_o \tag{2-36}$$

where n_o is the total number of neutrons per unit solid angle produced by the deuteron ion beam.

Since the energy of the emitted neutrons is known as a function of the angle θ between the emitted neutrons and the deuteron beam,[3] the angle θ for each set of (α,β) must be determined in order to get $E_1(\alpha,\beta)$ and $E_2(\alpha,\beta)$. The relationship between α, β and θ is given by

$$\cos\theta = \frac{1}{\sqrt{2}}(\sin\alpha\cos\beta + \cos\alpha) \tag{2-37}$$

Since there are no simple analytical functions for $E_1(\alpha,\beta)$ and $E_2(\alpha,\beta)$, the integration of equation (2-35) was carried out by a numerical method. With $\alpha_m = 60^o$, which is mostly the case in the present work, the average neutron energy was found to be 14.4 Mev with maximum and minimum energies at 14.8 and 13.9 Mev, respectively. The neutron spectrum estimated by grouping the neutrons in an energy interval of 100 keV is shown in Figure 2. It is seen that more than 90% of the neutrons received by the sample target have energies within 14.4 ± 0.4 Mev. The poor neutron energy resolution is a consequence of the geometry of the target system and the large size of the sample target. The geometry was chosen to facilitate the construction of a Si(Au) detector in the direction of 90^o to the deuteron beam. The detector is necessary to count the associated alpha particles from which the average decay constant of the neutron flux

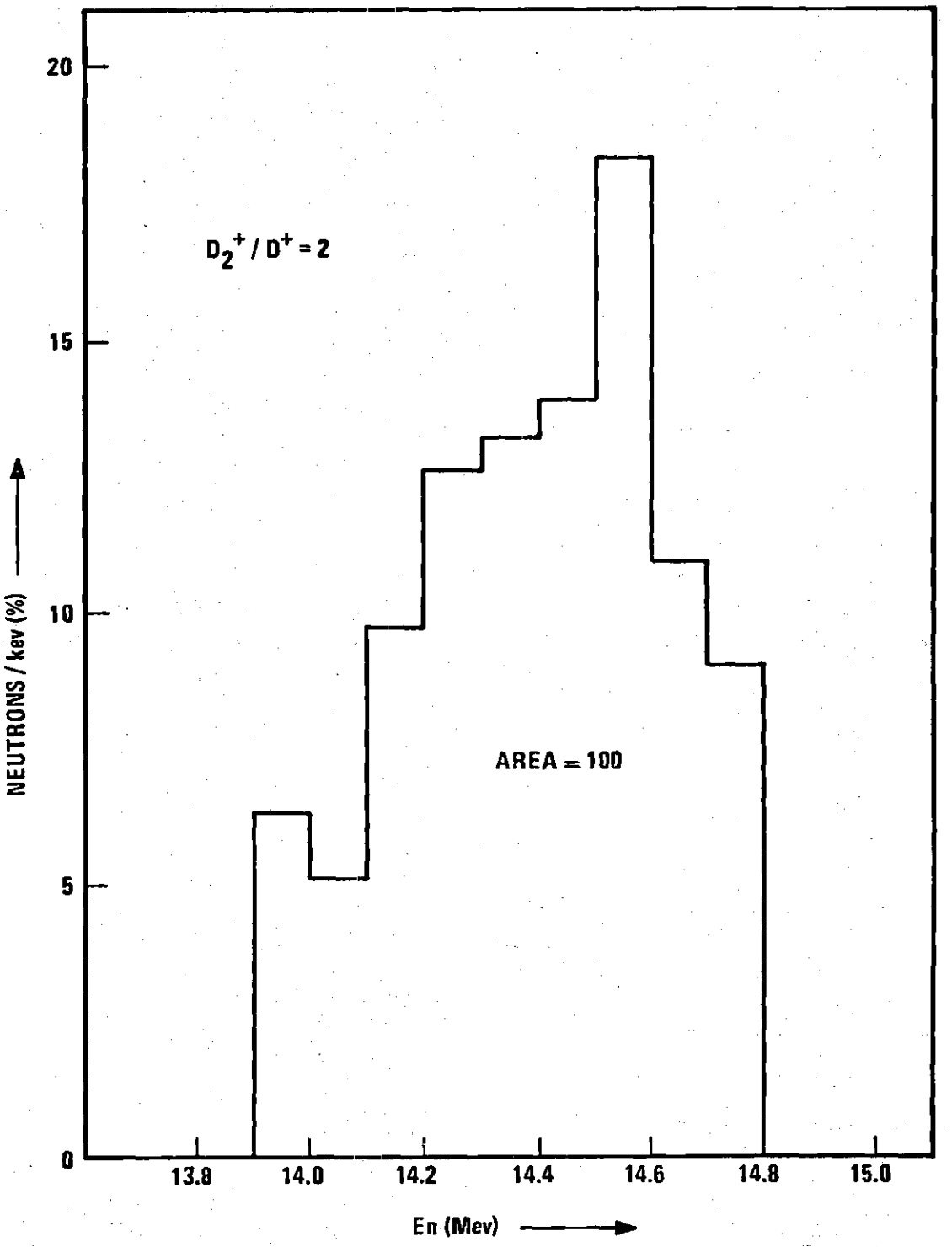

Figure 2 Neutron Spectrum Received by a Sample Target which Subtends an Angle of 120° at the Center of the Ti–T Target

can be estimated. The large sample target is necessary to get sufficiently strong product activities.

2.3. Irradiations and Radiochemical Procedures

To prepare the sample for irradiation, several grams of the sample material in powder form were mixed with iron and aluminum powders in an agate mortar. The mixture was then packed in a lucite holder with a hole of 1.5 to 1.8 cm in diameter and 3 to 6 mm thickness. The aluminum served to check the uniformity of the mixture, by comparing the measured cross section ratio of the $Al^{27}(n,\alpha)Na^{24}$ to the $Fe^{56}(n,p)Mn^{56}$ reaction to the known value of 1.14 ± 0.08 (see Section 3.2), since the uniformity of the mixture is essential to getting accurate results.[1,4,5] The weight of each component of the sample was determined to $\pm$ 1 mg. All the sample components, either in elemental form or in a chemical compound, had natural isotopic composition. The isotopic abundances needed in calculating the N_o's in equation (2-33) were taken from the Table of Isotopes edited by C. M. Lederer, et al.[6]

The sample target was placed about 3 mm behind the Ti-T neutron source for irradiation. The irradiation time varied from 30 seconds to 2 hours, depending on the half-life of the product activity of interest. For cases of very short-lived activities, a fast transfer rabbit system was used. This system can transfer a sample from the irradiation position to the detection position in less than one second. After irradiation the target was immediately brought to the detection position for gamma counting without further treatment, except in one case that needed radiochemical separation of Ag from Cd.

In the separation of Ag from Cd, about 3 grams of irradiated Cd was dissolved in 8 ml conc. HNO_3 and about 200 mg of Ag^+ carrier in 2 ml $AgNO_3$ solution was added. AgCl was then precipitated with conc. HCl. After filtration, the filtrate containing the Cd was evaporated to dryness and mounted in a lucite holder for gamma counting. The AgCl precipitate was washed with 0.1 N HCl several times to remove the contaminated Cd and then dissolved again with conc. NH_4OH. AgCl was reprecipitated with HCl, centrifuged, and then mounted on an aluminum planchet under an infrared lamp. After the AgCl was dried, the planchet was covered with Scotch® tape and gamma counted. No chemical yield determination was needed.

2.4. Detection of the Product Activities

After the end of irradiation, the gamma activities of the sample target were measured with a 16-cm^3 coaxial Ge(Li) detector having a resolution of 3.6-keV FWHM (full width at half maximum) at 1333 keV at < 1000 counts/sec. The detection efficiencies for various gamma energies were calibrated with standard essentially point sources supplied by the International Atomic Energy Agency (IAEA), Vienna. A typical calibration curve is shown in Figure 3. In the determination of the curve, the sources were placed about 4 mm from the detector window along the axis in essentially the same position in which the activities of the irradiated target were measured. The circular points in the figure were measured absolutely, while the triangular points were measured relatively. The normalization points are indicated by squares in the figure. The standard sources used, together with their half-lives, gamma energies, and intensities are summarized in Table 1. From the figure it is seen that a Log-Log plot

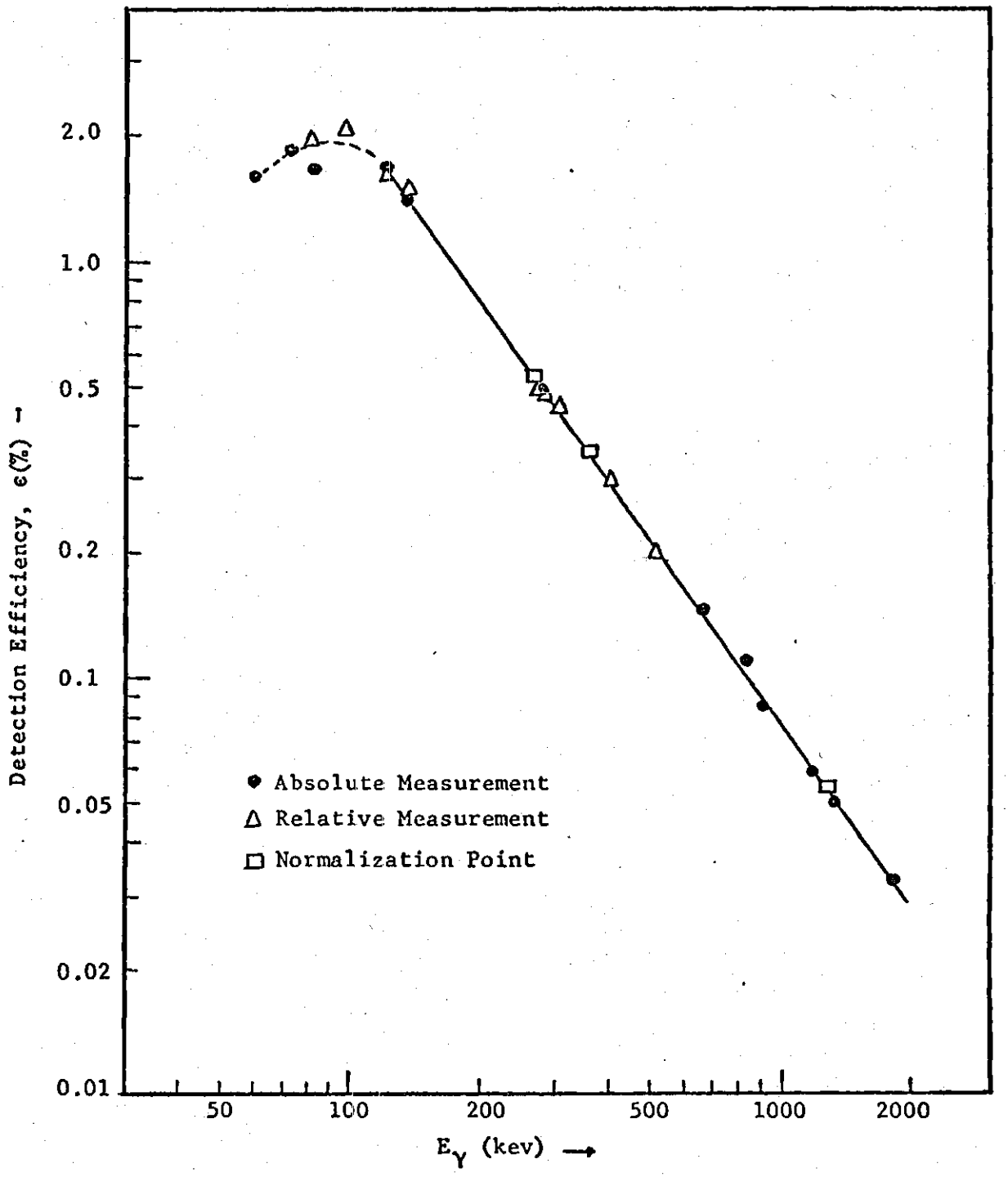

Figure 3. Detection Efficiency of 16 cm^3 Coaxial Ge(Li) Detector.

Table 1. Calibration Sources for Gamma Activities[a]

Sources	Half-life	E(keV)	Gammas per Disintegration (%)	
Am^{241}	432.9 yr	59.5	35.9	
Hg^{203}	46.6 day	72.9	9.7	
		82.5	2.8	
		279.2	81.6	
Co^{57}	271.6 day	122.0	85.0	
		136.3	11.4	
Na^{24}	2.602 yr	511.0	179.7	
		1274.6	99.95	
Cs^{137}	30.6 yr	661.6	85.1	
Mn^{54}	312.6 day	834.6	100.0	
Co^{60}	5.264 yr	1173.2	99.74	
		1332.5	99.85	
Y^{88}	107.4 day	898.0	91.4	
		1836.1	99.4	
Se^{75}	120.4 day	96.7	5.33	(b)
		121.1	27.8	
		136.0	94.9	
		264.6	100	
		279.6	43.0	
		400.1	22.3	
Ba^{133}	10.66 yr	80.9	58.2	(c)
		276.5	11.8	
		302.8	29.8	
		355.9	100	

(a) All values, unless otherwise stated, are taken from the calibration certificates by IAEA with the standard sources.

(b) P. Venugopala Rao and R. W. Fink, Nucl. Phys. 81, 296 (1966).

(c) H. E. Bosch and A. J. Haverfield, Nucl. Phys. A108, 209 (1968).

of detection efficiency vs. energy gives a straight line for gammas of energy greater than about 120 keV. Below 120 keV, absorption in the aluminum window becomes increasingly serious and causes the curve to turn down. The solid line is a least squares fitting which can be represented empirically by

$$\epsilon = 1820 E_{\gamma}^{-1.46} \tag{2-38}$$

where ϵ is in percent and E_{γ} in keV.

The gamma spectra of irradiated targets were recorded with a 400-channel analyzer successively at various time intervals after the end of irradiation. For short lived activities the target was brought to the detection position by a fast transfer rabbit system and its gamma spectra were recorded in a magnetic digital tape recorder. The recorder can record a 400-channel spectrum in 4 seconds and store up to 36 spectra on the tape cartridge. The spectra were later printed out with a fast Franklin printer which can print 40 digits/sec. From these spectra, the half-lives and energies of various gammas in the spectrum were determined simultaneously. The activities were then identified by both the half-life and the gamma energy.

The counting rate of a given gamma at a particular energy is obtained from the peak area less the background, which is estimated from the spectrum graphically. The average counting rate corrected to the end of the irradiation is given by

$$\overline{C^{o}} = \frac{1}{n} \sum_{i=1}^{n} C_i e^{\lambda t_i} \tag{2-39}$$

where the n is the number of the counting rates measured for a given gamma and C_i, the i^{th} counting rate at time t_i which is the middle point of the i^{th} counting period between t_{ia} and t_{ib} both measured from the end of irradiation. The zero time activity A^o is then calculated from the equation

$$A^o = \frac{C^o}{\epsilon f_d f_s} \tag{2-40}$$

where ϵ is the overall detection efficiency of the given gamma activity obtained from the calibration curve (Figure 3) or from equation (2-38), f_d, the number of gammas per decay of the nuclide from its decay scheme, and f_s, the correction factor for the self-absorption in the target. The f_s is calculated from

$$f_s = \frac{1 - e^{-(\mu/\rho)(\rho x)}}{(\mu/\rho)(\rho x)} \tag{2-41}$$

where (μ/ρ) is the mass absorption coefficient of the target material taken from Davisson's tables,[7] and (ρx), the thickness of the target in mg/cm^2. In the cases that the target is a mixture of several components, which is mostly the case in the present investigation, a weighted average of the component mass absorption coefficients, $(\mu/\rho)_{av}$, is substituted for (μ/ρ) in equation (2-41). The $(\mu/\rho)_{av}$ is given by

$$(\mu/\rho)_{av} = \sum_{i=1}^{n} (\mu/\rho)_i w_i \tag{2-42}$$

where $(\mu/\rho)_i$ is the mass absorption coefficient of the i^{th} component, w_i, the weight percentage of the component, and n, the number of components in the target.

It should be noticed that the zero time activity A^o so obtained is not the absolute disintegration rate; rather, it is a relative activity, because the standard sources used in the determination of the calibration curve are essentially point sources, whereas the sample target sources are not. Moreover, the geometrical position of the standard sources and that of the sample sources are not exactly the same. However, only the ratio of the activities is needed in the calculation of cross sections as is shown in equation (2-32). Therefore no absolute disintegration rate is necessary.

CHAPTER III

RESULTS AND ERRORS

3.1. Evaluation of Cross Sections

All the cross sections determined are either directly or indirectly relative to the cross section of the standard reaction

$$Fe^{56}(n,p)Mn^{56} \quad (2.57\ hr) \qquad \sigma = 100 \pm 6\ mb^{(8)}$$

Other standard reactions include

$$Al^{27}(n,\alpha)Na^{24} \quad (15\ hr) \qquad \sigma = 114 \pm 6\ mb^{(9)}$$

and

$$Si^{28}(n,p)Al^{28} \quad (2.238\ min) \qquad \sigma = 252 \pm 15\ mb^{(10)}$$

The parameters used in these reactions are listed in Table 2.

The cross sections determined are summarized in Tables 3 through 6. In these tables the half-lives, the gamma energies, and the f_d values of the gamma rays counted are all included.

Some special cases which need further discussion individually are given below.

3.1.1. $Ru^{96}[(n,np) + (n,pn) + (n,d)]Tc^{95g}(20\ hr)$

In this reaction the product nucleus, Tc^{95g}, is also the daughter of Ru^{95}, which is the (n,2n) reaction product. Therefore, the 20 hr gamma activity of Tc^{95g} measured arises from two sources. The situation is similar to the cases in which an isomeric state is involved in the reaction

Table 2. Parameters for Standard Reactions*

Reaction	Half-life	E (keV)	f_d	Cross Section (mb)
$Fe^{56}(n,p)Mn^{56}$	2.576 hr	847	0.987	100 ± 6 [8]
$Al^{27}(n,\alpha)Na^{24}$	15 hr	1369	1.0	114 ± 6 [9]
$Si^{28}(n,p)Al^{28}$	2.238 min	1780	1.0	252 ± 15 [10]

*All the values, unless otherwise stated, are taken from Reference 6. f_d is the number of gammas per decay.

product, i.e. the cross sections for the (n,2n) and (n,np) + ...reactions correspond respectively to the isomeric and ground state cross sections. Therefore, the cross section of the (n,np) +... reaction can be similarly determined. From the gamma activity of 1.65 hr Ru^{95} the (n,2n) cross section is determined to be

$$\sigma_{2n} = 569 \pm 30 \text{ mb} \tag{3-1}$$

After the activity of 1.65 hr Ru^{95} has died off, the measured 20 hr gamma activity of Tc^{95g} gives the composite cross section of the (n,2n) and (n,np) +... reactions

$$\sigma_{cps} = \sigma_{np} + \frac{\lambda^*_{2n}}{\lambda_{2n}-\lambda_{np}} \sigma_{2n} = 847 \pm 60 \text{ mb} \tag{3-2}$$

In equations (3-1) and (3-2) the subscripts 2n and np refer to the (n,2n) and (n,np) +... reactions, respectively. Substituting equation (3-1) into equation (3-2) for σ_{2n}, it is found that

$$\sigma_{np} = 227 \pm 70 \text{ mb} \tag{3-3}$$

However, the latter is obtained from the difference of two rather large values, and its accuracy is therefore very sensitive to the accuracies of both σ_{cps} and σ_{2n} values. Hence, a better method was used to check the accuracy of this result.

In the second method, the growth and decay of the 20 hr activity of Tc^{95g} was followed from the end of the irradiation. A least squares fitting of the counting rates to equation (2-23) gives (see Figure 4)

$$B = 577 \pm 14 \text{ cpm} \tag{3-4}$$

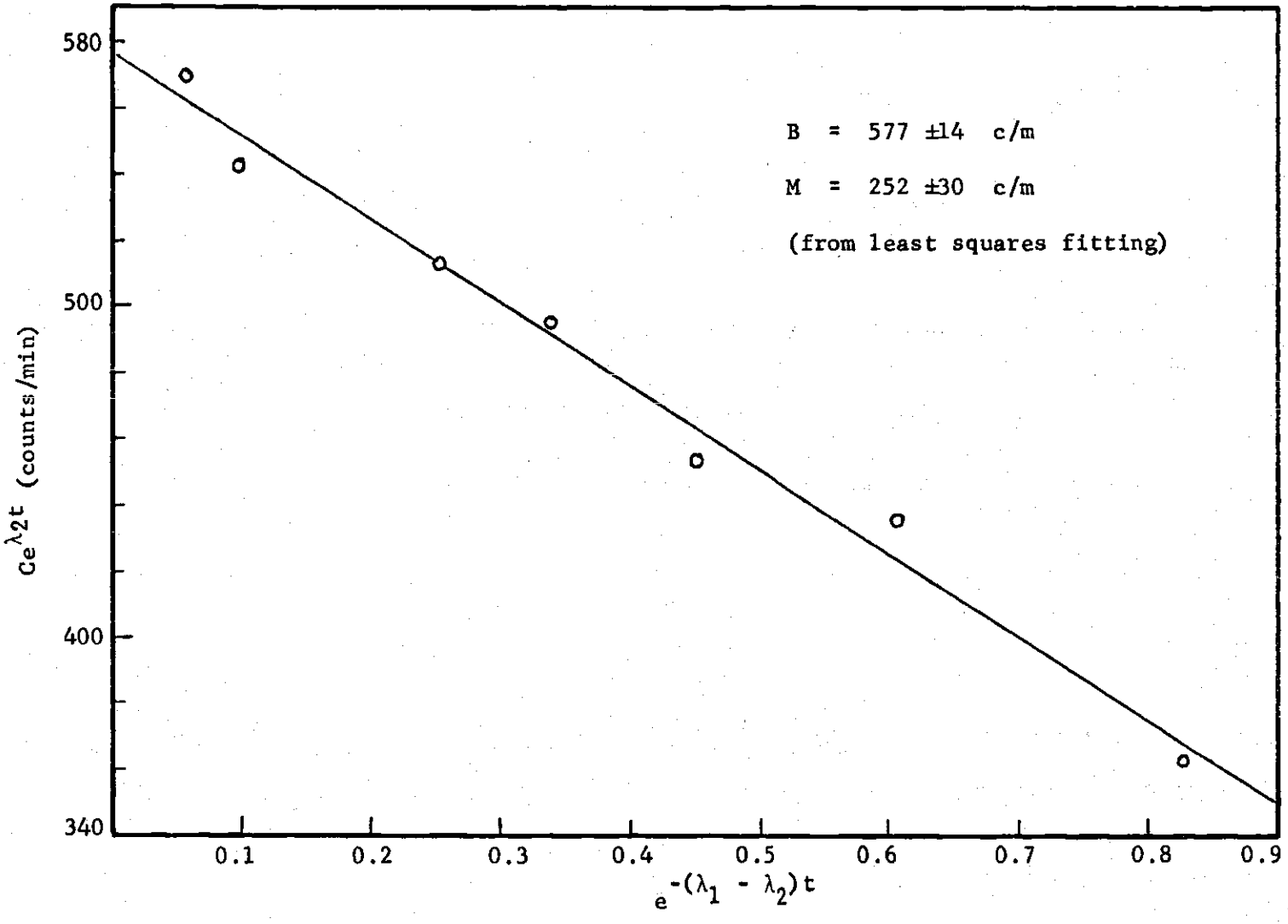

Figure 4. Resolution of the Components of the 768 kev Gamma Ray of the 20 hr Tc^{95g}.

and

$$M = 250 \pm 30 \text{ cpm} \tag{3-5}$$

From equations (2-26) and (2-27), together with the related equations, it is shown that the cross section ratio σ_{np}/σ_{2n} can be expressed by

$$\sigma_{np}/\sigma_{2n} = (B/M)(g_{2n}/g_{np}) \frac{k\lambda_{np}}{\lambda_{2n} - \lambda_{np}} - \frac{\lambda^*_{2n}}{\lambda_{2n} - \lambda_{np}} \tag{3-6}$$

where the subscripts 2n and np refer to (n,2n) and (n,np) +... reactions, respectively. When the numerical values were substituted into equation (3-6) it is found that

$$\sigma_{np}/\sigma_{2n} = 0.36 \pm 0.13^* \tag{3-7}$$

It should be noticed that the cross section ratio determined in this way is independent of the detection efficiency, the decay scheme of Tc^{95g}, and self-absorption, because the same activity is measured in the ratio and the parameters ϵ, f_d, and f_s cancel out. The large error is mainly due to counting statistics which can be improved by increasing the source strength or by a radiochemical separation of Tc from the target as was done in the Cd^{106} case discussed below.

---

* From the value previously reported by the author in Phys. Rev. C1 358 (1970), the quantity 0.46 should be subtracted for the term

$$\frac{\lambda^*_{2n}}{\lambda_{2n} - \lambda_{np}}\left(1 - \frac{\lambda_{np} g_{2n}}{\lambda_{2n} g_{np}}\right)$$

and the (n,np) +... cross section derived from the ratio given in that paper should be corrected accordingly to give 216 ± 50 mb.

From the (n,2n) cross section (equation (3-1)) measured from the activity of 1.65 hr Ru^{95} and the cross section ratio (equation (3-7)) from the activity of 20 hr Tc^{95g}, the cross section for the (n,np) +... reaction is found to be

$$\sigma_{np} = 205 \pm 75 \text{ mb} \tag{3-8}$$

The agreement between equation (3-3) and (3-8) is good. The weighted average* of these two values is

$$\sigma_{np} = 216 \pm 50 \text{ mb} \tag{3-9}$$

The cross section of the (n,2n) reaction can also be determined from the value of M in equation (3-5) and is found to be

$$\sigma_{2n} = 590 \pm 70 \text{ mb} \tag{3-10}$$

Also, from equations (3-2) and (3-7), it is found that

$$\sigma_{2n} = 572 \pm 50 \text{ mb} \tag{3-11}$$

Both of these values are in good agreement with the value 569 ± 30 mb which is determined from the activity of 1.65 hr Ru^{95}.

---

* The weighted average, $\bar{\sigma} \pm \bar{\delta}$, is defined by

$$\bar{\sigma} = \sum_{i=1}^{n} \frac{\sigma_i}{\delta_i^2} \Big/ \sum_{i=1}^{n} \frac{1}{\delta_i^2}$$

and

$$\bar{\delta} = 1 \Big/ \sqrt{\sum_{i=1}^{n} \frac{1}{\delta_i^2}}$$

where the δ's are percent errors.

3.1.2. $Cd^{106}(n,2n)Cd^{105}$(55 min) and $Cd^{106}(n,np)+...$ Ag^{105}(41.2 d)

Since the decay scheme of 55 min Cd^{105} is not sufficiently well known, the (n,2n) cross section of Cd^{106} cannot be determined directly from the activity of Cd^{105}. Therefore, the activity of the 41.2 d Ag^{105} was used to determine both the (n,2n) and the (n,np) +... cross sections. The method is similar to that described in Section 3.1.1. for the case of Ru^{96}. However, there is a difficulty in this case. Due to the long half-life of Ag^{105}(41.2 d) and the low isotopic abundance of Cd^{106}(1.22%) in natural Cd, the activity of Ag^{105} is not sufficiently strong to get several counting rates before the 55 min Cd^{105} dies off as required to resolve the measured Ag^{105} activity (see equation (2-23)). To overcome this difficulty, radiochemical separations of Ag^{105} from the irradiated target at various times were performed. The advantage of the separation is that the time scale in equation (2-23) is set by the time at which the Ag is separated, and the counting rate at that time can be obtained later by counting the separated sample. Thus, the sample can be counted for a longer period to improve the counting statistics. In addition, the Compton background of the separated sample is also reduced, because many of the unwanted activities are removed in the separation process. The reduction of the Compton background is important in this case, because the energy of the gamma activity of Ag^{105} measured is 281 keV which is lower than those of most of the gamma activities present in the target.

To avoid the necessity of determining the chemical yield of the separated sample, the 617 keV gamma of 3.14 hr Ag^{112} from the (n,p) reaction of Cd^{112} was used as an internal standard. With the value of 15.3 $\pm$ 1.3 mb for the $Cd^{112}(n,p)Ag^{112}$ reaction measured in the present

work, the composite cross section for both (n,2n) and (n,np) +... reaction of Cd^{106} is found to be

$$\sigma_{cps} = \sigma_{np} + \frac{\lambda^{*}_{2n}}{\lambda_{2n} - \lambda_{np}} \sigma_{2n} = 1190 \pm 105 \text{ mb} \qquad (3\text{-}12)$$

To determine the cross section ratio of the two reactions three separate runs with total of six Cd targets were made. The result is

$$\sigma_{np}/\sigma_{2n} = 0.220 \pm 0.023 \qquad (3\text{-}13)$$

The cross section ratio so determined is also independent of the detection efficiency and of the decay scheme of Ag^{105}. Since the separated samples were thin, the variation of the f_s values due to variations in the thickness of various samples was also negligible.

From the values in equations (3-12) and (3-13) it is found that

$$\sigma_{2n} = 975 \pm 86 \text{ mb} \qquad (3\text{-}14)$$

and

$$\sigma_{np} = 215 \pm 29 \text{ mb} \qquad (3\text{-}15)$$

The Ag^{105} activity in the Cd-fraction from which Ag has been separated arises entirely from the decay of Cd^{105}. Therefore, the (n,2n) cross section of Cd^{106} can also determined from the activity of Ag^{105} in the Cd-fraction. Using the Cd^{116} (n,2n) Cd^{115g} reaction as an internal standard, with σ = 820 ± 50 mb measured in the present work, the (n,2n) cross section of Cd^{106} was found to be 945 ± 85 mb which is in good agreement with the value in equation (3-14) obtained from the Ag^{105} activity in the Ag-fraction.

Recently, Hopke et al.[11] found a 7.23 min isomer in Ag^{105} which will affect the results obtained above if the isomer has branching to the levels of Pd^{105}. However, the branching was estimated to be only about 4%[11] and the effect on the cross sections obtained above is even smaller; therefore, no correction for the effect of branching from the 7.23 min Ag^{105m} isomer was made.

3.1.3. Sn^{112}((n,np) + (n,pn) + (n,d))In^{111} (2.8 d)

This cross section was also determined by the same method used in the case of Ru^{96}. From the 760 keV gamma ray of 35 min Sn^{111} the (n,2n) cross section was determined to be

$$\sigma_{2n} = 1100 \pm 80 \text{ mb} \tag{3-16}$$

The measurement of the 171 keV and 247 keV gammas of In^{111} after all Sn^{111} has decayed gives

$$\sigma_{cps} = \sigma_{np} + \frac{\lambda^*_{2n}}{\lambda_{2n} - \lambda_{np}} \sigma_{2n} = 1275 \pm 100 \text{ mb} \tag{3-17}$$

From these two values it is found that

$$\sigma_{np} = 175 \pm 128 \text{ mb} \tag{3-18}$$

To determine the latter value more accurately, the cross section ratio, σ_{np}/σ_{2n}, was determined by the same method used in the case of the Ru^{96}(n,np) +... reaction, and from three separate runs, the result was found to be

$$\sigma_{np}/\sigma_{2n} = 0.15 \pm 0.05 \tag{3-19}$$

From this ratio and the (n,2n) cross section in equation (3-16), the cross section of the Sn^{112} (n,np) +... In^{111} was found to be

$$\sigma_{np} = 165 \pm 66 \text{ mb} \quad (3\text{-}20)$$

The agreement of these two values is very good although the errors are large. The weighted average* of these two values is

$$\sigma_{np} = 168 \pm 59 \text{ mb} \quad (3\text{-}21)$$

From equations (3-17) and (3-19) the (n,2n) cross section is also found to be

$$\sigma_{2n} = 1110 \pm 100 \text{ mb} \quad (3\text{-}22)$$

The agreement of these two (n,2n) cross section values (equations (3-16) and (3-22)) is also very good.

3.1.4. Mo^{92} (n,2n) Mo^{91g} (15.5 min)

In this case there is no gamma transition in the decay of Mo^{92g}. The cross section ratio σ_g/σ_m was determined by following the decay of the positron annihilation radiation by use of a similar method to that described in Section 3.1.1. for the case of Ru^{96}. However, there is a modification required in that a term for the branching of Mo^{91m}, which also gives annihilation radiation, must be included in equation (2-23). The result is

$$\sigma_g/\sigma_m = 12.4 \pm 0.6 \quad (3\text{-}23)$$

---

* See footnote in Section 3.1.1., page 27.

The cross section for the metastable state was determined from the isomeric transition gamma ray to be

$$\sigma_m = 16.2 \pm 1.2 \text{ mb} \tag{3-24}$$

From these two values the ground state cross section is found to be

$$\sigma_g = 201 \pm 17 \text{ mb} \tag{3-25}$$

Generally, the detection efficiency for the positron annihilation radiation is not the same as that of the 511 keV gamma rays. Therefore, the positron annihilation radiation of Mo^{91g} is not used to determine the absolute cross section of the reaction. In the determination of the cross section ratio σ_g/σ_m in the present case the efficiency ratio of the positrons from Mo^{91m} to those from Mo^{91g} is taken as unity. Since these two groups of positrons have approximately the same maximum energy, the difference in the detection efficiencies for their annihilation radiations is expected to be negligible.

3.2. Errors in the Measured Cross Sections

In the present investigation, the mixed powders method first developed by Rao and Fink[1] was used. The advantages of this method were discussed by Fink.[4] The consistency of this method was confirmed by Rao[5] from a compilation of the $Fe^{56}(n,p)\ Mn^{56}$ to $Al^{27}(n,\alpha)\ Na^{25}$ cross section ratio made over a two year period by various investigators for many different cross section measurements. This procedure of intimately mixing of sample and standard materials eliminates the geometrical errors present in the procedure of sandwiching the sample between foils that act

as flux monitors, because the sample and standard materials are irradiated and counted together. This method gives more accurate results for cross section measurements, especially in cases where hard gammas are emitted.[1,4]

The errors quoted in the Tables 3 through 6 for the cross sections are root-mean-square errors and are comprised of the following:

(1) Errors in the photopeak efficiency of the detector. This represents the major error in the measurement. The standard sources used in the calibration of the detection efficiency curve are accurate to 1-2%[12] and the accuracy of the calibration curve is about 3%. The absolute detection efficiency for the sample sources may deviate from the calibration curve, because the size of the sample sources are much larger than the calibration standard sources which are essentially point sources. However, no serious departures in relative efficiencies were observed except at energies below 60 keV.[5] Since the ratio of two efficiencies is always involved in the calculation of the cross section, the error can be reduced by selection of a standard having a gamma ray with energy close to the one under investigation. In general this error is about 4% depending on the energy of the gamma ray measured.

(2) Statistical error. The error in counting statistics is in general small. Except for a few cases in which the gamma activities are weak, this error is about 1-2%.

(3) Error in the self-absorption correction. Thin samples were used whenever low energy gammas were involved to reduce the error in this correction. The error in f_s amounted to 1-2% at most, but is considerably lower than this for high-energy gamma rays.

(4) Error in weighing and mixing of the samples. Weighing errors

are negligible ($< 0.1\%$), but the error due to non-uniform mixing of the sample and standard powders can be considerable.[1,4,5] However, the non-uniform mixing becomes obvious from the measured activity ratio of Na^{24}/Mn^{56} from which the $Al^{27}(n,\alpha)Na^{24}$ to $Fe^{56}(n,p)Mn^{56}$ cross section ratio was derived, and runs in which the cross section ratio deviates from 1.14 ± 0.08 were repeated.

(5) Error in timing. For long irradiation and counting times the timing errors are negligible. When short-lived activites are involved, the irradiation and counting times were measured to 0.5 second. Spectra were generally taken with less than 20% dead-time in the analyzer. In general, timing errors were negligible.

The errors in the standard cross section and in f_d of the sample and standard activities are not included in the reported errors, because any revision in the decay schemes permits easy recalculation of the cross sections in the future, since the values of f_d used in the present work are given in the tables.

Table 3. (n,2n) Cross Sections at 14.4 ±0.4 Mev from the Present Work

Reaction	Half-Life	$E_{(kev)}$	f_d [a]	Measured Cross Section (mb) [b]
$Ni^{58}(n,2n)Ni^{57}$	36.0 hr	1370	0.86	38 ±5
$Zr^{90}(n,2n)Zr^{89m}$	4.19 min	588	0.87	79.5 ±5.6
$Zr^{90}(n,2n)\ Zr^{89g}$	78.4 hr	910	0.98	572 ±30
$Zr^{96}(n,2n)Zr^{95}$	65.5 d	724	0.431	1456 ±80
		756	0.555 [c]	
$Nb^{93}(n,2n)Nb^{92m}$	10.16 d	934	0.99	578 ±30
$Mo^{92}(n,2n)Mo^{91m}$	64 sec	658	0.54	16.2 ±1.2
$Mo^{92}(n,2n)Mo^{91g}$	15.49 min			201 ±17 [d]
$Ru^{96}(n,2n)Ru^{95}$	1.65 hr	340	0.75	569 ±30
$Mo^{100}(n,2n)Mo^{99}$	66.7 hr	740	0.12	1389 ±84
$Ru^{98}(n,2n)Ru^{97}$	2.88 d	215	0.91	1169 ±96
$Ru^{104}(n,2n)Ru^{103}$	39.5 d	497	0.88	1440 ±80
$Rh^{103}(n,2n)Rh^{102m}$	2.1 yr	698	0.422	435 ±35 [e]
		768	0.316	
		1050	0.316	
$Rh^{103}(n,2n)Rh^{102g}$	206 d	475	0.57	522 ±45
$Pd^{102}(n,2n)Pd^{101}$	8.4 hr	298	0.30	637 ±45
$Pd^{110}(n,2n)Pd^{109m}$	4.69 min	188	0.58	510 ±35
$Pd^{110}(n,2n)Pd^{109m+g}$	13.5 hr	88	0.036	1416 ±150
$Cd^{106}(n,2n)Cd^{105}$	55 min			975 ±86 [f]
$Cd^{108}(n,2n)Cd^{107}$	6.5 hr	93	0.049	865 ±100
$Cd^{110}(n,2n)Cd^{109}$	453 d	88	0.036	1221 ±150
$Cd^{112}(n,2n)Cd^{111m}$	48.6 min	247	0.94	725 ±50
$Cd^{111}(n,n')Cd^{111m}$				

Table 3 (Continued)

Reaction	Half-Life	$E_{(kev)}$	f_d [a]	Measured Cross Section (mb) [b]
$Cd^{116}(n,2n)Cd^{115m}$	43 d	934	0.02 [g]	569 ±60
$Cd^{116}(n,2n)Cd^{115g}$	2.23 d	528 335	0.275 0.45 [g]	820 ±50
$Sn^{112}(n,2n)Sn^{111}$	35 min	760	0.011	1100 ±100
$Sn^{114}(n,2n)Sn^{113}$	115 d	393	0.65	1239 ±130 [h]
$Sn^{118}(n,2n)Sn^{117m}$ $Sn^{117}(n,n')Sn^{117m}$	14 d	158	0.865	957 ±100
$Sb^{121}(n,2n)Sb^{120m}$	5.8 d	1030 1171	0.99 1.0	427 ±20
$Sb^{121}(n,2n)Sb^{120g}$	15.89 min	1171	0.0132	1188 ±60
$Sb^{123}(n,2n)Sb^{122}$	2.8 d	564 696	0.66 0.034	1542 ±80
$Te^{122}(n,2n)Te^{121m}$	154 d	212	0.83	890 ±100
$Te^{122}(n,2n)Te^{121g}$	17 d	573	0.81	725 ±40
$Te^{124}(n,2n)Te^{123m}$ $Te^{123}(n,n')Te^{123m}$	117 d	159	0.84	980 ±100
$Te^{128}(n,2n)Te^{127m}$	109 d	417	0.0082 [i]	949 ±150
$Te^{128}(n,2n)Te^{127g}$	9.4 hr	417	0.0083	712 ±60
$Te^{130}(n,2n)Te^{129m}$	34.1 d	460 487 696	0.06 0.012 [j] 0.038	885 ±45
$Te^{130}(n,2n)Te^{129g}$	68.7 min	460 487	0.083 0.015 [j]	570 ±30
$I^{127}(n,2n)I^{126}$	12.8 d	386	0.334	1649 ±80
$Cs^{133}(n,2n)Cs^{132}$	6.59 d	668	0.978	1542 ±75
$Ba^{130}(n,2n)Ba^{129}(ec)Cs^{129}$ $Ba^{130}(n,np)+...Cs^{129}$	32.1 hr	372 411	0.36 0.24 [k]	1371 ±70
$Ba^{132}(n,2n)Ba^{131}$	12 d	496	0.48	1574 ±100
$Ba^{134}(n,2n)Ba^{133m}$	38.9 hr	276	0.175	783 ±56
$Ba^{136}(n,2n)Ba^{135m}$ $Ba^{135}(n,n')Ba^{135m}$	28.7 hr	268	0.16	1149 ±80
$Ce^{136}(n,2n)Ce^{135}$	17 hr	265	0.444 [l]	1318 ±90
$Ce^{138}(n,2n)Ce^{137m}$	34.4 hr	255	0.11	958 ±100

Table 3 (Continued)

Reaction	Half-Life	$E_{(kev)}$	f_d (a)	Measured Cross Section (mb) (b)
$Ce^{140}(n,2n)Ce^{139m}$	54 sec	746	0.93	621 ±70
$Ce^{140}(n,2n)Ce^{139m+g}$	140 d	165	0.81	1593 ±130
$Ce^{142}(n,2n)Ce^{141}$	32.5 d	145	0.48	1730 ±170

(a) All values, unless otherwise stated, are taken from Reference 6.

(b) The cross sections of $Mo^{92}(n,2n)Mo^{91m}$ and $Ce^{140}(n,2n)Ce^{139m}$ are based on the $Si^{28}(n,p)Al^{28}$ standard reaction with σ=252 ±15 mb (Ref. 10). All other cross sections are based on the $Fe^{56}(n,p)M_n56$ reaction with σ=100 ±6 mb (Ref. 8). The errors are discussed in Section 3.2

(c) L. Broman and S. Boreving, Arkiv Fysik 34 259 (1967).

(d) See text (Section 3.1-4).

(e) M. Adachi, H. Taketani, and K. Hisatake, J. Phys. Soc. (Japan) 24 227 (1968).

(f) See text (Section 3.1-2).

(g) G. Graeffe, C. W. Tang, C. D. Coryell, and F. E. Gordon, Phys. Rev. 149, 884 (1966).

(h) This is a composite cross section including only 91% metastable state, i.e. $\lambda_1^*/(\lambda_1 - \lambda_2) = 0.91$.

(i) Nuclear Data Sheets, compiled by K. Way et al. (Printing and Publishing Office, National Academy of Sciences--National Research Council, Washington, D. C. 20418).

(j) G. Berzins, L. M. Beyer, and W. H. Kelly, Nucl. Phys. A93, 456 (1967).

(k) G. Graeffe and W. B. Walters, Phys. Rev. 153, 1321 (1967).

(l) A. Abdulmalek and R. A. Nauman, Phys. Rev. 166, 1194 (1968).

Table 4. (n,p) Cross Sections at 14.4 ±0.4 Mev from the Present Work

Reaction	Half-Life	$E_{(kev)}$	f_d[a]	Measured Cross Section (mb)[b]
$Ni^{58}(n,p)Co^{58}$	71.3 d	810	0.99	331 ±30
$Zr^{90}(n,p)Y^{90m}$	3.1 hr	202 482	0.97 0.91	12.9 ±1.0
$Zr^{91}(n,p)Y^{91m}$	50.3 min	551	0.95	18.6 ±1.9
$Zr^{92}(n,p)Y^{92}$	3.53 hr	934	0.14	18.5 ±2.7
$Mo^{96}(n,p)Nb^{96}$	23.35 hr	569 778 1092 1200	0.59 0.97 0.49 0.21	21.3 ±1.5
$Mo^{97}(n,p)Nb^{97m}$	1 min	747	0.98	7.4 ±0.8
$Mo^{97}(n,p)Nb^{97g}$	72 min	658	0.98[c]	8.5 ±1.0
$Mo^{98}(n,p)Nb^{98g}$	51 min	720 787	0.75 1.0	4.1 ±0.5
$Ru^{96}(n,p)Tc^{96}$	4.35 d	778 810 851	1.0 0.84 1.0	146 ±7
$Rh^{103}(n,p)Ru^{103}$	39.5 d	497	0.88	16.9 ±1.5
$Pd^{105}(n,p)Rh^{105}$	35.9 hr	319	0.19	37.6 ±2.0[d]
$Pd^{106}(n,p)Rh^{106m}$	130 min	512	1.0[e]	6.0 ±0.4
$Pd^{106}(n,p)Rh^{106g}$	30 sec	512	0.097[f]	18 ±4
$Pd^{108}(n,p)Rh^{108}$	16.8 sec	434 620	0.43 0.22	8.3 ±1.5
$Cd^{106}(n,p)Ag^{106m}$	8.5 d	512	0.97[f]	50 ±6
$Cd^{106}(n,p)Ag^{106g}$	24 min	512 511	1.43[f]	103 ±30
$Cd^{112}(n,p)Ag^{112}$	3.14 hr	617	0.43[g]	15.0 ±1.3[h]
$Sn^{112}(n,p)In^{112m}$	20.7 min	617	0.06	49 ±15
$Sn^{112}(n,p)In^{112g}$	14.4 min	617	0.06	68 ±20
$Sn^{116}(n,p)In^{116m}$	54.0 min	417	0.36	7.9 ±0.8
$Sn^{117}(n,p)In^{117m}$	1.93 hr	314 565	0.31 0.47	5.7 ±1.5
$Sn^{117}(n,p)In^{117g}$	45 min	565	1.0	9.8 ±1.6

Table 4. (Continued)

Reaction	Half-Life	$E_{(kev)}$	f_d[(a)]	Measured Cross Section (mb)[(b)]
$Ba^{138}(n,p)Cs^{138}$	32.2 min	463	0.23	3.8 ±0.6
$Ce^{140}(n,p)La^{140}$	40.22 hr	329 487 1596	0.21 0.48 0.96 } (i)	6.3 ±0.5

(a) All the values, unless otherwise stated, were taken from Reference 6.

(b) The cross sections are based on the standard reaction $Fe^{56}(n,p)Mn^{56}$ with σ = 100 ±6mb. The errors are discussed in Section 3.2.

(c) G. Graeffe and A. Siivola, Nucl. Phys. A109, 380 (1968).

(d) There is possible contribution from the $Pd^{106}(n,np)$ +... Rh^{105} reaction.

(e) J. Vrzal, E. P. Grigorev, A. V. Zolotavin, J. Liptak, V. D. Sergeev, and J. Urbanet, Bull. Acad. Sci. USSR, Phys. Ser. 31, 692 (1967).

(f) P. Venugopala Rao and R. W. Fink, Nucl. Phys. A103, 385 (1967).

(g) E. W. A. Lingeman, J. Kowijn, and L. G. R. Mathod, Nucl. Phys. A113 33 (1968).

(h) There is possible contribution from the $Cd^{113}(n,np)$ +... Ag^{112} reaction.

(i) H. W. Baer, J. J. Reidy, and M. L. Wiedenbeck, Nucl. Phys. A113, 33 (1968).

Table 5. (n,α) Cross Sections at 14.4 ±0.4 Mev from the Present Work

Reaction	Half-Life	$E_{(kev)}$	f_d [a]	Measured Cross Section (mb) [b]
$Zr^{94}(n,\alpha)Sr^{91}$	9.67 hr	1025	0.30	5.0 ±1.0
$Nb^{93}(n,\alpha)Y^{90m}$	3.1 hr	482	0.91	5.3 ±0.5
$Mo^{92}(n,\alpha)Zr^{89m}$	4.18 min	588	0.87	9.4 ±0.9
$Mo^{92}(n,\alpha)Zr^{89g}$	78.4 hr	910	0.99	18.7 ±1.5
$Mo^{98}(n,\alpha)Zr^{95}$	65.5 d	758	0.54 [c]	8.1 ±1.0
$Pd^{106}(n,\alpha)Ru^{103}$	39.5 d	497	0.88	5.6 ±0.7
$Pd^{108}(n,\alpha)Ru^{105}$	4.44 hr	470	0.19 [d]	2.7 ±0.3
$Cs^{133}(n,\alpha)I^{130}$	12.3 hr	538	0.99 [e]	1.96 ±0.15 [f]
$Ba^{138}(n,\alpha)Xe^{135m}$	15.6 min	527	0.80	0.55 ±0.05
$Ba^{138}(n,\alpha)Xe^{135g}$	9.14 hr	250	0.97 [g]	2.0 ±0.2
$Ce^{142}(n,\alpha)Ba^{139}$	82.9 min	166	0.266 [h]	6.0 ±1.0

(a) All the values, unless otherwise stated, were taken from Reference 6.

(b) The cross sections are based on the standard reaction $Fe^{56}(n,p)Mn^{56}$ with σ = 100 ±6 mb. The errors are discussed in Section 3.2.

(c) L. Foin, J. Oms, J. Blachet and J. Crancon, Nucl. Phys. A123, 513 (1969).

(d) S. O. Schriber and M. W. Johns, Nucl. Phys. A96, 337 (1967).

(e) D. D. Wilkey and J. E. Willard, J. Chem. Phys. 44, 970 (1966).

(f) This is a composite cross section including 77% of the metastable state, i.e. $\lambda_1^*/(\lambda_1 - \lambda_2) = 0.77$.

(g) P. Alexander and J. P. Lau, Nucl. Phys. A121, 612 (1968).

(h) J. C. Hill and M. L. Wiedenbeck, Nucl. Phys. A119, 53 (1968).

Table 6. [(n,np) + (n,pn) + (n,d)] Cross Sections at 14.4 ±0.4 Mev from the Present Work**

Target	Product	Half-life	E (kev)	f_d	Measured Cross Section (mb)
Ni^{58}	Co^{57}	272 d	122	0.85[a]	509 ±51[b]
Ru^{96}	Tc^{95m}	61 d	204	0.835[c]	52 ±10
Ru^{96}	Tc^{95g}	20 hr	768	0.94[c]	216 ±50[d]
Cd^{106}	Ag^{105}	41.2 d	281	0.32[e]	215 ±29[f]
Sn^{112}	In^{111}	2.81 d	173 247	0.89[a] 0.93[a]	168 ±59[g]

** The cross sections are based on the standard reaction $Fe^{56}(n,p)Mn^{56}$ with σ = 100 ±6 mb (Reference 8). The errors are discussed in Section 3.2.

(a) Reference 6.

(b) The small contribution from the corresponding (n,2n) reaction has been corrected.

(c) G. Chilos, E. Eichler, and N. K. Aras, Nucl. Phys. A123, 327 (1969).

(d) See text (Section 3.1.1).

(e) W. R. Pierson and K. Pengan, Phys. Rev. 159, 939 (1967).

(f) See text (Section 3.1.2).

(g) See text (Section 3.1.3).

CHAPTER IV

DISCUSSION OF THE RESULTS

4.1. Fundamental Equations for the Statistical Model Calculation of Cross Sections

According to the statistical theory[13] of nuclear reactions, the cross section $\sigma(n,x)$ for a reaction, in which a neutron is absorbed by a target nucleus A forming a compound nucleus (A + 1) which subsequently emits a particle x, can be represented by

$$\sigma(n,x) = \sigma_c \frac{F_x}{\sum_i F_i} \tag{4-1}$$

where σ_c is the compound nucleus formation cross section; and F_i is the relative probability of emission of particle i. The F_i functions are given by

$$F_i = K g_i m_i \int_0^{E_m} E \sigma_i(E) w_i(U_i) dE \tag{4-2}$$

where K is a constant; g_i is a statistical weight factor given by $2s_i + 1$ where s_i is the spin of the emitted particle i; m_i is the reduced mass; E is the kinetic energy of the particle i; $\sigma_i(E)$ is the inverse reaction cross section of the particle i at energy E with the residual nucleus at excitation energy U_i; and $w_i(U_i)$ is the level density of the residual nucleus at excitation energy U_i given by

$$U_i = E_n + Q_{(n,i)} - E \tag{4-3}$$

where E_n is the incident neutron energy in the center of mass system,

$Q_{(n,i)}$ is the Q-value of the (n,i) reaction, with no correction for pairing energy. The upper limit E_m for the integration is the maximum energy available to the emitted particle i and is given by

$$E_m = E_n + Q_{(n,i)} \tag{4-4}$$

The (n,2n) cross section can be represented by

$$\sigma(n,2n) = \sigma_c \frac{F_{2n}}{\sum_i F_i} = \sigma_c \frac{1}{\sum_i F_i/F_n} \frac{F_{2n}}{F_n} \tag{4-5}$$

$$(i = n,\ p,\ \alpha,\ \text{etc.})$$

where F_{2n} is the relative probability of emitting two neutrons from the compound nucleus (A + 1), and F_n is the relative probability of emitting a neutron irrespective whether or not more particles or gamma rays will be emitted following the neutron emission. The relative probability of two particle emission has been calculated[14] but a relatively crude model is usually used[15-17] for multiple neutron emissions. The model assumes that the compound nucleus A resulting from the emission of a first neutron from the compound nucleus (A + 1) will emit a second neutron or even a third neutron whenever it is energetically possible.* The ratio F_{2n}/F_n can then be calculated from

$$\frac{F_{2n}}{F_n} = \frac{\int_0^{E_n - S_n} E\sigma(E)w(E)dE}{\int_0^{E_n} E\sigma(E)w(E)dE} \tag{4-6}$$

---

* This assumption is of doubtful validity as is discussed in Section 3.2.

where S_n is the separation energy of a neutron from the target nucleus A.

In the use of equation (4-6) for calculations, the variation of the inverse reaction cross section $\sigma(E)$ with E is usually ignored and an exponential function for the level density is used,[13,15-17] e.g.

$$w(U) = ke^{2\sqrt{aU}} \tag{4-7}$$

where k is a constant and a is a level density parameter assumed to be constant with excitation energy U.

For simplicity the following quantities are defined.

$$G_o = 2(X_o^2 - 3X_o + 3) \tag{4-8}$$

and

$$G_1 = X_o^2(X_1 - 1) - X_1^3 + 3(X_1^2 - 2X_1 + 2) \tag{4-9}$$

where

$$X_o = \sqrt{4aE_n} \tag{4-10}$$

and

$$X_1 = \sqrt{4aS_n} \tag{4-11}$$

In terms of the above quantities equation (4-6) can be integrated to give

$$\frac{F_{2n}}{F_n} = \frac{G_o e^{X_o} - G_1 e^{X_1}}{G_o e^{X_o} + X_o^2 - 6} \tag{4-12}$$

Since $G_o e^{X_o}$ is very large compared with $X_o^2 - 6$, equation (4-12) can be approximated by

$$F_{2n}/F_n = 1 - (G_1/G_o)e^{-2\sqrt{a}\,(\sqrt{E_n} - \sqrt{S_n})} \tag{4-13}$$

The ratio F_{3n}/F_n can be calculated by substituting S_{2n}, the separation energy of two neutrons, for S_n in equation (4-13) and related equations.

For charged particles emission, the probability ratio F_q/F_n can be expressed by

$$F_q/F_n = j_q \frac{\int_{B_q}^{E_n+Q_{n,q}} E\sigma_q(E)w_q(U_q)dE}{\int_0^{E_n} E\sigma_n(E)w_n(U_n)dE} \qquad (4\text{-}14)$$

where the subscripts q and n refer to charged particles and neutrons, respectively; j_q is given by

$$j_q = g_q m_q / g_n m_n \qquad (4\text{-}15)$$

$Q_{(n,q)}$ is the Q-value of the (n,q) reaction; and B_q is the effective Coulomb barrier that a charged particle must overcome to escape from the compound nucleus and is given by

$$B_q = k_q V_q \qquad (4\text{-}16)$$

where k_q is a coefficient varying with atomic number Z obtained from Dostrovsky et al.,[18] and V_q is given by

$$V_p = 1.019(Z - 1)/(A^{1/3} + 1) \quad \text{Mev} \qquad (4\text{-}17)$$

and

$$V_\alpha = \frac{2.038\ (Z-2)}{(A-3)^{1/3} + 4^{1/3}} \quad \text{Mev} \qquad (4\text{-}18)$$

where A and Z are, respectively, the mass number and atomic number of the target nucleus, and a unit radius of 1.4 fermis was used to give the numerical coefficients.

In the use of equation (4-14) in calculations, the inverse reaction cross sections has been assumed to be[13,18]

$$\sigma_q(E) = \sigma_o(1 - B_q/E) \quad \text{for} \quad E > B_q \tag{4-19}$$

and

$$\sigma_q(E) = 0 \quad \text{for} \quad E < B_q \tag{4-20}$$

where σ_o is a constant.

Using Bodansky's method[19] of expansion with the modification that the logarithm of the level density was expanded in a Taylor series about U_o instead of about $U_o - E + B_q$, it can be shown that

$$w_i(U_i) = w_i(U_o)e^{(U_i-U_o)/T} \tag{4-21}$$

$$(i = n,p,\alpha, \text{ etc.})$$

where

$$U_i = E_n + Q_{(n,i)} - \delta_i - E \tag{4-22}$$

$$U_o = E_n + \tfrac{1}{2}Q_{(n,q)} - \tfrac{1}{2}B_q \tag{4-23}$$

$$(q = p,\alpha, \text{ etc.})$$

and the nuclear temperature T is defined by

$$\frac{1}{T} = \frac{d}{dU}[\text{Log}_e w(U)]_{U=U_o} \tag{4-24}$$

In equation (4-22), δ_i is the pairing energy of the product nucleus of the (n,i) reaction.

In the derivation of equation (4-21), the nuclear temperature T was assumed to be constant so that only the first two terms in the Taylor series need be used. For simplicity, the following parameters are defined.

$$E_{mq} = E_n + Q_{(n,q)} - B_q \tag{4-25}$$

and

$$D_q = Q_{(n,q)} + \delta_T - \delta_R - B_q \tag{4-26}$$

$$(q = p, \alpha, \text{ etc.})$$

where δ_T and δ_R are respectively the pairing energies of the target and the product nuclei obtained from Cameron and Elkin[20] with positive sign. Equation (4-14) is then integrated to give

$$F_q/F_n = j_q(I_q/I_n)e^{D_q/T} \tag{4-27}$$

where

$$I_q = 1 - (1 + E_{mq}/T)e^{-E_{mq}/T} \tag{4-28}$$

$$(q = p, \alpha, \text{ etc.})$$

and

$$I_n = 1 - (1 + E_n/T)e^{-E_n/T} \tag{4-29}$$

In obtaining equation (4-27), the difference in level densities of different residual nuclei at the same excitation energy U_o was ignored, i.e. the ratio $w_q(U_o)/w_n(U_o)$ was taken as unity. For 14 Mev neutrons, I_n in equation (4-29) is essentially unity, and the probability ratios of

charged particles emission to neutron emission can then be expressed by

$$F_p/F_n = I_p e^{Dp/T} \tag{4-30}$$

and

$$F_\alpha/F_n = 2I_\alpha e^{D\alpha/T} \tag{4-31}$$

Since the probability of emitting an alpha-particle or other kind of charged particle is very small compared with that of neutron emission, the following approximate expressions were obtained.

$$\sigma(n,p) = \sigma_c I_p e^{Dp/T}/(1 + I_p e^{Dp/T}) \tag{4-32}$$

$$\sigma(n,\alpha) = \sigma_c (2I_\alpha e^{D\alpha/T})/(1 + I_p e^{Dp/T}) \tag{4-33}$$

and

$$\sigma(n,2n) = \sigma_c (F_{2n}/F_n)/(1 + I_p e^{Dp/T}) \tag{4-34}$$

where

$$F_{2n}/F_n = 1 - (1 + \frac{E_n - S_n}{T}) e^{-(E_n - S_n)/T} \tag{4-35}$$

is obtained from equation (4-6) with the level density given by equation (4-21) and is the same as given by Blatt and Weisskopf.[13]

4.2. Comparison of the Present Results with Previous Work

Most of the previous measurements were made with beta-counting or gamma-counting with NaI(Tl) detectors. Beta-counting has the problem of resolving a continuous beta-spectrum into its components by the difference in half-lives and is highly unreliable when many activities or thick sources are involved. Gamma counting with NaI(Tl) detectors often suffers

from the defect of poor resolution. Some of the early results were not corrected for the decay of the neutron flux during the irradiation, which occasionally can give rise to substantial error when the activities compared do not have comparable half-lives.[21] Finally, when annihilation radiation from β^+ sources is counted, the detection efficiency becomes highly uncertain due to the uncertain effective "size" of the source.

In Tables 7 through 10, the total cross sections measured in the present work are compared with previously reported values,* together with various theoretical or semiempirical predictions. In general, the present values agree with previously reported values whenever the latter are in good agreement with each other. However, discrepancies were observable for cases in which only one or a few previous values were available. In the present work, the cross sections were determined from at least two separate runs and/or from several gamma transitions and they were all consistent.

4.3. (n,2n) and [(n,np) + (n,pn) + (n,d)] Reactions

4.3.1. Systematics of the (n,2n) Cross Sections

Taking all of the experimental values reported in the literature and plotting them against mass number in separate curves for even-Z and odd-Z cases, Bormann[22] observed apparent shell structure effects around the magic neutron numbers. A similar study was made by Manero,[23] and he implied that effects can also be seen at the closure of proton shells. Cuzzocrea and Notarrigo[24] reported that at neutron shell and subshell closures in the target nuclei, (n,2n) cross sections are found to increase

*The previously reported values were at various neutron energies ranging from about 14.1 to 14.8 Mev.

Table 7. Comparison of Total (n,2n) Cross Sections Measured in the Present Work with Various Predictions and with Previous Values

Target	S_n [a] (Mev)	σ_{exp} (mb)	Theoretical Predictions: Pearlstein [b] (mb)	Gardner [c] (mb)	Present [d] (mb)	Previous Values [e] (mb)
$_{28}Ni^{58}$	12.35	38 ±4	26	77	36	37 ±3, 40 ±5, 39 ±4, 39.3±2, 38 ±2.7, 31.7±2.5, 40.6 ±12, 34.3 ±1.7, 33.4 ±2.7, 38.8 ±8.2, 34.2 ±2.6, 31 ±4, 52 ±5, 36 ±3
$_{40}Zr^{90}$	11.54	652 ±31	617	645	685	877 ±51, 973 ±97, 768 ±23, 502 ±36, 544 ±22, 750 ±50, 800 ±120
$_{40}Zr^{96}$	7.55	1456 ±90	1463	1317	1570	
$_{42}Mo^{92}$	12.68	217 ±18	350	326	240	256 ±35, 158 ±5, 170 ±14, 107 ±7, 155 ±10, 132 ±21, 211 ±16, 130 ±29, 310 ±87, 315 ±35, 191 ±40
$_{42}Mo^{100}$	8.34	1389 ±84	1520	1329	1530	1510 ±180, 3790 ±1900, 2039 ±210, 1910 ±190, 1762 ±200
$_{44}Ru^{96}$	10.37	569 ±30	832	1023	982	634 ±55, 478 ±90, 2600 ±300, 860 ±43, 616 ±50
$_{44}Ru^{98}$	9.94	1168 ±96	1047	1127	1245	
$_{44}Ru^{104}$	8.72	1440 ±80	1573	1356	1470	2500 ±500
$_{45}Rh^{103}$	9.29	957 ±57	1342	1287	1390	

Table 7. (Continued)

Target	S_n (a) (Mev)	σ_{exp} (mb)	Theoretical Predictions: Pearlstein (mb) (b)	Gardner (mb) (c)	Present (mb) (d)	Previous Values (mb) (e)
$_{46}Pd^{102}$	10.53	637 ±45	978	1062	1020	
$_{46}Pd^{110}$	8.78	1416 ±150	1590	1428	1360	1948±100,2570±160, 2942±200,1590±80, 1590±140
$_{48}Cd^{106}$	10.62	975 ±88	978	1091	1050	827 ±63, 820 ±80, 1358 ±136
$_{48}Cd^{108}$	10.43	865 ±100	1153	1154	1130	504 ±76
$_{48}Cd^{110}$	9.96	1221 ±150	1333	1272	1235	
$_{48}Cd^{116}$	8.63	1387 ±71	1670	1510	1625	1587±127,1634±116, 1180±180
$_{50}Sn^{112}$	10.85	1100 ±100	1065	1096	1000	1508±112, 725±80, 1110±127,1217±138
$_{50}Sn^{114}$	10.46	1239 ±130 (f)	1240	1214	1165	1800 ±100
$_{51}Sb^{121}$	9.04	1615 ±63	1611	1533	1540	1562 ±156,1546±197, 1841 ±115
$_{51}Sb^{123}$	8.88	1542 ±80	1680	1566	1610	1245±300,1950±200, 1263±135,1706±100 2280±200
$_{52}Te^{122}$	9.88	1615 ±110	1484	1413	1360	1280 ±128
$_{52}Te^{128}$	8.70	1661 ±161	1730	1624	1665	
$_{52}Te^{130}$	8.36	1455 ±55	1765	1668	1725	457 ±120,753 ±107, 676 ±58, 599 ±120

Table 7. (Continued)

Target	S_n (a) (Mev)	σ_{exp} (mb)	Theoretical Predictions: Pearlstein (mb) (b)	Gardner (mb) (c)	Present (mb) (d)	Previous Values (mb) (e)
$_{53}I^{127}$	9.31	1649 ±80	1636	1552	1544	1120±400, 1320±132, 1300±80, 1660±140
$_{55}Cs^{133}$	9.12	1542 ±75	1646	1639	1605	1289 ±46, 1625±135, 1550 ±250
$_{56}Ba^{130}$	10.34	1371 ±80 (g)	1410	1406	1255	
$_{56}Ba^{132}$	9.90	1574 ±100	1509	1516	1450	
$_{57}Ce^{136}$	9.97	1318 ±90	1460	1545	1395	
$_{58}Ce^{140}$	8.97	1593 ±130	1710	1731	1690	2280 ±200, 1804 ±105, 1740 ±100, 3000 ±400
$_{58}Ce^{142}$	7.07	1730 ±170	1180 (h)	1200 (h)	1740 (h)	1695±102, 1600 ±300, 1860±170

(a) Values are taken from Reference 39.
(b) The values are calculated from Pearlstein's method[16] using the non-elastic cross section values of Mani et al.[38]
(c) The values are calculated from Gardner's method[15] with the modification that the cross sections are calculated directly from equation (4-43) without using the ratio equation and that the level density parameter a is given by a = A/25.
(d) The values were calculated from equation (4-34) with effective thresholds given by equations (4-46) and (4-47). For the case of Ni^{58} the correction for the (n,np) reaction is also made according to equation (4-55).
(e) The values are for $14.4 < E_n < 14.8$ Mev taken from CINDA-69, An Index to the Literature on Microscopic Neutron Data, USAEC Division of Technical Information Extension (USAEC DTIE), USSR Nuclear Data Information Centre (USSR NDIC), ENEA Neutron Data Compilation Centre (ENEA NDCC), IAEA Nuclear Data Unit (IAEA NDU).
(f) This is not exactly the total cross section but a composite cross section including only 91% metastable state.
(g) This value includes the [(n,np)+(n,pn)+(n,d)] cross section which is estimated from equation (4-49) to be about 80 mb within the error limits quoted.
(h) The (n,3n) contribution has been corrected for.

Table 8. Comparison of the Total [(n,np) + (n,pn) + (n,d)] Cross Sections Measured in the Present Work with Statistical Model Calculations and with Literature Values

Target	σ_{exp} (mb)	σ_{cal} (mb) (a)				Literature Values (b) (mb)
		(n,np) (c)	(n,pn) (c)	(n,d)	σ_{sum}	
$_{28}Ni^{58}$	509 ±51	320 (d)	131 (193)	10	461	520 ±120, 527 ±63, 540 ±50
$_{44}Ru^{96}$	268 ±51	1.9	6.6 (23)	2.7	11	
$_{48}Cd^{106}$	215 ±29	0.1	1.3 (13)	2.0	3.4	
$_{50}Sn^{112}$	168 ±59	0	0	1.2	1.2	

(a) The values are calculated from equations (4-52) through (4-55) and related equations derived from the statistical model with a constant nuclear temperature of 1.5 Mev.

(b) Values are from CINDA-69 for $14.1 < E_n < 14.8$ Mev.

(c) The values without brackets are calculated by adding 0.5 Mev to the thresholds for second emitted neutrons. The values in brackets are calculated by using ground state thresholds for neutron emissions.

(d) The cross section of the (n,np) component of Ni^{58} has been measured by Glover and Purser[45] to be 340 mb in agreement with the present estimation.

Table 9. Comparison of Total (n,p) Cross Sections Measured in the Present Work with Various Predictions and with Previous Values

Target	$Q_{n,p}$ [a] (Mev)	σ_{exp} (mb)	Theoretical Predictions: Levkovskii (mb) [b]	Gardner (mb) [c]	Present (mb) [d]	Previous Values (mb) [e]
$_{28}Ni^{58}$	0.39	331 ±30	344	398	353	560 ±110, 534 ±70, 411 ±30, 393 ±40, 316 ±20, 290 ±32, 280 ±35, 418 ±11, 318 ±25
$_{40}Zr^{92}$	-2.85	18.5 ±1.7	18.6	24.4	23.5	22 ±4, 25 ±5, 20.7 ±5, 76 ±16
$_{42}Mo^{96}$	-2.37	21.3 ±1.3	22.7	28.6	37.8	36.6 ±9.2, 21 ±7, 16 ±3
$_{42}Mo^{97}$	-1.15	15.9 ±1.3	17.0	20.3	18.6	108 ±54, 68 ±14, 110 ±20, 17.7 ±1.5
$_{44}Ru^{96}$	0.57	146 ±7	89.9	49.2	154	170 ±30
$_{45}Rh^{103}$	0.05	16.9 ±1.5	22.7	9.3	19.7	11 ±3
$_{46}Pd^{105}$	0.35	37.6 ±2.0	24.8	23.7	35.8	743 ±500
$_{46}Pd^{106}$	-2.73	24 ±4	19.0	8.7	23.6	
$_{46}Pd^{108}$	-3.81	8.3 ±1.5	11.3	3.3	11.9	
$_{48}Cd^{106}$	0.60	153 ±30	66.0	74.2	153	76 ±24
$_{48}Cd^{112}$	-3.22	15.0 ±1.3	13.7	5.3	12.0	11 ±3, 11 ±1.1
$_{50}Sn^{112}$	0.12	117 ±25	44.7	149	110	21.7±1.3, 145±30, 10 ±2.6
$_{50}Sn^{117}$	-0.69	15.5 ±2.1	13.0	24.4	14.5	9.6 ±0.9, 23±5, 12 ±3

Table 9. (Continued)

Target	$Q_{n,p}$ [a] (Mev)	σ_{exp} (mb)	Theoretical Predictions: Levkovskii (mb) [b]	Gardner (mb) [c]	Present (mb) [d]	Previous Values (mb) [e]
$_{56}Ba^{138}$	-4.05	3.8 ±0.6	3.4	--	3.5	1.9 ±0.5, 6.3 ±2, 3.1 ±0.2, 2.5 ±1.0, 2.2 ±0.3
$_{58}Ce^{140}$	-2.99	6.3 ±0.5	6.1	--	5.9	12.2 ±1.2, 10 ±2, 7.7 ±0.9

(a) The Q-values are taken from Reference 44.

(b) The values are calculated from Levkovskii's formula (equation 4-71).

(c) The values are taken from Reference 51.

(d) The values are calculated from equation (4-32) derived in the present work. The (n,pn) contributions whenever exists is corrected using equation (4-53) with $E_{pn} = E_{np} - 0.5$ Mev.

(e) The values are for $14.1 < E_n < 14.8$ Mev taken from CINDA-69.

Table 10. Comparison of Total (n,α) cross sections measured in the Present Work with Theoretical Predictions and with Literature Values

Target	$Q_{n,\alpha}$ (a) (Mev)	σ_{exp}	σ Theory Present (mb) (b)	σ Theory Facchini (mb) (c)	Literature Value (mb) (d)
$_{40}Zr^{94}$	2.06	5.0 ±1.0	6.7	0.72	4.3 ±1.1, 3.99 ±0.16, 4.9 ±0.5, 3.6 ± 0.5, 3.9 ±0.5, 6.0 ±0.4, 4.7 ±0.8, 5.5 ±0.5
$_{42}Mo^{92}$	3.69	28.1 ±2.0	12.4 24.2 (e)		20 ±8
$_{42}Mo^{98}$	3.20	8.1 ±1.0	12.7		
$_{46}Pd^{106}$	3.01	5.6 ±0.7	4.3		
$_{46}Pd^{108}$	2.12	2.7 ±0.7	2.1	0.18	2.3 ±0.4
$_{53}Cs^{133}$	4.38	1.96 ± 0.15 (f)	2.06	0.25	1.98 ±0.2, 1.0 ±0.9, 1.0 ±0.3, 1.05±0.15, 2.5 ±0.4
$_{56}Ba^{138}$	3.77	2.6 ±0.3	1.1 2.1 (e)		13 ±2(g), 3.6 ±0.5(g), 13 ±2(m), 4.9 ±0.7(g), 3.6 ± 0.5
$_{58}Ce^{142}$	6.15	6.0 ±1.0	3.6	3.0	7.0 ±0.7, 8 ±2, 4.5 ±0.9

(a) The Q-values are taken from Reference 44.
(b) The values are calculated from equation (4-33), based on the statistical model with constant nuclear temperature of 1.5 Mev.
(c) The values are taken from Reference 54.
(d) The values are taken from CINDA-69 for $14.1 < E_n < 14.8$ Mev.
(e) 1 Mev is added to the pairing energy for neutron shell closure at N = 50 or 82.
(f) This is not exactly the total cross section but a composite cross section including only 77% metastable state.

by a factor of as much as 3. They suggested that this enhancement may be due to direct interactions. Rieder[25] has shown that there is no significant shell effect in the (n,2n) cross sections of nuclei with neutron numbers close to 50. Csikai and Peto[26] pointed out that (n,2n) cross section values differ greatly even for nuclides with the same target neutron number and so no significant shell effect can be recognized by plotting the cross sections against target neutron or mass number. They observed an (N-Z) dependence of (n,2n) cross sections at 3 Mev residual excitation and that the (n,2n) cross section increases with increase in (N-Z) for a given neutron number. They suggest that the (N-Z) dependence is probably due to the influence of direct inelastic scattering (n,n'γ) reaction. Barr et al.[27] noted a dependence of (n,2n) cross sections on the asymmetry parameter (N-Z)/A. Hille[28] pointed out that shell effects can only cause minor deviations from the smooth trend of increasing (n,2n) cross section with increase in (N-Z)/A. Later, Bormann and Lammers,[29] from their study on (n,2n) cross sections at fixed reaction energies of 3 Mev and 6 Mev above the threshold, concluded that neutron shell effects in the (n,2n) cross sections are absent for cross sections at the same reaction energy. Adam and Jeki[30] compared the measured (n,2n) cross sections at 3 Mev residual excitation energy above thresholds with the values predicted by an empirical formula which is a function of (N-Z)/A, and concluded that shell effects produced by the pairing energy or the level density are nonexistent and that the so-called "shell effect" appearing in the (n,2n) cross sections seems to be due to the Q-value only.

The (n,2n) cross sections measured in the present work are plotted

against (N-Z)/A in Figure 5. From the figure it is seen that the (n,2n) cross sections increase with increasing (N-Z)/A. No difference between odd-Z and even-Z nuclei were seen, and shell effects corresponding to the proton shell closure at Z = 50 and that corresponding to neutron shell closure at N = 82 are not observable. The apparent shell effect at N = 50 for the cases of Mo^{92} and Zr^{90} can be removed if their high reaction thresholds (12.68 and 11.54 Mev, respectively) are taken into consideration. The average reaction energy (E_n - $E_{threshold}$) of all the nuclides investigated in the present work is about 5 Mev. By use of the excitation functions[31] of Mo^{92} and Zr^{90}, these (n,2n) cross sections at 5 Mev reaction energy were estimated to be 540 mb and 800 mb, respectively. Therefore, if the latter values are used in the plot, no shell effect at N = 50 is observed.

A least squares fitting of the measured (n,2n) cross sections to an exponential function of (N-Z)/A with the limiting condition that the (n,2n) cross section cannot exceed the geometric cross section, the following expression is obtained

$$\sigma(n,2n) = 61.6(A^{1/3} + 1)^2(1 - 1.319e^{-8.744(N-Z)/A}) \text{ mb} \qquad (4\text{-}36)$$

The above expression reproduces the (n,2n) cross sections measured in the present work to within about ± 20% except for a few cases as is shown in Figure 6a. To test the applicability of equation (4-36) for nuclei in other regions, the (n,2n) cross sections measured by other investigators[1,5,10,32-35] using the same method and experimental conditions as are used in the present work are compared with the predictions from the empirical formula, equation (4-36). The results are shown in Table 11 and

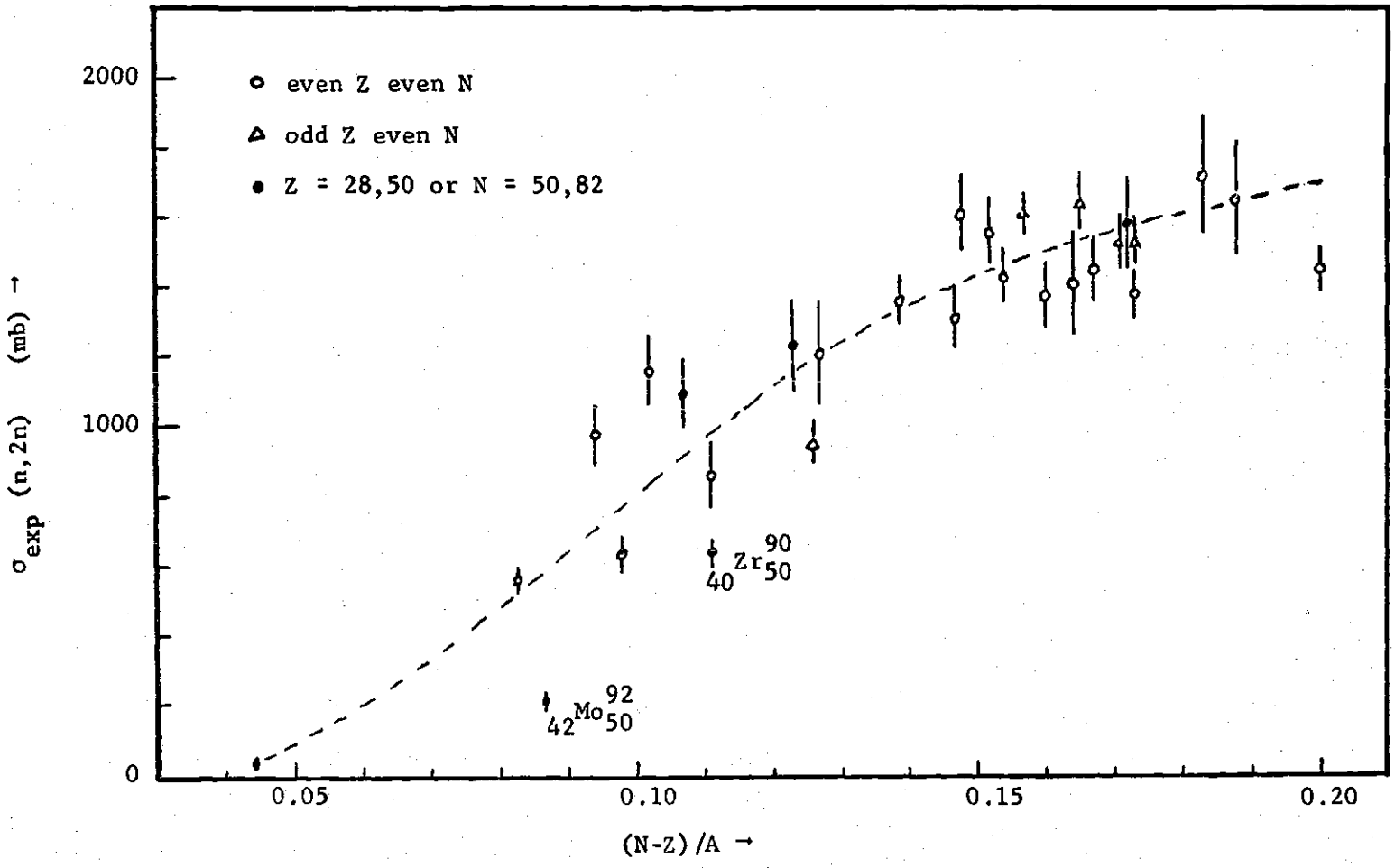

Figure 5. Linear Plot of Experimental (n,2n) Cross Sections at 14.4 Mev from the Present Work against the Asymmetry Parameter (N-Z)/A. This Plot Indicates that there are No Significant Shell Structure Effects and No Odd-Even Effects of Z in (n,2n) Cross Sections. The Apparent Dips of Mo^{92} and Zr^{90} Are Thought to be Due to Q-value Effects as Is Discussed in the Text.

Figure 6b. The agreement between the predictions and experimental values is still satisfactorily within ±20% except for a few cases. For heavy nuclei from Os to Pb, the predicted values are in general about 10% too large. It is interesting to notice that those nuclei with large discrepancies from the predicted values are the lightest stable isotopes of even-Z elements. The small (n,2n) cross sections of these nuclei may be due to the competition of the (n,np) reaction which is energetically favored, because the proton separation energy of these nuclei is much smaller than the corresponding neutron separation energy. However, as the atomic number Z is increased, the competition will decrease because of the increasing Coulomb barrier. In general, the empirical formula represented by equation (4-36) is believed to give good predictions, i.e. within about ± 20%, of (n,2n) cross sections for nuclei ranging from Ni to Pb, except in the rare earth region which needs experimental measurement.

From the measured (n,2n) cross sections listed in Table 7, it is seen that for a given element (fixed Z) the (n,2n) cross sections in general increase with increasing neutron number.

4.3.2. Theoretical Predictions of (n,2n) Cross Sections

By using the statistical compound nucleus model approach, attempts have been made to interpret measured (n,2n) cross sections semi-empirically.[15-17] Pearlstein[16] calculated (n,2n) cross sections by using the relation

$$\sigma(n,2n) = \sigma_{ne}(\sigma_{n,M}/\sigma_{ne})(\sigma_{n,2n}/\sigma_{n,M}) \qquad (4\text{-}37)$$

where σ_{ne} is the non-elastic cross section and $\sigma_{n,M}$ is the sum of the neutron emission cross sections $\sigma_{n,n'} + \sigma_{n,2n} + \sigma_{n,3n}$ + etc. The values

Table 11. Comparison of the (n,2n) Cross Sections Calculated from the Empirical Equation (Equation 4-36) with the Experimental (n,2n) Cross Sections Measured by Other Investigators Using the Same Method as Used in the Present Work

Target	$\sigma^{(a)}_{exp}$ (mb)	$\sigma^{(b)}_{emp}$ (mb)	Reference
$_{30}Zn^{64}$	150 ±12	364	10
$_{30}Zn^{66}$	650 ±150	633	10
$_{32}Ge^{76}$	1236 ±120	1129	32
$_{33}As^{75}$	1016 ±102	902	5
$_{34}Se^{74}$	358 ±33	584	1
$_{34}Se^{76}$	808 ±81	802	1
$_{34}Se^{82}$	1119 ±91	1238	1
$_{35}Br^{79}$	741 ±74	885	5
$_{35}Br^{81}$	1128 ±84	1045	5
$_{36}Kr^{78}$	245 ±20	560	33
$_{36}Kr^{80}$	810 ±78	781	33
$_{54}Xe^{124}$	1130 ±110	1266	33,34
$_{54}Xe^{126}$	1355 ±165	1385	33,34
$_{54}Xe^{128}$	1530 ±170	1491	33,34
$_{54}Xe^{134}$	1698 ±170	1748	33,34
$_{54}Xe^{136}$	1700 ±100	1818	33,34
$_{76}Os^{192}$	1993 ±200	2220	35
$_{78}Pt^{192}$	2035 ±150	2100	35
$_{78}Pt^{198}$	1716 ±173	2280	35
$_{79}Au^{197}$	1986 ±150	2195	35
$_{80}Hg^{196}$	1980 ±180	2100	35

Table 11. (Continued)

Target	$\sigma_{exp}^{(a)}$ (mb)	$\sigma_{emp}^{(b)}$ (mb)	Reference
$_{80}Hg^{198}$	2010 ±190	2165	35
$_{80}Hg^{204}$	2077 ±166	2337	35
$_{81}Tl^{203}$	1950 ±200	2256	35
$_{82}Pb^{204}$	1737 ±140	2228	35

(a) These values are from the references given in the last column. They were measured using the same method as was used in the present work.

(b) The values are calculated from the empirical formula (equation 4-36) obtained in the present work.

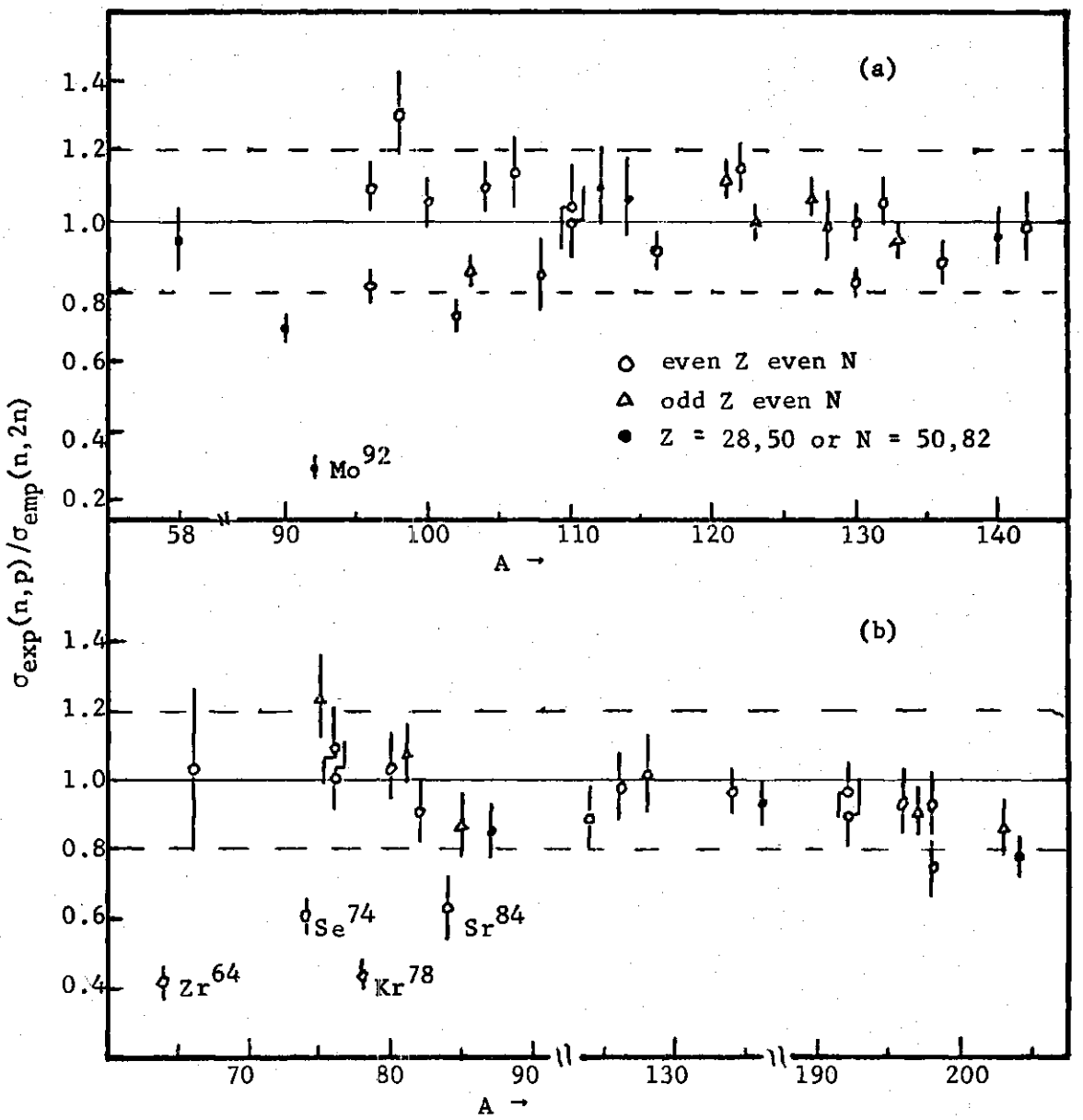

Figure 6. Comparison of the Experimental (n,2n) Cross Sections at 14.4 Mev with Those Calculated from the Empirical Equation (Equation 4-36) Obtained in the Present Work.
(a) The σ_{exp} (n,2n) Values are from the Present Work.
(b) The σ_{exp} (n,2n) Values are from References 1, 5, 10 and 32-35 Using the Same Method as is used in the Present Work.

of σ_{ne} used by Pearlstein were from Flerov and Talyzin's[36] empirical formula

$$\sigma_{ne} = 3.142(0.12A^{1/3} + 0.21)^2 \quad \text{barn} \tag{4-38}$$

The ratio $\sigma_{n,M}/\sigma_{ne}$ was obtained using the empirical formula of Barr et al.[27]

$$\sigma_{n,M}/\sigma_{ne} = 1 - 1.764e^{-18.14(N-Z)/A} \tag{4-39}$$

and the ratio $\sigma_{n,2n}/\sigma_{n,M}$ was calculated from the statistical model as given in equation (4-13) and related equations. The values of the level density parameter as used by Pearlstein[16] were calculated from

$$a = 0.154(j_Z + j_N + 1)A^{1/3} \quad \text{Mev}^{-1} \tag{4-40}$$

where j_Z and j_N are the effective spins for protons and neutrons, respectively. The values of j_Z and j_N were taken from Newton.[37]

A comparison of the measured (n,2n) cross sections with those calculated by Pearlstein[16] showed good agreement, in general. However, a close examination indicates that the present values are about 10% smaller than Pearlstein's predictions. It was found that the values of σ_{ne} used by Pearlstein were about 7% larger than those tabulated by Mani et al.[38] from optical model calculations. Therefore, the (n,2n) cross sections were recalculated by using the σ_{ne} values from Mani et al. The results are given in Table 7. The comparison with measured values is shown in Figure 7a and is found to be good within about $\pm$20%, except for a few cases discussed later.

Gardner[15] on the other hand calculated the cross section ratios

of two adjacent isotopes of a given element by the expression

$$\sigma_{n,2n}(Z,A+1)/\sigma_{n,2n}(Z,A) = R(Z,A+1)/R(Z,A) \qquad (4\text{-}41)$$

where

$$R = G_o e^{-X_o} - G_1 e^{-X_1} \qquad (4\text{-}42)$$

where G_o, X_o, G_1, and X_1 are given in equations (4-8) through (4-11). The absolute (n,2n) cross section of the isotope closest to the stability line with even N was calculated from

$$\sigma_{n,2n}(Z,A_Z) = \sigma_{ne}(\sigma_{n,2n}/\sigma_{n,M})G(Z) \qquad (4\text{-}43)$$

where A_Z is the mass number of the isotope closest to the stability line for a given element, and G(Z) is a normalization function given in Reference (15). The absolute cross sections of the other isotopes of the element were then obtained from the product of the cross section ratio and the normalizing cross section. The method has been tested[34] with Xe isotopes and found to be unsatisfactory in that the predicted values depend very much on which isotope is taken as the normalization point and in that some of the predictions exceed σ_{ne}. However, when the (n,2n) cross sections were calculated directly from equation (4-43) for each isotope without using the ratio equation, the results were found to be satisfactory. In the calculations, the values of σ_{ne} were taken from Mani et al.,[38] the G(Z)'s were read from the curve of Gardner[15] shown in the inset of Figure 8. The ratio $\sigma_{n,2n}/\sigma_{n,M}$ was calculated from equation (4-13) with $a = A/25$ Mev^{-1}. The results are given in Table 7

and a comparison with measured values is shown in Figure 7b. The agreement is about equally good (±20%) as that from Pearlstein's method.[16]

Gilbert and Gomberg[17] found that using the experimental (n,2n) and (n,3n) thresholds gave spurious results in the statistical model estimations and suggested that effective thresholds be used. In their method the normalization function is given by

$$\sigma_{n,M}/\sigma_{ne} = 1/(1 + 11.5e^{32.5(Z-N)/A}) \qquad (4\text{-}44)$$

and the level density parameter a was from Gilbert and Cameron.[40] The values of σ_{ne} were also taken from Mani et al.[38] The results taken directly from the tables of Gilbert and Gomberg[17] were compared with the presently measured (n,2n) cross sections in Figure 7c. It is seen that the predictions are in general too large by about 10-15% compared with values measured in the present work.

From Figures 7a, b, and c, it is seen that there are several nuclides which show large discrepancies in each prediction method, i.e. Ni^{58}, Mo^{92}, Ru^{96}, Pd^{102}, Rh^{103}, and Ce^{142}. The discrepancies of the cases of Ni^{58}, Mo^{92}, and Ce^{142} can be removed when the method of constant nuclear temperature approximation with effective thresholds is used. The method is discussed later. For the case of Ni^{58} the correction for the competition of the corresponding (n,np) reaction has to be taken into account. The estimation of the (n,np) cross section is given in Section 4.3.3.

For the case of Mo^{92}, there are two discrepant values for the reported neutron separation energy S_n, e.g. 12.68[39] and 13.1 Mev.[41] If the value 13.1 Mev is used in the calculation, the (n,2n) cross section

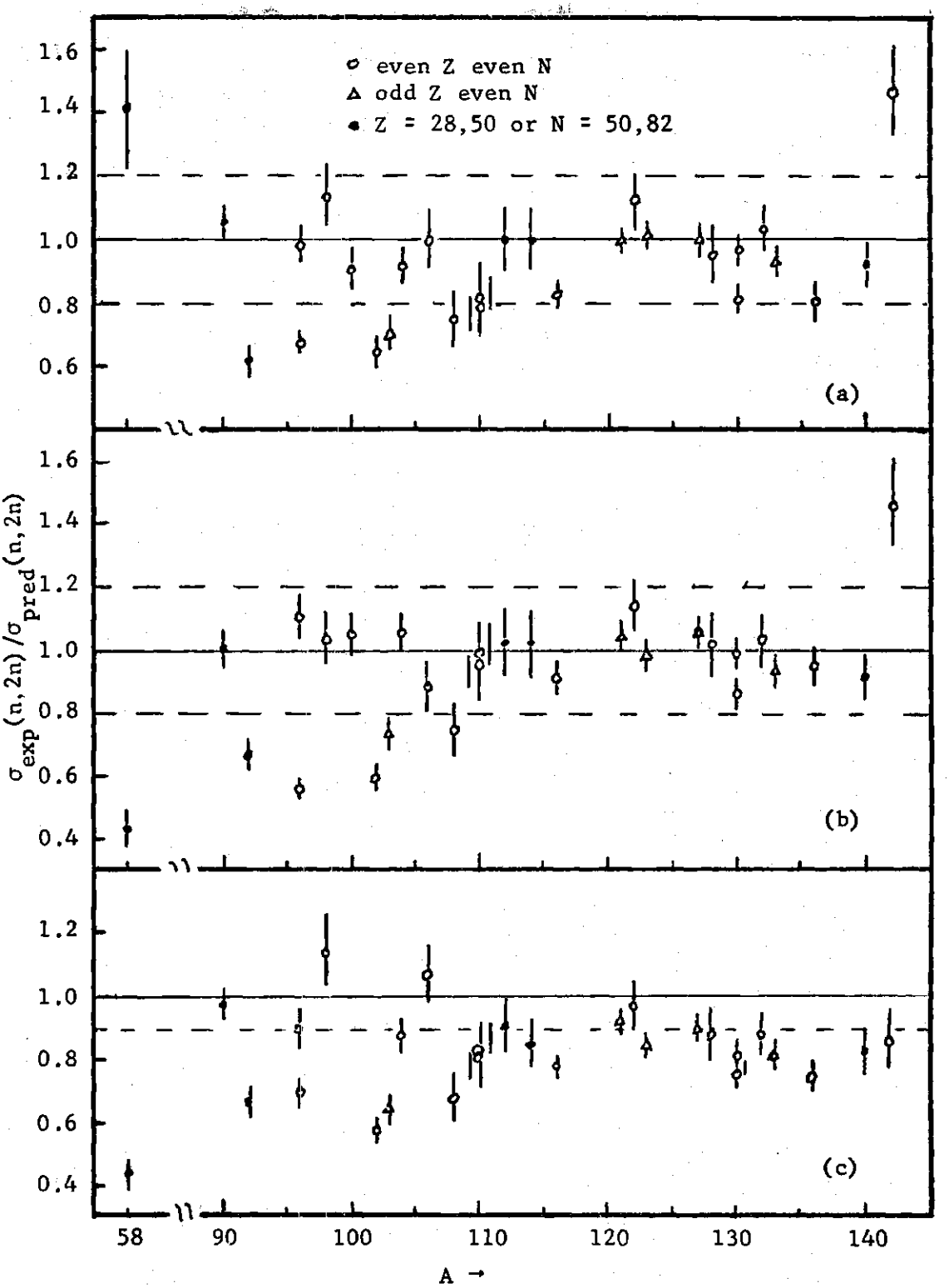
even Z even N
odd Z even N
Z = 28,50 or N = 50,82
(a)
(b)
(c)
$\sigma_{exp}(n,2n)/\sigma_{pred}(n,2n)$
A →
58
90
100
110
120
130
140

Figure 7.

Figure 7. Comparison of the experimental (n,2n) cross sections at 14.4 Mev from the present work with the predictions of

(a) Pearlstein,[16] with the modification that values of the non-elastic cross section σ_{ne} are from Mani et al.[38]

(b) Gardner, with the modification that the individual (n,2n) cross sections are calculated directly from the relation

$$\sigma(n,2n) = \sigma_{ne}(\sigma_{n,2n}/\sigma_{n,M})G(Z)$$

without using his cross section ratio equation and the level density parameter is given by a = A/25, and

(c) Gilbert and Gomberg,[17] using effective thresholds.

The predictions of both Pearlstein and Gardner are generally in agreement with the experimental values with a few exceptions, while the predictions of Gilbert and Gomberg are in general larger than the experimental values by about 10-20%.

of Mo^{92} is calculated to be 211 mb from both the method of Pearlstein and the modified method of Gardner. The value of 211 mb agrees very well with the measured value of 217± 18 mb. Therefore, an accurate measurement of the neutron separation energy of Mo^{92} will help to clarify this problem. This result shows that the estimated cross section is very sensitive to the fluctuation of the value of S_n when the incident neutron energy is close to the threshold.

From a comparison of equation (4-5) with equation (4-37), it is seen that the normalization functions, $\sigma_{n,M}/\sigma_{ne}$ or G(Z), correspond to the term $(\sigma_c/\sigma_{ne})(1/\sum_i F_i/F_n)$. The factor $1/\sum_i F_i/F_n$ accounts for the competition from the charged particle emission and is generally close to unity for cases investigated in the present work. The ratio σ_c/σ_{ne} represents the fraction of the non-elastic cross section that goes by compound nucleus formation. Therefore, the normalization function $\sigma_{n,M}/\sigma_{ne}$ or G(Z) appeared to account essentially for the influence of the direct interaction if the direct interaction cross section σ_d is defined by

$$\sigma_d = \sigma_{ne} - \sigma_c \tag{4-45}$$

The normalization functions of the three methods are plotted in Figure 8. It is seen that Gardner's G(Z)[15] values are approximately constant with (N-Z)/A, while the other two functions[16,17] increase with (N-Z)/A. It appeared that the functions used by Pearlstein[16] and by Gilbert and Gomberg[17] are about the same while Gardner's G(Z) function gives larger values for isotopes of small (N-Z)/A. The normalization function $\sigma_{n,M}/\sigma_{ne}$ used by Pearlstein or by Gilbert and Gomberg was intended to account for

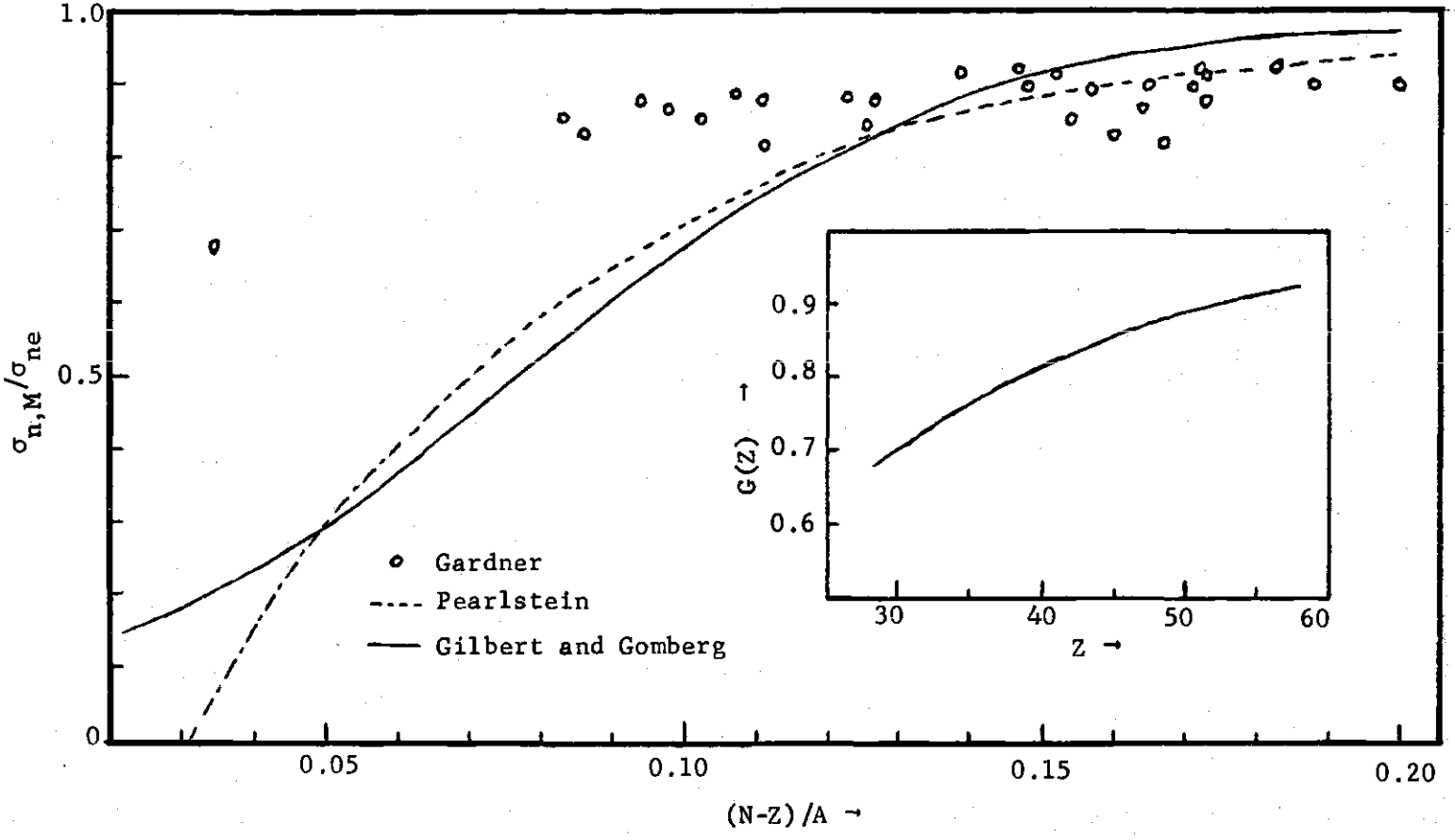

Figure 8. Comparison of the Normalization Functions Used by Gardner,[15] Pearlstein,[16] and Gilbert and Gomberg.[17] The Normalization Function G(Z) used by Gardner is a Function of Z as is shown in the Inset. The Circles shown in the Main Figure are Gardner's Values of G(Z) for the Nuclei Investigated in the Present Work.

the competition of charged particle emission.[16,17,27] However, qualitatively, this function appears to account instead essentially for direct interaction effects, most likely the direct inelastic $(n,n'\gamma)$ reaction.[26] A systematic study of total $(n,n'\gamma)$ cross sections from which the contribution of the direct interaction may be estimated may help to understand the effects.

A close look at equation (4-13) reveals that the ratio $\sigma_{n,2n}/\sigma_{n,M}$ is mainly governed by the exponential term in

$$\sigma_{n,2n}/\sigma_{n,M} = 1 - (G_1/G_o)e^{-2\sqrt{a}\,(\sqrt{E_n} - \sqrt{S_n})} \qquad (4\text{-}13)$$

when E_n is close to S_n. The parameters G_1 and G_o are given in equations (4-8) and (4-9). The ratio G_1/G_o is a slowly varying function of E_n, S_n, and a. The values of the ratio in the present work vary from about 2 to 6. If $\sqrt{E_n} - \sqrt{S_n} > 1$ and $a > 5$, the second term in equation (4-13) is less than 0.1 and the ratio $\sigma_{n,2n}/\sigma_{n,M}$ is rather insensitive to the variations of a and S_n for a fixed E_n. However, if S_n is very close to E_n, the second term is close to unity and the ratio $\sigma_{n,2n}/\sigma_{n,M}$ becomes very sensitive to the variations of a and S_n. For the case of Mo^{92} the effective threshold used by Gilbert and Gomberg[17] was 13.1 Mev, but the level density a used was 10.1 Mev^{-1}. It was this large value of a that canceled the effect of the effective threshold and failed to improve the prediction of the (n,2n) cross sections of Mo^{92}.

In general, the values of the level density parameter a used by Gilbert and Gomberg[17] are much larger than those used in the other two calculation methods as is shown in Figure 9. From equation (4-13), it is

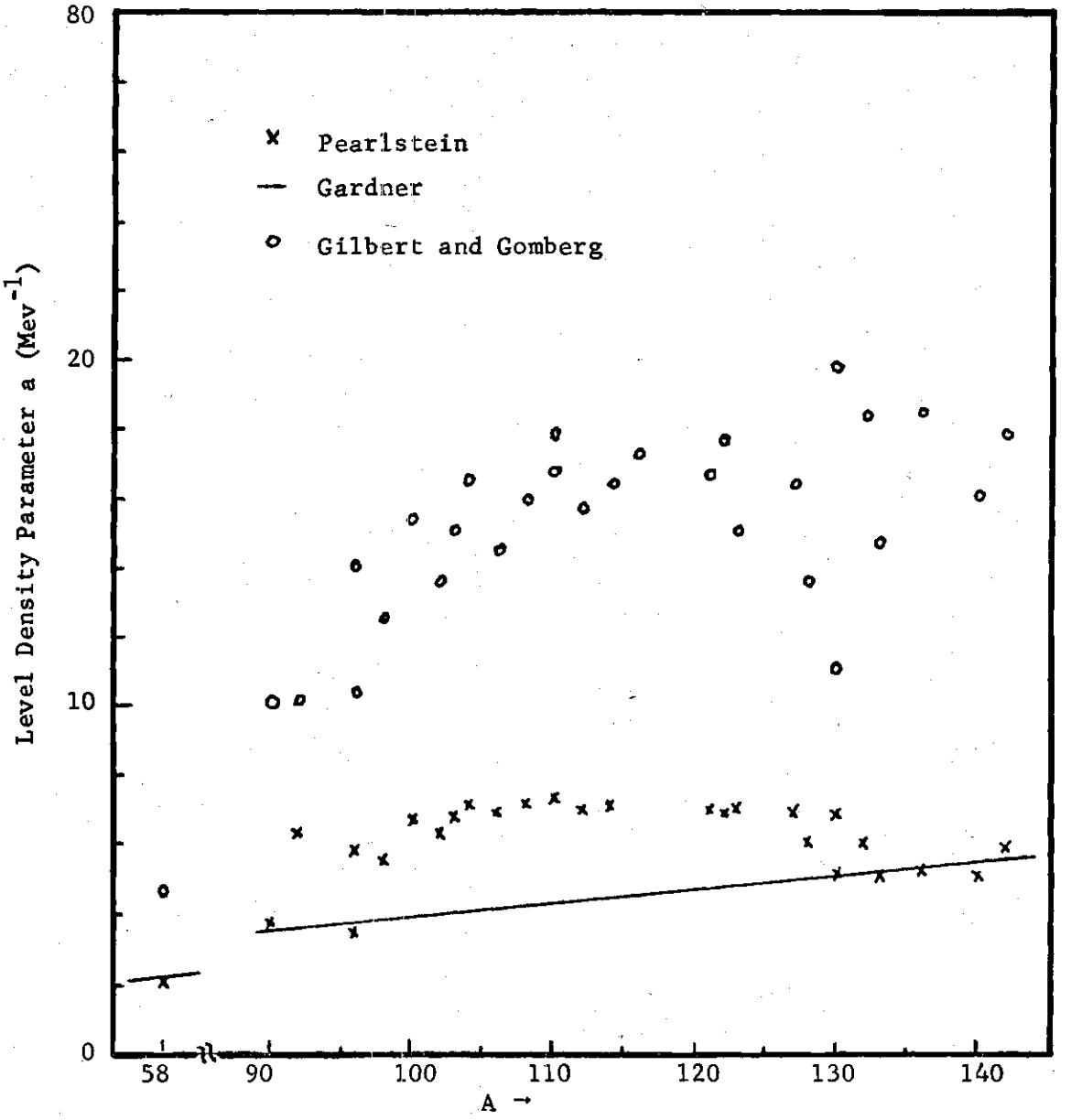

Figure 9. Comparison of the Values of the Level Density Parameter a used in the Calculation Methods of Gardner,[15] Pearlstein (16), and Gilbert and Gomberg.[17] Although there are Wide Differences in Choice of the Level Density Parameter a by the Authors, the Calculated (n,2n) Cross Sections do not differ as much as would be expected, owing to the use of Different Normalization Functions.

seen that the effects of increasing a and S_n are in the opposite direction. Therefore, in the calculation method of Gilbert and Gomberg[17] the effect of using larger effective thresholds is effectively canceled by their use of larger level density parameters.

In the above mthods, the statistical model was involved only in the calculation of the ratio $\sigma_{n,2n}/\sigma_{n,M}$ which was not directly measured. Since a normalization function is used in each method to get absolute (n,2n) cross sections, they all give comparable results, even though the level density parameters used in the calculation of $\sigma_{n,2n}/\sigma_{n,M}$ are quite different. As pointed out before, the ratio $\sigma_{n,2n}/\sigma_{n,M}$ is rather insensitive to the values of the level density parameter a at excitation energies well above the (n,2n) thresholds. Therefore, the agreement between the measured (n,2n) cross sections and calculated ones in the above methods can hardly be regarded as a confirmation of the statistical theory because of the normalization procedures involved in the methods. In addition, the excitation function of (n,2n) reactions appears unsuitable for the extraction of accurate level density parameters unless the small part of the excitation function close to the (n,2n) threshold is used.

As a comparison, the constant nuclear temperature approximation[13] was also used to calculate the (n,2n) cross sections. In this calculation, an average nuclear temperature of 1.5 Mev suggested by Cuzzocrea et al.[42] was used for all nuclides investigated in the present work. The average nuclear temperature of 1.5 Mev was confirmed from the (n,p) and (n,α) cross sections measured in the present work, as is discussed later. The (n,2n) cross sections were calculated from equation (4-34) and related equations. Again the non-elastic cross sections of Mani et al.[38] were

used for the compound nucleus formation cross section σ_c. The results are compared with the measured values in Figure 10a. It is seen that the predicted values are generally about 10% larger than the measured ones. However, if the effective thresholds E_1 and E_2 for one neutron and two neutron emission, respectively, given by

$$E_1 = S_n + 0.5 \text{ Mev} \tag{4-46}$$

and

$$E_2 = S_{2n} + 1.0 \text{ Mev} \tag{4-47}$$

are used for the neutron separation energies, the agreement between the predictions and the measured (n,2n) cross sections is improved. The results are given in Table 7 and a comparison with the measured values is shown in Figure 10b. The predicted values are seen to be good within about ±15% except for the cases of Ru^{96}, Pd^{102}, and Rh^{103} which deviate by about 30-40%. These deviations are thought to be due to direct interaction effects; i.e., the compound nucleus formation cross section σ_c is not equal to the non-elastic cross section. The concept of effective thresholds suggested by Gilbert and Gomberg[17] is supported by the present results. However, the odd-even effects observed by Gilbert and Gomberg[17] are not seen in the present results. Therefore, the adjustments for the odd-even effects made by Gilbert and Gomberg[17] appear to be unnecessary.

For the case of Rh^{103}, Nagel and Aten[43] have measured the (n,n'γ) cross section to be 508 mb. The (n,n'γ) cross section calculated in the constant nuclear temperature method with effective threshold is 287 mb. If the assumption that the direct interaction produces mainly

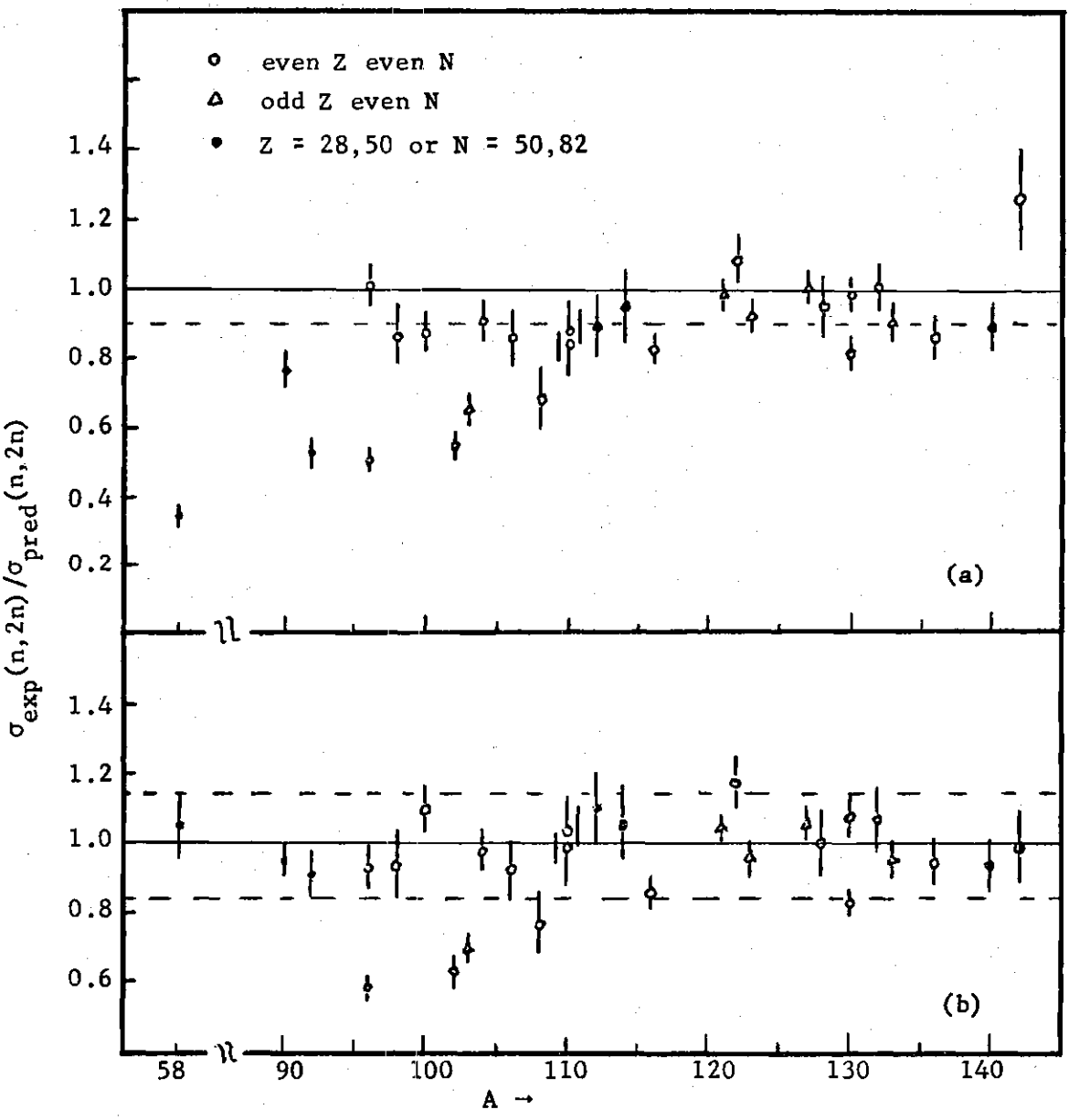

Figure 10. Comparison of the Experimental (n,2n) Cross Sections at 14.4 Mev from the Present Work with the Predictions using an Average Nuclear Temperature of 1.5 Mev and with
(a) Ground State Reaction Thresholds
(b) Effective Thresholds given by $E_1 = S_n + 0.5$ Mev and $E_2 = S_{2n} + 1$ Mev.

It is clear that Method (b) gives better agreement with Experiment, i.e. within about ±15%; while the Predictions of Method (a) are generally too large by about 10%.

the $(n,n'\gamma)$ reaction is made, the fraction of the non-elastic cross section attributed to the direct interaction can be estimated by

$$\frac{\sigma_d}{\sigma_{ne}} = \frac{\sigma_t(n,n'\gamma) - \sigma_s(n,n'\gamma)}{\sigma_{ne} - \sigma_s(n,n'\gamma)} \qquad (4\text{-}48)$$

where σ_d is the direct interaction cross section, $\sigma_t(n,n'\gamma)$ is the measured total $(n,n'\gamma)$ cross section, and $\sigma_s(n,n'\gamma)$ is the $(n,n'\gamma)$ cross section calculated from the statistical model in which σ_{ne} is used for σ_c and no normalization is involved. With

$$\sigma_t(n,n'\gamma) = 508 \text{ mb}; \quad \sigma_s(n,n'\gamma) = 287 \text{ mb}; \text{ and } \sigma_{ne} = 1778 \text{ mb}$$

it is found that

$$\sigma_d/\sigma_{ne} = 0.15 \quad \text{(i.e. 15\% direct interaction)}$$

Since only the $(n,n'\gamma)$ reaction was considered in the above estimation, it is a lower limit of the direct effect. For Ru^{96}, a rather large $[(n,np) + (n,pn) + (n,d)]$ cross section (268 mb) was observed in the present work. The contribution from evaporation of the compound nucleus was estimated to be negligibly small. The cross section was therefore very likely produced by direct interactions. Two other rather large $[(n,np) + (n,pn) + (n,d)]$ cross sections of Cd^{106} and Sn^{112} (216 and 165 mb, respectively) were also observed (see Section 4.3.3.) It was noticed that the nuclides Ru^{96}, Cd^{106}, and Sn^{112} are all the lightest isotopes of the corresponding elements. Therefore, it is very likely that Pd^{102} may also have comparable $[(n,np) + (n,pn) + (n,d)]$ cross sections. Thus for these lightest stable isotopes of the elements with even-Z, the direct $[(n,np) + (n,pn) + (n,d)]$ reactions in addition to

the direct inelastic (n,n'γ) reaction may be also important and affect the (n,2n) cross sections.

The direct interaction effects so far discussed are all negative effects on the (n,2n) cross sections. However, there is also the probability that (n,2n) reactions may be produced by a reaction in which the first neutron is knocked out by direct interaction leaving the target nucleus in an excited state which subsequently emits a second neutron.

4.3.3. [(n,np) + (n,pn) + (n,d)] Reactions

Bramlitt and Fink[21] studied a number of rare reactions of which the [(n,np) + (n,pn) + (n,d)] reaction is especially interesting because of its effects on the corresponding (n,2n) and (n,p) reactions. In the present work, four [(n,np) + (n,pn) + (n,d)] cross sections were measured, three of them for the first time. The total (n,np) +... cross sections measured in the present work, together with statistical model estimations for the components and available literature values, are summarized in Table 8. The cross section of Ni^{58} is seen to be in good agreement with literature values. A plot of the total cross section vs. atomic number Z or mass number A of the target nuclei is shown in Figure 11a or 11b, respectively. It is seen that the total cross sections are linearly related to both Z and A. Least squares fitting to linear functions of Z or A gives

$$\sigma(n,np + pn + d) = 934 - 15.14Z \qquad (4\text{-}49)$$

and

$$\sigma(n,np + pn + d) = 834 - 5.85A \qquad (4\text{-}50)$$

Either of the above empirical equations reproduces the total (n,np) +... cross section about equally well. From an examination of the atomic

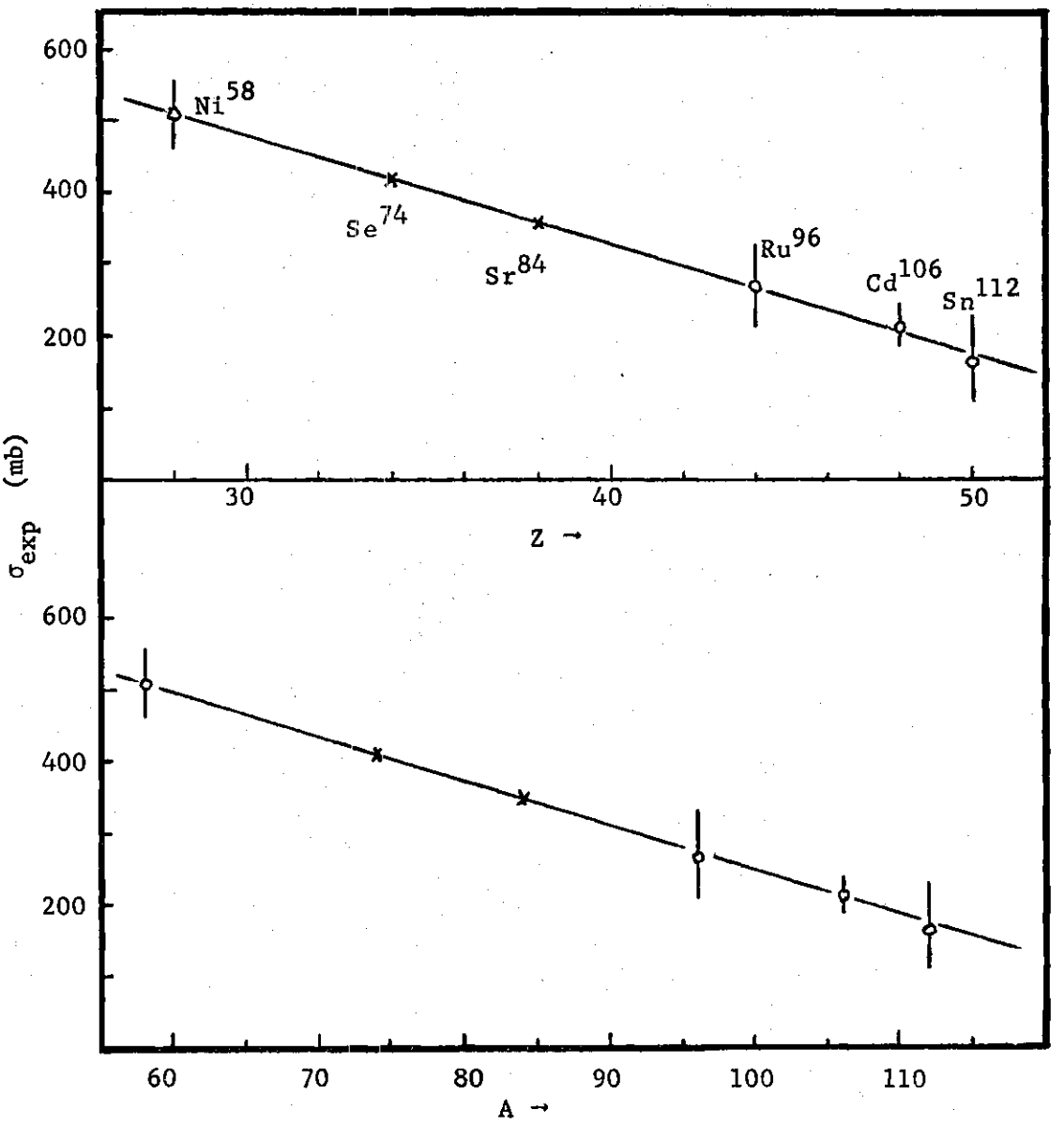

Figure 11. Plot of Total $[(n,np)+(n,pn)+(n,d)]$ Cross Sections at 14.4 Mev from the Present Work against
(a) Atomic Number Z and
(b) Mass Number A of the Target Nuclei
The Straight Lines are least squares fittings represented by (a) $\sigma(n,np+pn+d) = 934-15.14Z$ mb, and
(b) $\sigma(n,np+pn+d) = 834-5.85A$ mb.
The Nuclei Se^{74} and Sr^{84} are suggested to test the above Empirical Equations.

number Z and mass number A of the target nuclides Ni^{58}, Ru^{96}, Cd^{106}, and Sn^{112}, it is found that their Z and A are linearly related by an empirical equation

$$Z = 0.412(A + 10) \tag{4-51}$$

Since equations (4-49) and (4-50) are obtained from the cross sections corresponding only to the lightest stable isotopes of even-Z elements with Z and A related by equation (4-51), they should apply to only that kind of nuclides.

To test the applicability of the empirical equations (equations (4-49) and (4-50)) to other lightest stable isotopes of even-Z elements, additional (n,np) +... cross section measurements are needed. The nuclides Se^{74} and Sr^{84} are found to be good candidates for this purpose, because fairly large cross sections are predicted, e.g. 419 mb and 359 mb, respectively, from equation (4-49). In addition, the half-lives involved are not too long or too short, and, although the isotopic abundances are small, they are large enough that natural elements may be used with radiochemical separations of the products.

The rather large (n,np) +... cross sections can affect the corresponding (n,2n) and (n,p) cross sections in two ways, i.e. by direct interactions and competition in the evaporation process of the compound nucleus. The individual contributions of the components to the total (n,np) +... cross section were estimated using the statistical model with the constant nuclear temperature approximation. The equations used in the estimation are summarized below:

$$\sigma(n,d) = 3\sigma_c I_d e^{D_d/T}/(1 + F_p/F_n) \tag{4-52}$$

$$\sigma(n,pn) = \sigma_c I_{pn} e^{D_p/T}/(1 + F_p/F_n) \tag{4-53}$$

and

$$\sigma(n,np) = \begin{cases} \sigma_c I_{np} P_{np}/(1 + F_p/F_n) & \text{if } E_{np} < E_{nn} \quad (4\text{-}54) \\ \sigma_c (I_{np} - I_{nn} P_{nn})/(1 + F_p/F_n) & \text{if } E_{np} > E_{nn} \quad (4\text{-}55) \end{cases}$$

where

$$P_{nn} = 1/(1 + I'_{np} e^{D_{np}/T}/I'_{nn}) \tag{4-56}$$

where T is nuclear temperature assumed to be constant for all types of reactions and for all nuclei,

$$P_{np} = 1 - P_{nn} \tag{4-57}$$

$$D_{np} = S_n - S_p + \delta(Z,N-1) - \delta(Z-1,N) - B_p(Z,N-1) \tag{4-58}$$

where S_n and S_p are respectively the neutron and the proton separation energies, the δ's are pairing energies, and B_p is the effective Coulomb barrier for a proton given by equation (4-16); the ratio F_p/F_n is given in equation (4-30), D_p and D_d are given in equation (4-26), and the I_i's are given by

$$I_i = \int_0^{E_i/T} x e^{-x} dx \tag{4-59}$$

$$(i = p,\ d,\ nn,\ np,\ \text{and } pn).$$

The E_i's in equation (4-59) are defined by

$$E_q = E_n + Q_{n,q} - B_q \tag{4-60}$$

$$(q = p \text{ and } d)$$

$$E_{nn} = E_n - S_n \tag{4-61}$$

$$E_{np} = E_{pn} = E_n - S_p - B_p \tag{4-62}$$

where the slight difference between $B_p(Z,N)$ and $B_p(Z,N-1)$ is ignored,

$$E'_{nn} = E_{nn} - \bar{e}_n \tag{4-63}$$

and

$$E'_{np} = E_{np} - \bar{e}_n \tag{4-64}$$

where E_n is the incident neutron energy in the center of mass system, B_d is the effective Coulomb barrier for a deuteron given by

$$B_d = k_d \frac{1.029(Z-1)}{(A-1)^{1/3}+2^{1/3}} \quad \text{Mev} \tag{4-65}$$

where $k_d = k_p + 0.06$ is from Dostrovsky et al.,[18] and $\bar{e}_n$ is the average energy of the first emitted neutrons averaged from 0 to E_{np} or E_{nn}, whichever is smaller, and is given by

$$\bar{e}_n = \int_0^{E_{ns}} E^2 e^{-E/T} dE \Big/ \int_0^{E_{ns}} E e^{-E/T} dE \tag{4-66}$$

where $E_{ns} = E_{np}$ or E_{nn} whichever is smaller. All the parameters, unless otherwise specified, refer to a target nucleus (Z,N).

In equation (4-53), it is assumed that a neutron is emitted following the proton emission whenever energetically possible.* In equation (4-54), the branching ratio P_{np} or P_{nn} is estimated by assuming a compound nucleus with an average excitation energy of $E_n - \bar{e}_n$.

In the calculations all the Q-values of stable nuclei are from Maples et al.,[44] all the neutron separation energies and Q-values of

*This assumption is of doubtful validity, see discussions later.

unstable nuclei are from the mass table of Garvey et al.,[39] the pairing energies are from Cameron and Elkin[20] with positive sign. The results are summarized in Table 8.

For the case of Ni^{58}, Büttner et al.[14] has made accurate statistical model calculations using a complicated level density equation from Newton[37] given by

$$w(U) = \text{const. } a^{-\frac{1}{4}}(U+t)^{-5/4}\, e^{2\sqrt{aU}} \tag{4-68}$$

where

$$a = 0.0748(j_N + j_Z + 1)A^{2/3} \tag{4-69}$$

and

$$t = U/a \tag{4-70}$$

The results are

$$\sigma(n,np + pn + d) = \begin{cases} 370 \text{ mb} & \text{at } 14.1 \text{ Mev} \\ 480 \text{ mb} & \text{at } 14.8 \text{ Mev} \end{cases}$$

At 14.4 Mev, it is interpolated to be 420 mb, which is in good agreement with the value 461 mb calculated in the present work with rather crude approximations. Glover and Purser[45] have measured the angular and energy distributions of emitted protons at 14.8 Mev neutrons for the case of Ni^{58}. The total cross section of the [(n,p) + (n,pn) + (n,np)] reactions of Ni^{58} was found to be[45] 830 ± 70 mb, of which 60 mb was attributed to the direct interactions for the [(n,p) + (n,pn)] reaction from the angular and energy distributions. Also from the emitted deuterons, a value of 25 ± 6 mb was obtained for the $Ni^{58}(n,d)Co^{57}$ reaction.[45] In the present work the (n,p) cross section of Ni^{58} is measured to be 331 ± 30 mb, so the total cross section of Ni^{58} for the

[(n,p) + (n,pn) + (n,np) + (n,d)] reactions is 331 + 509 = 840± 60 mb which is in very good agreement with the value 855 ± 70 mb obtained from emitted proton and deuteron measurements by Glover and Purser.

Glover and Weigold[46] compared their activation cross section of the (n,p) reaction for Ni^{58} with that deduced from the energy spectrum of emitted protons.[45] To obtain the latter they assumed that, after emission of the first proton, neutron emission will occur if energetically possible in preference of gamma de-excitation. On this basis they obtained an (n,p) cross section significantly smaller than the activation (n,p) cross section, although the sum of [(n,p) + (n,np) + (n,pn) + (n,d)] cross sections is in good agreement with both activation and emitted particle measurements. They concluded that[46] the assumption that gamma ray de-excitation can be neglected as soon as the excited nucleus can decay by particle emission is of doubtful validity. They gave a qualitative explanation as follows:

The compound nucleus Ni^{59} resulting from addition of a neutron contributing all possible values of the orbital angular momentum quantum number ℓ will be formed in a wide range of spin states. Emission of low energy protons which will carry away little angular momentum will tend to leave in Co^{58} a similar distribution of states. Neutron emission will then lead to Co^{57}, which has a (7/2)-ground state and excited states at 1.36, 1.49, and 1.89 Mev. Therefore, until the Q-value is exceeded by 1.36 Mev, the only state open for neutron emission is the ground state. Since low energy neutrons can carry away little or no angular momentum, only states of Co^{58} within a limited range of spins will decay by neutron emission. By contrast, since Co^{58} is an odd nucleus and therefore has a

high level density, there will be many states through which gamma ray de-excitation may occur. Hence, these spin considerations imply that neutron emission in this case is not favored, although energetically possible.

The above explanation can be similarly applied to (n,2n) reactions. Glover[47] has demonstrated the importance of competition between gamma ray emission and particle emission within about 2 Mev of reaction thresholds. Therefore, in statistical model calculations of (n,2n) and (n,pn) cross sections, the gamma ray emission competition to the second neutron emission cannot be neglected, if the excitation energy of the emitting nucleus is close to the reaction threshold. In addition, near the reaction threshold, the number of states of the product nucleus open to the second neutron emission will be very few, which violates the basic continuum assumption of the statistical model. For (n,2n) reactions there is also possible competition from the corresponding (n,np) reaction, especially for the lightest stable isotopes of even-Z elements in the low-Z region. To account for these effects, the concept of effective thresholds proposed by Gilbert and Gomberg[17] is used. The effective thresholds are obtained by adding 0.5 Mev or 1 Mev, respectively, to the first or second neutron separation energy. The values 0.5 Mev and 1 Mev used to get effective thresholds are quite arbitrary; however, the results so calculated are in general fairly satisfactory compared with measured (n,2n) cross sections, as is shown in Figure 10b.

From Table 8, it is seen that the equations (4-52) through (4-55) and related equations derived from statistical model with a constant nuclear temperature of 1.5 Mev can describe well the (n,np) +... cross section for the case of Ni^{58}, but failed completely for other cases.

From the angular and energy distributions of emitted protons in the case of Ni^{58} measured by Glover and Purser,[49] it was shown that most of the (n,p) and (n,pn) reactions (about 85%) and all the (n,np) reactions go by compound nucleus formation, which is in agreement with the present estimations, both for the total [(n,p) + (n,pn) + (n,np) + (n,d)] cross section and for the (n,np) component. The failure of the equations to describe the (n,np) +... cross sections for Ru^{96}, Cd^{106}, and Sn^{112} suggests that for these nuclides, the (n,np) +... reactions are likely to go by direct interactions. However, to understand the reaction mechanism for these cases the measurements of the angular and energy distributions of the emitted protons and deuterons are needed.

The energetic parameters related to the [(n,np) + (n,pn) + (n,d)] reactions are summarized in Table 12.

From Table 12, it is seen that the decreasing trend of the [(n,np) + (n,pn) + (n,d)] cross sections with increasing Z shown in Figure 11b may be understood by Coulomb barrier effects and competition effects from the (n,2n) reaction. However, the good linearity of the cross sections with Z or A may be somewhat fortuitous.

4.4. (n,p) and (n,α) Reactions

4.4.1. Systematics of (n,p) and (n,α) Cross Sections

From the examination of old data in the literature, Levkovskii[48] noticed in 1956-1958 that the cross section of (n,p) and (n,α) reactions in a series of stable isotopes of one element decrease as a rule with increasing atomic weight of the isotope by approximately a factor of 2. Later, from his measured cross sections Levkovskii[49] obtained an empirical formula which describes the (n,p) cross sections at 14-15 Mev

Table 12. Energetic Parameters Related to the [(n,np) + (n,pn) + (n,d)] Reactions for Ni^{58}, Ru^{96}, Cd^{106}, and Sn^{112}

Target	$Q_{n,d}$ [(a)] (Mev)	$Q_{n,p}$ [(a)] (Mev)	S_n [(b)] (Mev)	S_p [(b)] (Mev)	B_p [(c)] (Mev)	E_f [(d)] (Mev)	B_d [(e)] (Mev)
$_{28}Ni^{58}$	-5.954	0.392	12.35	8.31	3.80	2.04	3.89
$_{44}Ru^{96}$	-5.086	0.572	10.37	7.37	5.95	0.98	6.11
$_{48}Cd^{106}$	-5.063	0.597	10.62	7.21	6.42	0.70	6.59
$_{50}Sn^{112}$	-5.549	0.123	10.85	7.81	6.61	-0.12	6.84

(a) Values are from Reference 44.

(b) Values are from Reference 39.

(c) Values are calculated from equation (4-16) and related equations.

(d) $E_f = E_n - S_p - B_p$, is the maximum excitation energy of the final product nucleus resulting from multiple particles emission in cascade.

(e) Values are calculated from equation (4-65).

quite well in the range $12 < A < 150$ as compared with the published (n,p) cross section values up to 1963. The empirical formula has a simple form given by

$$\sigma(n,p) = 45.2(A^{1/3} + 1)^2 \, e^{-33(N-Z)/A} \qquad (4\text{-}71)$$

A more thorough systematic study of (n,p) cross sections at 14 Mev was made by Gardner.[50] He observed that the (n,p) cross section of each succeeding isotope of any element was about one half the value of the preceding isotope and obtained an empirical equation as a function of Z and A with five adjustable parameters to predict the (n,p) cross sections of all the stable isotopes up to $Z \approx 94$ with a few exceptions. The factor of 2 in the empirical equation was explained by a cross section ratio equation obtained from the statistical model with crude approximations.[50] This cross section ratio equation with the refinement of including effects due to Coulomb barrier was later used by Gardner and Rosenblum[51] to recalculate the (n,p) cross sections of nuclei in the range $6 < Z < 50$. The results are generally in agreement with Levkovskii's predictions.[51] However, it was pointed out[51] that there are many cases in which the two predictions are in substantial disagreement. Some of the discrepant (n,p) cases were investigated in the present work, e.g. Ru^{96}, Rh^{103}, Pd^{106}, Pd^{108}, Cd^{106}, Cd^{112}, Sn^{112}, and Sn^{117}. The present results are generally in favor of Levkovskii's predictions, although in some cases, both predictions are in bad disagreement as discussed later.

Chatterjee[52,53] observed marked dips at proton shell and subshell closures for both (n,p) and (n,α) cross sections when the cross

sections of most abundant isotopes of the corresponding elements were plotted against the atomic number Z_R of the residual nucleus. But Gardner and Rosenblum[51] pointed out that these apparent "shell effects" resulted from the choice of the isotope which was to represent an element and are not true shell effects. Rao and Fink[5] also pointed that it is a consequence of the absence of stable isotopes to cover all possible values of Z_R.

Cuzzocrea and Notarrigo[24] showed that the experimental cross sections of (n,p) and (n,α) reactions at about 14 Mev for nuclei outside neutron shell and subshell closures can be described by means of a semi-empirical relation that gives roughly the predictions of the statistical model throughout the entire range of mass number. The relation is based on a pure exponential dependence for the level density of the residual nucleus and a nuclear temperature of about 2.3 Mev[24] taken to be constant for all types of reactions and for all nuclei. It was found that[24] at neutron shell and subshell closures of the target nucleus the cross sections were larger by factors up to 10 and 100, respectively, for (n,p) and (n,α) reactions and suggested that this enhancement may be due to direct interaction mechanisms. Later, an average nuclear temperature of 1.5 Mev was suggested by Cuzzocrea et al.[42] on the basis of an analysis of all the known values of the (n,p), (n,2n), and (n,α) cross sections at 14 Mev. The equations used for the calculation of the (n,p) and (n,α) cross sections are, respectively,[42]

$$\sigma(n,p) = \sigma_c e^{E_p^*/T} \tag{4-72}$$

and

$$\sigma(n,\alpha) = 2\sigma_c e^{E_\alpha^*/T} \tag{4-73}$$

where the E_q^*'s (q = p,α) are the same as the D_q's given in equation (4-26).

An average nuclear temperature of 1.5 Mev is confirmed by the present (n,p) and (n,α) cross sections by a semilog plot of the ratio $j_q\sigma_{ne}/\sigma_{exp}(n,q)$ against $-D_q$ as is shown in Figure 12. The parameter j_q is given in equation (4-15), the others are obvious. The solid straight line in Figure 12 is a least squares fit. From the slope of the straight line, an average nuclear temperature of 1.5 Mev is found. A comparison of equations (4-72) and (4-73) with equations (4-32) and (4-33) shows that the former equations may be considered as approximations of the latter ones. In general, in the region of low Z the integrals, I_q, in equations (4-32) and (4-33) are close to unity at 14 Mev, and so can be approximated by unity, but the term $e^{D_p/T}$ in the denominator which accounts for the competition of charged particles emission cannot be neglected. On the other hand, in the region of large Z, the competition of charged particle emission can be neglected, i.e. $e^{D_p/T}$ is close to 0, but the integral, I_q, is usually much smaller than unity, especially for (n,α) reactions, because of high Coulomb barrier and cannot be neglected. Therefore, one can either put I_q = 1 or put $e^{D_p/T}$ = 0 depending on the region of application to get good approximations.

4.4.2. Comparison of the (n,p) and (n,α) Cross Sections with Various Predictions

The total (n,p) cross sections measured in the present work, together with various predictions, are summarized in Table 9. The comparisons for various predictions are shown in Figures 13a, b, and c. It is seen that the values predicted by Gardner and Rosenblum[51] are almost

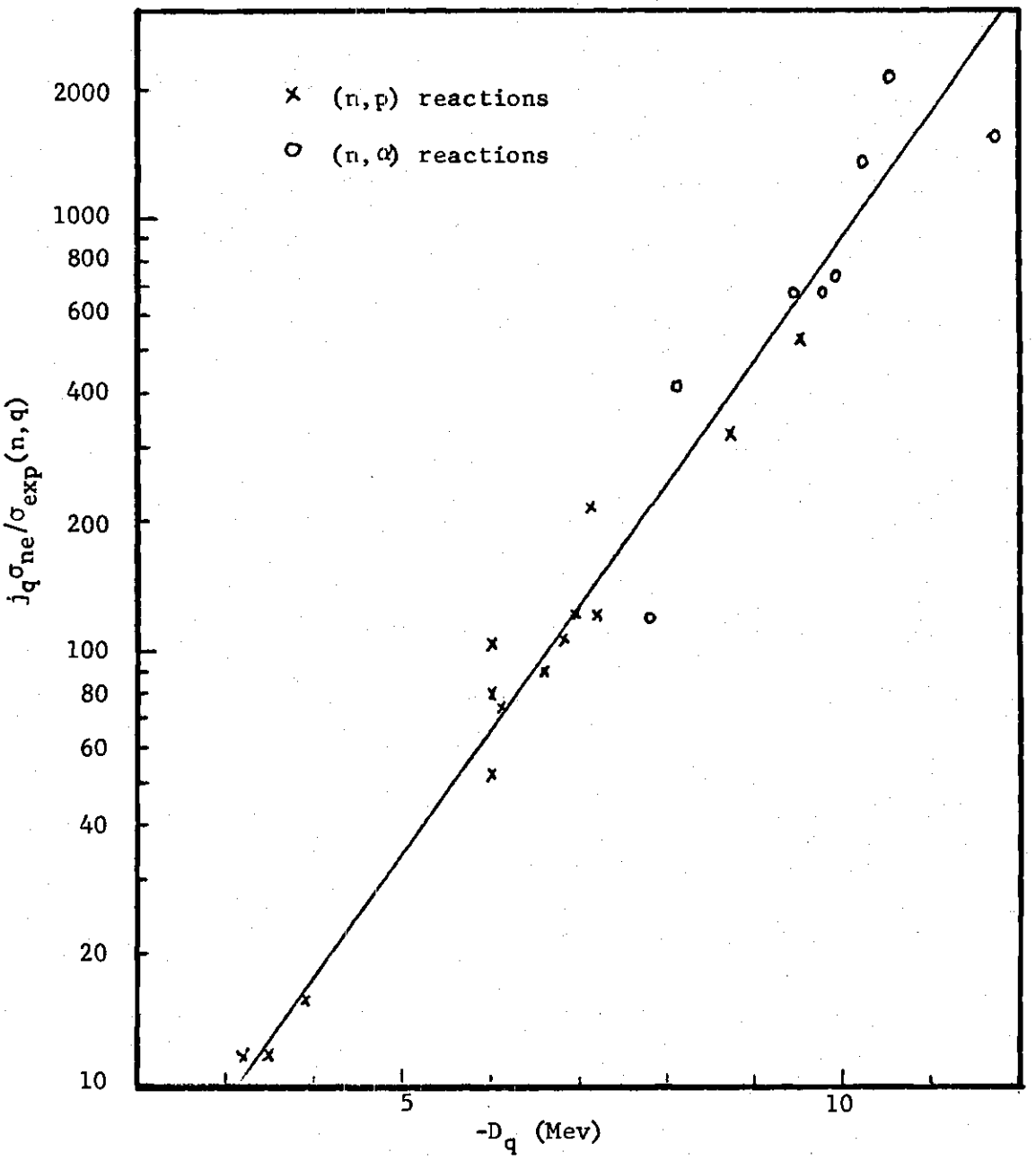

Figure 12. Semi-log Plot of the Ratio $j_q\sigma_{ne}/\sigma_{exp}(n,q)$ against $-D_q$, where j_q=1 if q=p, j_q=2 if q= α, and D_q is the Difference of the Q-value of the (n,q) Reaction corrected for pairing Energies and the Effective Coulomb Barrier. The Solid Line is a least squares fitting. From the slope of the line an Average Nuclear Temperature of 1.5 Mev is obtained. The value 1.5 Mev is the same as was suggested by Cuzzocrea et al. (42).

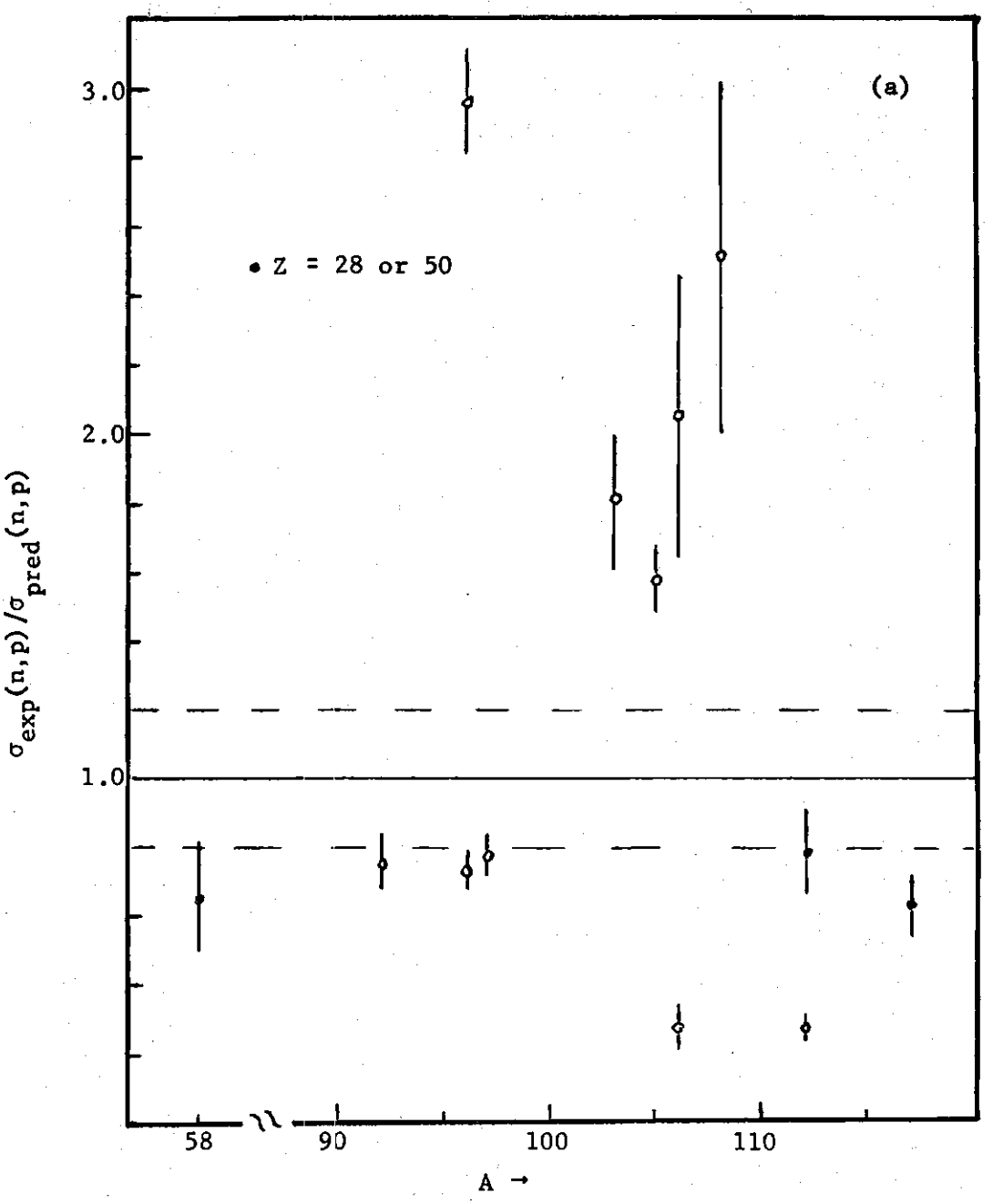

Figure 13. Comparison of the (n,p) Cross Sections at 14.4 Mev from the Present Work with the Predictions of
(a) Gardner and Rosenblum (51),
(b) Levkovskii (48,49), and
(c) Present Work using an Average Nuclear Temperature of 1.5 Mev.
It is seen that there are no significant Shell Effects in (n,p) Cross Sections, and that Method (c) gives the best agreement with the Present Experimental Results, i.e. within ±20%.

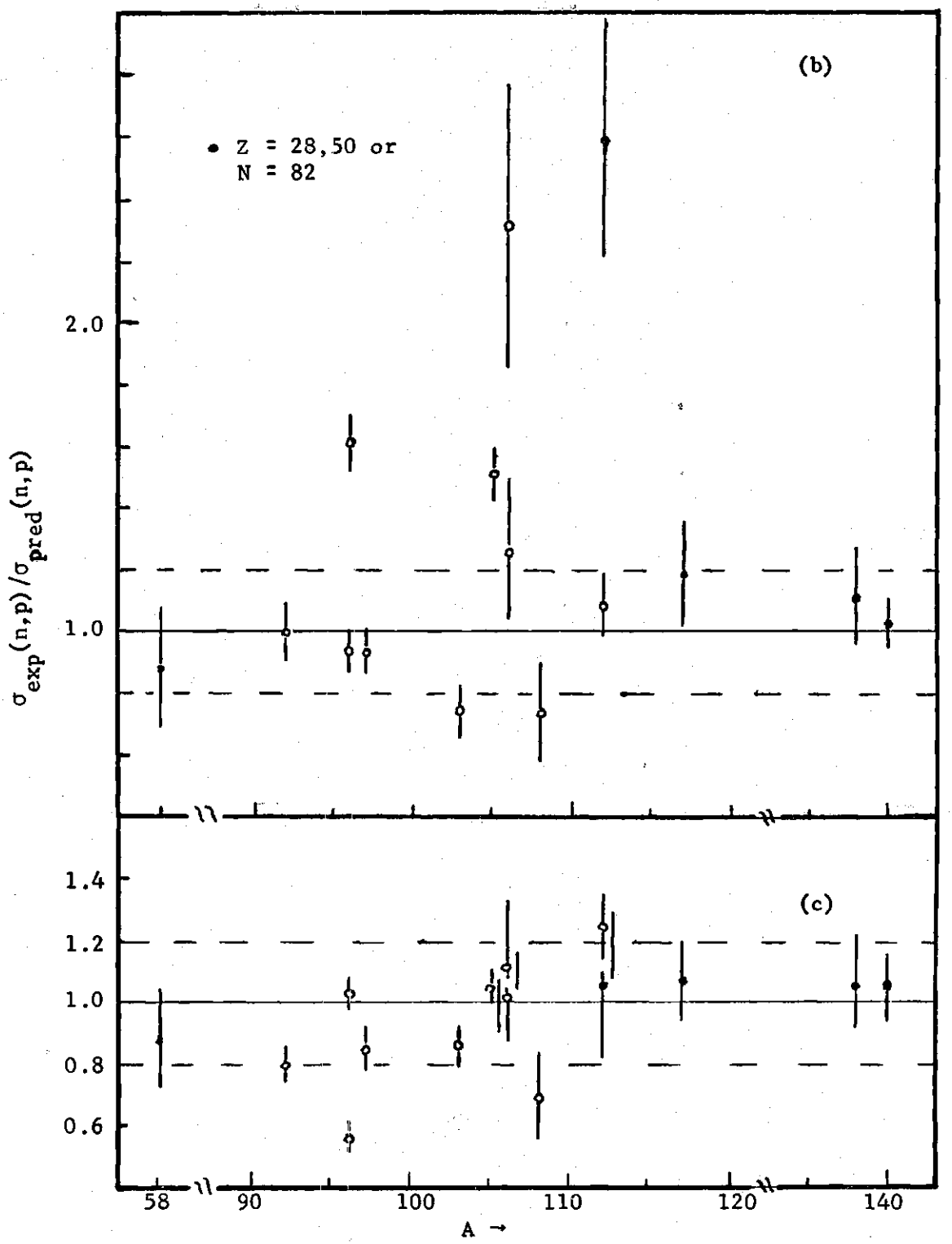

Figure 13. (b) and (c)

completely in disagreement with the presently measured (n,p) cross sections, while Levkovskii's predictions give much better agreement. However, Levkovskii's formula[49] failed to predict the (n,p) cross sections of Ru^{96}, Pd^{105}, Cd^{106}, and Sn^{112}. The predicted values for these cases are always too small, the measured cross sections being larger than the predicted ones by factors up to 2.5. It is seen that the values calculated from equation (4-32) derived in the present work are in good agreement with the measured ones within about ± 20% except for the cases of Mo^{96} and Rh^{103}.

The resemblance in form between Levkovskii's empirical formula and equation (4-32) derived from the statistical model with the constant nuclear temperature approximation for level densities suggests that there may be some relation connecting these two equations. To search for this relation, the values of D_p in equation (4-32) are plotted against (N-Z)/A in Figure 14. It is very interesting that D_p is seen to vary approximately linearly with the asymmetry parameter (N-Z)/A. A least squares fitting gives

$$D_p = 0.73 - 52.3(N-Z)/A \qquad (4\text{-}74)$$

or

$$D_p/T = 0.73/T - (52.3/T)(N-Z)/A \qquad (4\text{-}75)$$

With a constant temperature of 1.5 Mev, the coefficient of (N-Z)/A in equation (4-75) is found to be 34.8. The coefficient 33 in Levkovskii's formula corresponds to a nuclear temperature of 1.58 Mev. The form of equation (4-74) may be derived from a mass equation, but the numerical coefficients cannot be obtained from the parameters of the mass equation. The coefficients derived from a mass equation are averaged values of

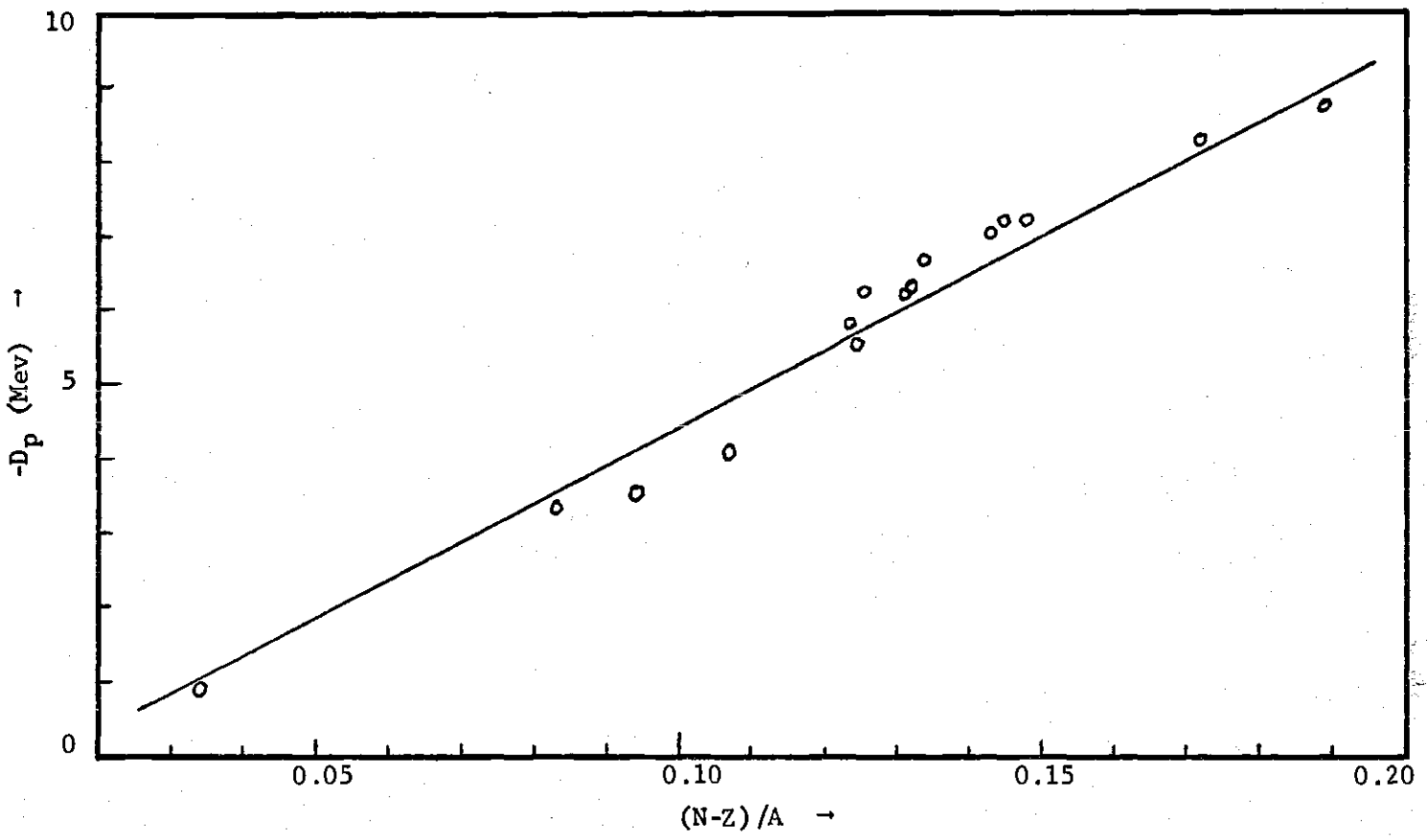

Figure 14. Plot of $-D_p$ against the Asymmetry Parameter (N-Z)/A, where D_p is the Difference of the Q-value of the (n,p) Reaction corrected for Pairing Energies and the Effective Coulomb Barrier. The Solid Line is a Least Squares Fitting Represented by

$$D_p \approx 0.73 - 52.3\ (N-Z)/A \text{ Mev.}$$

The Linear Relationship of D_p with (N-Z)/A enables one to relate the Levkovskii's Empirical Formula for (n,p) Cross Sections to the Equation Derived from Statistical Model with the Constant Nuclear Temperature Approximation for Level Densities, as discussed in the Text.

functions of Z and A, being approximately constant in a limited range. It appeared that Levkovskii's formula may be considered as an approximation of equation (4-32).

Facchini et al.[54] have calculated a number of (n,α) cross sections at 14 Mev by the statistical model for nuclei ranging from Na to U. In their calculations a complicated level density equation with level density parameter a was used. The results are in good agreement with measured (n,α) cross sections for nuclei with $A < 80$ but for nuclei of medium Z the calculated values are usually too small compared with the experimental values by factors of 5-10.[54] The (n,α) cross sections calculated from equation (4-33) with a constant nuclear temperature of 1.5 Mev are listed in Table 10, together with the values measured in the present work and with literature values. A comparison is shown in Figure 15. It is seen that the measured (n,α) cross sections are in general larger than the calculated ones, especially for the cases of Mo^{92}, Ba^{138}, and Ce^{142}, in which Mo^{92} and Ba^{138} have neutron shell closures at N = 50 and 82, respectively. The enhancement of (n,α) cross sections at neutron closures of the target nuclei is in accordance with that observed by Cuzzocrea et al.[24] The large discrepancies for the cases of Mo^{92} and Ba^{138} may be due to shell effects. If 1 Mev is added to the pairing energy for the neutron shell closure, the large discrepancies in the cases of Mo^{92} and Ba^{138} can be removed, as is shown in Figure 15. After doing so the (n,α) cross sections calculated from equation (4-33) derived in the present work generally agree with the measured ones within about $\pm 30\%$. The large discrepancies for the cases of Mo^{92}, Ba^{138}, and Ce^{142} may be also due to direct interactions with virtual preformed alpha

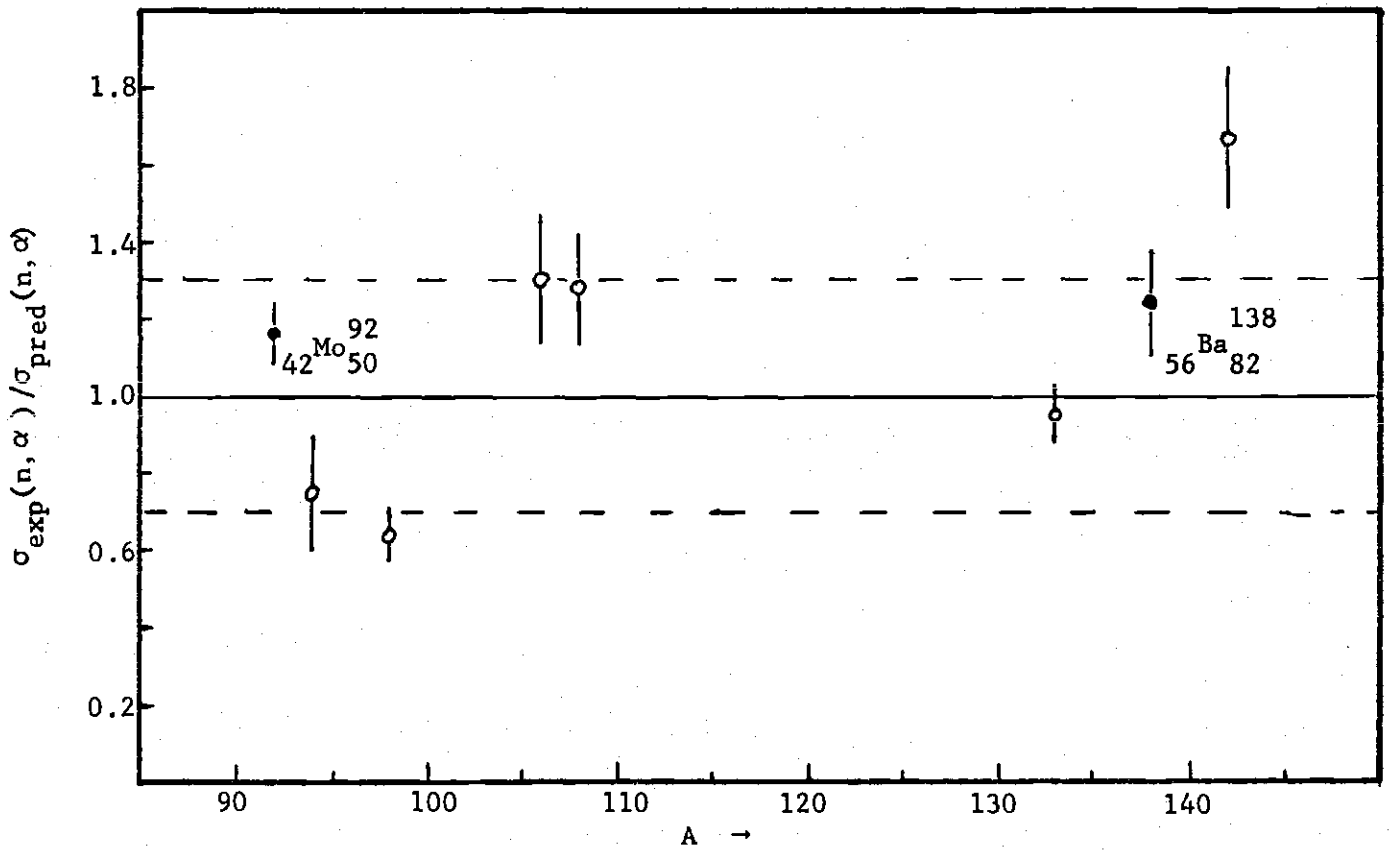

Figure 15. Comparison of the Experimental (n,α) Cross Sections at 14.4 Mev from the Present Work with the Predictions Based on an Average Nuclear Temperature of 1.5 Mev. For the Cases of Mo^{92} and Ba^{138}, 1 Mev is added to the Pairing Energy for the Neutron Shell Closures at N= 50 and N=82, respectively, suggesting that there may be Shell Effects in (n,α) Cross Sections. It is seen that this procedure gives agreement with Experiment within about ±30%.

clusters in the nuclear surface.[55-58]

In all cross section calculations in the present work, the non-elastic cross section σ_{ne} from Mani et al.[38] is used for the compound cross section σ_c. In general, however, σ_c is not equal to σ_{ne}, when direct interactions are present. Generally, direct interactions can have two opposite effects on a particular reaction, as is mentioned in the discussion of the direct interaction effects on (n,2n) cross sections. The general reaction (n,x) can be produced in principle both by direct interaction and through compound nucleus formation. The cross section measured by the activation method cannot distinguish between these two mechanisms. The activation cross section can be represented by

$$\sigma(n,x) = \sigma_s(n,x) + \sigma_d(n,x) \tag{4-76}$$

where $\sigma_s(n,x)$ and $\sigma_d(n,x)$ are cross sections described by the statistical model and due to direct interaction, respectively. For simplicity, let

$$r_{sx} = \sigma_s(n,x)/\sigma(n,x) \tag{4-77}$$

$$r_{dx} = \sigma_d(n,x)/\sigma(n,x) \tag{4-78}$$

$$r_c = \sigma_c/\sigma_{ne} \tag{4-79}$$

and

$$r_d = \sigma_d/\sigma_{ne} \tag{4-80}$$

where σ_d is the total cross section of direct interactions, i.e.

$$\sigma_d = \sum_x \sigma_d(n,x) \tag{4-81}$$

and

$$\sigma_{ne} = \sigma_c + \sigma_d \tag{4-82}$$

Then it is seen that

$$r_c + r_d = 1 \tag{4-83}$$

and

$$r_{sx} + r_{dx} = 1 \tag{4-84}$$

It is assumed that the cross section $\sigma_s(n,x)$ can be calculated from the statistical model as described in Section 4.1, i.e.

$$\sigma_s(n,x) = \sigma_c P_x \tag{4-85}$$

where P_x is the branching ratio of a particular reaction, given by

$$P_x = F_x / \sum_i F_i \tag{4-86}$$

in which the F_i's are defined in equation (4-2). The activation cross section of the (n,x) reaction can then be expressed by

$$\sigma(n,x) = \frac{1 - r_d}{1 - r_{dx}} \sigma_{ne} P_x \tag{4-87a}$$

$$= \frac{1 - r_d}{1 - r_{dx}} \sigma_{cal}(n,x) \tag{4-87b}$$

where $\sigma_{cal}(n,x) = \sigma_{ne} P_x$ is the calculated cross section for the (n,x) reaction from the statistical model with the non-elastic cross section σ_{ne} in place of the compound cross section σ_c.

From equation (4-87b), it is seen that if the calculated cross section $\sigma_{cal}(n,x)$ is about equal to the measured cross section $\sigma(n,x)$, the

ratio $(1 - r_d)/(1 - r_{dx})$ will be about equal to unity. In that case, r_d will be zero or very small compared with unity if r_d is zero or very small, which means little or no direct interaction. However, r_{dx} may be considerable when r_d is considerable, which means that direct interactions of the (n,x) reaction exist. Therefore, the agreement between the cross section calculated by the statistical model and the measured one does not necessarily mean that the reaction goes by compound nucleus formation, unless r_d is known to be zero from other experiments. In addition, r_{dx} may be smaller or greater than r_d so the calculated cross sections can also be greater or smaller than the measured cross sections. Qualitatively, it may be said that for a given (n,x) reaction, if the measured cross section $\sigma(n,x)$ is greater than the statistical model calculated cross section $\sigma_{cal}(n,x)$, e.g. $r_{dx} > r_d$, a contribution from direct interactions to $\sigma(n,x)$ is expected. On the other hand, if the measured cross section $\sigma(n,x)$ is smaller than the calculated $\sigma_{cal}(n,x)$, e.g. $r_d > r_{dx}$, direct interactions for the particular (n,x) reaction may or may not exist, but direct interactions of other reactions are expected, e.g. $\sigma_d \neq 0$. Therefore, the statistical model calculation cannot be definitively tested by activation cross sections alone, unless the direct interaction effects can be estimated independently, e.g. by emitted particle studies of energy and angular distributions from which r_d and r_{dx} may be estimated.

For medium and high Z nuclides the charged particles emission is generally negligibly small compared with neutron emission, so that the total direct interaction cross section σ_d is likely to be mainly due to the direct inelastic (n,n') reaction.[59] Therefore, systematic studies of the (n,n') reactions may help to estimate the value of r_d. If r_{dx} can

also be estimated from angular and energy distributions of emitted particles, then the method to calculate $\sigma_{cal}(n,x)$ can be justified.

The statistical model has various versions or approximations of the level density and inverse reaction cross section, etc. Sometimes quite different values for a parameter in the same version were used in the calculation of cross sections, as in the calculation of (n,2n) cross sections by Gardner,[15] Pearlstein,[16] and Gilbert and Gomberg.[17] For the (n,α) cross sections, the calculation method used by Facchini et al.[61] is different from the one used in the present work and quite different results are obtained as is shown in Table 10. However, the values from the present calculations are generally in fairly good agreement with the measured (n,α) cross sections.

4.5. Conclusions

From comparisons of the various predictions with experiments discussed above, the following conclusions are reached.

(1) The total (n,2n) cross sections at 14.4 Mev increase with increasing (N-Z)/A. An empirical formula was obtained from the (n,2n) cross sections measured in the present work. The formula reproduces the measured (n,2n) cross sections within about ±20% except for a few cases. The formula was further tested by (n,2n) cross sections measured by other investigators using the same method for nuclei ranging from Zn to Pb. The agreement is about equally good, i.e. within about ±20% with the exception of the lightest stable isotopes of even-Z elements where the competition from the (n,np) reaction may be important, especially for small Z nuclei.

(2) No odd-even effects in Z and no shell effects at Z = 28 and 50 and N = 82 for the (n,2n) reactions were observed for the nuclei investigated in the present work. The apparent shell effects seen for the cases of Mo^{92} and Zr^{90} at N = 50 are thought to be due to a Q-value effect.

(3) The calculated (n,2n) cross sections by Pearlstein's method and from the modified method of Gardner are generally in good agreement with the (n,2n) cross sections measured in the present work except for a few cases. The agreements in both methods are generally within about ±20%. Since in both methods a normalization procedure is involved to get absolute (n,2n) cross sections, this can hardly be regarded as a confirmation of the statistical theory with energy independent level density parameters.

(4) The equation

$$\sigma(n,2n) = \sigma_c(F_{2n}/F_n)/(1 + I_p e^{D_p/T}) \qquad (4\text{-}34)$$

derived from the statistical model with the constant nuclear temperature approximation for level densities, predicts the (n,2n) cross sections within about ±15% except for the cases of Ru^{96}, Pd^{102}, and Rh^{103} if effective thresholds proposed by Gilbert and Gomberg are used, i.e. the ground state threshold is raised by 0.5 Mev or 1 Mev for the second or third emitted neutrons, respectively. The large discrepancies for the cases of Ru^{96}, Pd^{102}, and Rh^{103} may be due to direct interaction effects in that the compound cross section σ_c is much smaller than the non-elastic cross section σ_{ne}, which was used for σ_c in the calculations. Since no normalization procedure is used in this method, it seems that the statistical

model with constant nuclear temperature approximation for level densities and with effective thresholds is confirmed by the present data.

(5) The assumption that neutron emission will occur whenever energetically possible appears to be questionable. Firstly, near the threshold, the competition from the gamma ray emission may not be negligible; the importance of this competition within about 2 Mev of thresholds has been demonstrated by Glover, theoretically. R. N. Glover and Weigold also pointed out qualitatively that near the threshold the spin states of the excited nucleus which can decay by neutron emission are limited, while there are many states through which gamma ray decay may occur, thus neutron emission may not be favored. In addition, the competition of (n,np) reactions may be also important as appears to be the case for Ni^{58}. Secondly, near the threshold, the level density of the residual nucleus is likely to be very small which violates the continuum assumption of the statistical model. Therefore, an effective threshold is used to compensate for these effects. The values 0.5 Mev or 1 Mev added to the ground state thresholds to get effective thresholds are quite arbitrary; however, they gave fairly satisfactory fits in general. For the cases of Ru^{96}, Pd^{102}, and Rh^{103}, the large discrepancies between calculated and measured (n,2n) cross sections may be also due to insufficient compensation of these effects, i.e. a higher effective threshold may be needed. The adjustments in effective thresholds for odd-even effects of Z suggested by Gilbert and Gomberg appear to be unnecessary, while the odd-even effects of N cannot be tested, because no (n,2n) cross sections of odd-N nuclei are available.

(6) The (n,2n) cross sections calculated from the statistical

model with an energy independent level density parameter a appeared to be rather insensitive to the value of a when the excitation energy is well above the threshold. Therefore, excitation functions of (n,2n) reactions seem not suitable for use to extract accurate values of the level density parameter a, unless the small part of the excitation function near the threshold is used. For cases in which the neutron separation energy S_n is close to the incident neutron energy, i.e. Mo^{92}, the calculated (n,2n) cross sections are very sensitive to the fluctuation of the values of S_n.

(7) The $[(n,np) + (n,pn) + (n,d)]$ cross sections of the lightest stable isotope of even-Z elements measured in the present work showed a simple regularity in that the cross sections decrease linearly with both Z and A of the target nucleus. Either of the empirical equations

$$\sigma\ (n,np + pn + d) = 934 - 15.14Z \qquad (4\text{-}49)$$

and

$$\sigma\ (n,np + pn + d) = 834 - 5.85A \qquad (4\text{-}50)$$

may be used to predict the $[(n,np) + (npn) + (n,d)]$ total cross sections for the lightest stable isotopes of even-Z elements. Two candidates, Se^{74} and Sr^{84}, are suggested to test the empirical equation. The good linearity of the cross section with Z or A may be just fortuitous. The generally decreasing trend of $[(n,np) + (n,pn) + (n,d)]$ cross sections may be understood from the increasing Coulumb barrier and the increasing competition of (n,2n) reactions. For the case of Ni^{58}, angular and energy distribution measurements of the emitted protons made by Glover and Purser showed that the reactions mainly go by compound nucleus and the statistical model calculations with a constant average nuclear temperature of 1.5 Mev agree well both with the total cross section and with the (n,np)

component. For the cases of Ru^{96}, Cd^{106}, and Sn^{112}, the values calculated from statistical model are far too small compared with the measured cross sections, suggesting that they are likely to go by some kind of direct interactions.

(8) An average nuclear temperature of 1.5 Mev obtained by Cuzocrea et al. is confirmed by the present (n,p) and (n,α) cross section data. The equation (equation 4-32) given by

$$\sigma(n,p) = \sigma_c I_p e^{D_p/T}/(1 + I_p e^{D_p/T}) \qquad (4\text{-}32)$$

predicts 14 out of 15 measured (n,p) cross sections within about ±20%, being better than the predictions from Levkovskii's formula. The predictions of Gardner and Rosenblum are almost completely in disagreement with the measured values. No shell effects at Z = 28, 50, and N = 82 for (n,p) cross sections were observed.

(9) Levkovskii's empirical formula

$$\sigma(n,p) = 45.2(A^{1/3} + 1)^2 e^{-33(N-Z)/A} \qquad (4\text{-}71)$$

is found to be closely related to equation (4-32) derived from the statistical model with the constant nuclear temperature approximation for level densities. The parameter D_p in equation (4-32), which is the Q-value of the (n,p) reaction corrected by pairing energies and Coulumb barrier, is found to be approximately a linear function of (N-Z)/A, i.e.

$$D_p/T = 0.73/T - (52.3/T)(N-Z)/A \qquad (4\text{-}75)$$

The coefficient 33 before (N-Z)/A in Levkovskii's formula corresponds to a nuclear temperature of 1.58 Mev. The linear form of the function for

D_p may be derived from a mass equation, but the numerical coefficients have to be determined empirically. The coefficients derived from a mass equation are functions of Z and A, being approximately constant in a limited range, so they may be different in different regions. It appeared that Levkovskii's empirical formula can be obtained from equation (4-32) by neglecting the term $I_p e^{0.73/T}/(1 + I_p e^{D_p/T})$ and replacing σ_c by the geometric cross section $45.2(A^{1/3} + 1)^2$.

(10) Since the cross sections measured by the activation method cannot distinguish direct interactions from compound nucleus formation and since in the statistical model calculations the non-elastic cross section σ_{ne} usually used for the compound cross section is in general not equal to σ_c due to direct interactions, one can hardly draw definite conclusions about reaction mechanisms from the comparison of measured activation cross sections at one energy with statistical model calculations. However, one may qualitatively say that, if the measured activation cross section is greater than the one calculated from the statistical model, direct interactions for the particular reaction are likely to exist; if the measured cross section is smaller than the calculated one, direct interaction for the particular reaction may or may not exist but direct interactions other than the particular reaction are likely to exist, i.e. σ_c is smaller than σ_{ne}. When a calculated cross section agrees with the measured one within experimental error, it does not necessarily mean that the reaction goes by compound nucleus formation unless the non-elastic cross section is known to equal the compound cross section σ_c.

(11) the (n,α) cross sections calculated from equation (4-33)

derived in the present work are generally in agreement with measured cross sections within about ±30%. The measured (n,α) cross sections of Mo^{92}, Ba^{138}, and Ce^{142} are larger than the calculated ones by factors of 2.3, 2.4, and 1.7, respectively. The large discrepancies of these cases may be due to direct interaction effects. For the cases of Mo^{92} and Ba^{138}, which have neutron shell closures at N = 50 and 82, respectively, a shell effect may exist. If 1 Mev is added to the pairing energy for the neutron shell closure, the discrepancies are removed. Therefore, both direct interaction effects and shell effects may affect the (n,α) cross sections of Mo^{92} and Ba^{138}.

(12) The statistical model has various versions or approximations and the results from different versions may be quite different. For the case of (n,α) cross sections Facchini, et al. have made calculations by the statistical model using a complicated level density equation with an energy independent level density parameter a. The results are in general an order of magnitude smaller than the ones calculated from equation (4-33) which also is derived from the statistical model, but with the constant nuclear temperature approximation for level densities, and with other rather crude approximations. In spite of the crudeness of the present calculation method, all the (n,2n), (n,p), and (n,α) cross sections measured in the present work ranging from Zr to Ce can be well described by the equations (4-34), (4-32), and (4-33), respectively. The average nuclear temperature of 1.5 Mev used for all types of reactions and for all nuclei in the present work is a rather crude approximation, although it generally gives fairly satisfactory agreement with experiment. The validity of the average nuclear temperature of 1.5 Mev may break down

in other regions or in particular cases. Therefore, the discrepancies between calculated cross sections and measured ones for particular cases may be also due to this crude approximation, i.e. the actual nuclear temperature for the particular cases may not be equal to 1.5 Mev. The same argument may apply to the effective thresholds.

4.6. Suggestions for Further Research

(1) Test the empirical linear relation of $[(n,np)+(n,pn)+(n,d)]$ cross sections with Z or A with the Se^{74} and Sr^{84} cases. If it turns out to be what is expected from the empirical equations, there may be theoretical significance connected to this linearity.

(2) Test the applicability of the constant nuclear temperature approach presented in the present work to the rare earth region.

(3) Do angular and energy distribution measurements of emitted particles on $[(n,np)+(n,pn)+(n,d)]$ reactions for cases other than Ni^{58} to test the mechanism of the reactions of Ru^{96}, Cd^{106}, and Sn^{112}.

(4) Measure the angular and energy distributions of the emitted alpha particles from the (n,α) reactions of Mo^{92} and Ba^{138}, which have neutron shell closures at N = 50 and 82, respectively, to test the mechanism of the reactions. The results may clarify the question of which causes the enhancement of the (n,α) cross sections of Mo^{92} and Ba^{138}, i.e. direct interactions? shell effects? or both?

REFERENCES

1. P. V. Rao and R. W. Fink, Phys. Rev. 154, 1023 (1967).

2. T. R. Fewell, US AEC report Sc-R-68-1704 (1968).

3. J. D. Seagrave, E. R. Graves, S. J. Hipwood and C. J. McDole, US AEC report LAMS-2162 (1967).

4. R. W. Fink, Proceedings of the Conference on the Use of Small Accelerators for Teaching and Research, U. S. Atomic Energy Report CONF-680411, Oak Ridge, Tenn. (1970).

5. P. V. Rao and R. W. Fink, submitted to Nucl. Phys. (1970).

6. C. M. Lederer, J. M. Hollander and I. Perlman, "Table of Isotopes," 6th Edition, (John Wiley and Sons, Inc., N. Y. 1967).

7. K. Siegbahn, Ed. "Alpha- Beta- and Gamma-ray Spectroscopy," Vol. I, Appendix 1, (North-Holland Publishing Co., Amsterdam, 1965).

8. H. Liskien and A. Paulsen, J. Nucl. Energy 19, 73 (1965).

9. H. Liskien and A. Paulsen, EURATOM Report, EUR-119e (1966) unpublished.

10. N. Ranakumar, E. Kondaiah and R. W. Fink, Nucl. Phys. A122, 679 (1969).

11. P. K. Hopke, R. A. Naumann, E. H. Spejewski and A. Strigachev Phys. Rev. 187, 1704 (1969).

12. IAEA standard source data sheet.

13. J. M. Blatt and V. F. Weisskopf, "Theoretical Nuclear Physics," (John Wiley and Sons, Inc., New York, 1952), pp. 311-564.

14. H. Büttner, A. Linder, and H. Meldner, Nucl. Phys. 63, 615 (1965).

15. D. G. Gardner, U. S. AEC Report UCRL-14575 (1966) (unpublished).

16. P. S. Pearlstein, Nucl. Data A3, 327 (1967); and U. S. AEC Report BNL-897 (T-365), (1964) (unpublished).

17. A. Gilbert and R. Gomberg, U. S. AEC Report UCRL-50736 (1969) (unpublished).

18. I. Dostrovsky, Z. Fraenkel, and G. Friedlander, Phys. Rev. 116, 683 (1960).

19. D. Bodansky, Ann. Rev. Nucl. Sci. 12, 79 (1962).

20. A. G. W. Cameron and R. M. Elkin, Can. J. Phys. 43, 1288 (1965).

REFERENCES (Continued)

21. E. T. Bramlitt and R. W. Fink, Phys. Rev. 131, 2649 (1963).

22. M. Bormann, Nucl. Phys. 65, 257 (1965).

23. F. Manero, International Conference on the Study of Nuclear Structure with Neutrons, Antwerp, 1965 (North-Holland Publishing Co., Amsterdam, 1966), p. 546.

24. P. Cuzzocrea and S. Notarrigo, ibid, p. 544.

25. R. Rieder, Sitzber. Osterr. Akad. Wiss. 175, 53 (1966).

26. J. Csikai and G. Peto, Phys. Letters 20, 52 (1966); Acta Phys. Acad. Sci. Hung. 23, 87 (1967).

27. D. W. Barr, C. I. Browne, and J.S. Gilmore, Phys. Rev. 123, 859 (1961).

28. P. Hille, Nucl. Phys. A107, 49 (1968).

29. M. Bormann and B. Lammers, Nucl. Phys. A130, 195 (1969).

30. A. Adam and L. Jeki, Acta Phys. Acad. Sci. Hung. 26, 335 (1969).

31. A. Abbound, P. Decowski, W. Grochulski, A. Marcinkowski, J. Piotrowski, K. Siwek, and Wilhelmi, Nucl. Phys. A139, 42 (1969).

32. R. E. Wood, W. S. Cook, Jr., R. Goodgame, and R. W. Fink, Phys. Rev. 154, 1108 (1967).

33. E. Kondaiah, N. Ranakumar, and R. W. Fink, Nucl. Phys. A120, 337 (1968).

34. W. Lu, N. Ranakumar, and R. W. Fink, Phys. Rev. C1, 350 (1970).

35. A. K. Hankla, private communication, (1970).

36. N. N. Flerov and V. M. Talyzin, J. Nucl. Energy 4, 529 (1957).

37. T. D. Newton, Can. J. Phys. 34, 804 (1956).

38. G. Mani, M. Melkanoff, and I. Iori, French Report CEA-2380 (1963) (unpublished).

39. G. T. Garvey, W. J. Gerace, R. C. Jaffe, I. Talmi, and I. Kelson, Revs. Mod. Phys. 41, No. 4, Part II, (1969).

40. A. Gilbert and A. G. W. Cameron, Can. J. Phys. 43, 1446 (1965).

REFERENCES (Continued)

41. J. Mattauch, W. Thiele, and Wapstra, Nucl. Phys. 67, 1 (1965).

42. P. Cuzzocrea, S. Notarrigo, and E. Perillo, Nuovo Cimento 52B, 476 (1967).

43. W. Nagel and A. H. W. Aten, J. Nucl. Energy 20, 475 (1966).

44. C. Maples, G. W. Goth, and J. Cerny, Nucl. Data A2, 429 (1966).

45. R. N. Glover and K. H. Purser, Nucl. Phys. 24, 431 (1961).

46. R. N. Glover and E. Weigold, Nucl. Phys. 29, 309 (1962).

47. J. R. Glover, Phys. Rev. 123, 267 (1961).

48. V. N. Levkovskii, J. Expl. Theoret. Phys. 31, 360 (1956), 33, 1520 (1957); Sov. Phys. JETP 4, 291 (1957), 6, 1174 (1958).

49. V. N. Levkovskii, J. Expl. Theoret. Phys. 45, 305 (1963), Sov. Phys. JETP 18, 213 (1964).

50. D. G. Gardner, Nucl. Phys. 29, 373 (1962).

51. D. G. Gardner and S. Rosenblum, Nucl. Phys. A96, 121 (1967).

52. A. Chatterjee, Nucl. Phys. 60, 273 (1964).

53. A. Chatterjee, Nucl. Phys. 47, 511 (1963), 49, 686 (1963); Phys. Rev. 134B, 374 (1964).

54. U. Facchini, E. Saetta-Menichella, F. Tonolini, and L. Tonolini-Severgnini, Nucl. Phys. 51, 460 (1964).

55. M. Jaskola, W. Osakiewicz, J. Turkiewicz, and Z. Wilhelmi, Nucl. Phys. 53, 270 (1964).

56. W. Osakiewicz, J. Turkiewicz, Z. Wilhelmi, and M. Jaskola, Nucl. Phys. 66, 361 (1965).

57. P. Kulisic, N. Cindro, and P. Strohal, Nucl. Phys. 73, 548 (1965).

58. W. R. Dixon, Nucl. Phys. 42, 27 (1963).

59. G. Peto, P. Bormmisza-Pauspertl, and J. Karolyi, Acta Phys. Acad. Sci. Hung., 25, 91 (1968).

APPENDIX

Material appearing in the foregoing dissertation has been published in part in the following journals:

Wen-deh Lu and R. W. Fink

Radiochemical Determination of the (n,2n) and (n,np)+(n,pn)+(n,d) Cross Sections of Cd^{106} at 14.4 Mev

Radiochimica Acta 12 62 (1969)

Wen-deh Lu, N. Ranakumar, and R. W. Fink

Activation Cross Sections for (n,2n) Reactions at 14.4 Mev in the Region Z = 40-60: Precision Measurements and Systematics

Phys. Rev. C1, 350 (1970)

Wen-deh Lu, N. Ranakumar, and R. W. Fink

Activation Cross Sections for (n,p), (n,np)+(n,pn) +(n,d), and (n,α) Reactions in the Region of Z = 40 to 58 at 14.4 Mev

Phys. Rev. C1, 358 (1970)

VITA

Winston Wen-deh Lu was born in a small town of Chekiang province, Chinese mainland, on June 6, 1932. After he graduated from high school in 1949, he joined in the army and came to Taiwan. Ten years later, he got an opportunity to enter National Taiwan University to continue his education. He obtained his B.S. degree in chemistry in 1963, and received an M.S. degree in chemistry in 1965 from the same university. Then he entered Chung Shan Institute of Science and Technology as an assistant investigator. In January, 1967, he was admitted to Georgia Institute of Technology to study toward the doctorate in nuclear chemistry.